The Role Hypothalamic Kisspeptin Neurons Play in Estradiol Negative and Positive Feedback Regulation of Reproduction

by

Luhong Wang

A dissertation submitted in partial fulfillment
of the requirements for the degree of
Doctor of Philosophy
(Molecular and Integrative Physiology)
in the University of Michigan
2018

Doctoral Committee:

Professor Suzanne M. Moenter, Chair
Associate Professor Carol F. Elias
Professor Martin G. Myers, Jr.
Professor Leslie S. Satin
Associate Professor Michael A. Sutton

A writer should have the precision of a poet and the imagination of a scientist.

- Vladimir Nabokov

Luhong Wang

wanglh@umich.edu

ORCID iD: 0000-0002-1085-841X

Dedication

To my parents and my beloved Shiwei

Acknowledgements

I am extremely thankful to my mentor, Sue, for her dedication, guidance and encouragement. The productive and collaborative work environment you create has made my time here truly enjoyable. You are encouraging and always give me the freedom to develop new ideas and to explore cutting-edge technologies. You have trained me to grow as a research scientist and transmitted your enthusiasm for science to me. From you, I learned to temper my excitement for new data with scientific rigor and organized skepticism. You always prioritize the interests of students beyond your own. My deep gratitude is beyond words.

I would like to thank the members of my thesis committee, Carol, Martin, Mike and Les for their guidance and encouragement throughout the duration of my thesis. You have provided intellectual inputs to my projects and challenged me to do the best. Special thanks go to Martin and Carol. Martin, you have shared your knowledge, resources, and time as my mentor for a rotation and it never ends. Carol, your kindness, generosity and scientific criticism are valuable. You provide me endless support for all my works.

I'd like to acknowledge the entire Moenter lab- past and present. Tony, thank you for sharing your knowledge in electrophysiology as well as in rock music. I have learned how to eliminate noise in the rig but to enjoy the noise as music. Thank you, Beth and Laura, I cannot imagine the lab without you. You have kept the lab running smoothly and fed us well with treats. You are amazing. Kasia and Kristen, you were the very model of successful graduate students. Tova, thank you for being a great rig partner. It is pleasant to work with you. Caroline, I always enjoy your sense of humor and sarcasm. You initiated the lab lunch tour that I love so much. Charlotte, for sharing so many thoughts on art, culture, food

and fashion. Thank you, Jeff, Eden, and Rudi, your being critical, supportive helps me solve my problems and perform better. Thank you all. Our talks together always filled me with insight and inspiration.

I own so much to my parents. Specially thanks to you, for unconditional and endless love and understanding of my career choice even when sometimes it meant being far away from you. You installed the independence, love of reading, curiosity in me. I am tremendously grateful to my beloved Shiwei, for encouraging me keep pursuing science, for bringing me Taikō, Zelda, and Mario games, and for many music albums, many postcards, many Skype phone calls and many flights. Thinking of you makes everything better.

Last but not least, I want to acknowledge Vladimir Nabokov and Marcel Proust. Your works keep inspiring me and have accompanied me during the most struggle time.

Table of Contents

List of Tables

List of Figures

List of Abbreviations

4AP	4-aminopyridine
AAV	adeno-associated virus
ACSF	artificial cerebrospinal fluid
ADP	afterdepolarization
AHP	afterhyperpolarization
AMPA	α-amino-3-hydroxy-5-methyl-4-isoxazolepropionic acid
APV	6-cyano-7-nitroquinoxaline
ARC	arcuate nucleus of the hypothalamus
AVPV	anteroventral periventricular nucleus
CNQX	6-cyano-7-nitroquinoxaline
CRISPR	clustered regularly interspaced short palindromic repeats
DIB	depolarization-induced burst
DMEM	Dulbecco's Modified Eagle Medium
DynA	dynorphin A
EPSCs	excitatory post-synaptic currents
ERα	estrogen receptor alpha
ERβ	estrogen receptor beta
FSCV	fast-scan cyclic voltammetry
FSH	follicle-stimulating hormone
FWHM	full width at half maximum
GABA	gamma-aminobutyric acid
GnRH	gonadotropin-releasing hormone
HCN	hyperpolarization-activated cyclic nucleotide-modulated channel
HPG	hypothalamic-pituitary-gonadal
I_A	A-type potassium current
I_h	hyperpolarization-activated nonspecific cation current
I_{NaP}	persistent sodium current
I_T	T-type calcium current
IF	instantaneous frequency

KERKO	kisspeptin-specific ERα knockout
KNDy	arcuate neurons co-expressing kisspeptin, neurokinin B and dynorphin
LH	luteinizing hormone
MBH	mediobasal hypothalamus
MUA	multi-unit activity
NKB	neurokinin B
NMDA	N-methyl-D-aspartate
norBNI	nor-binatorphimine
OVX	ovariectomized mice
OVX+E	ovariectomized mice treated with estradiol implant
OVX+E+P	ovariectomized mice treated with estradiol implant and progesterone injection
POMC	Pro-opiomelanocortin
POA	preoptic area
PPT	4,4',4''-(4-Propyl-[1H]-pyrazole-1,3,5-triyl) trisphenol
sgRNA	single-guide RNA
TERKO	neurokininB-specific ERα knockout
TTX	tetrodotoxin
VIP	vasoactive intestinal peptide
VMH	ventromedial hypothalamus
ZT	Zeitgeber time

Abstract

The brain regulates fertility through gonadotropin-releasing hormone (GnRH) neurons. Estradiol induces negative feedback on pulsatile GnRH/luteinizing hormone (LH) release and positive feedback generating GnRH/LH surges. Negative and positive feedback are postulated to be mediated by kisspeptin neurons in arcuate and anteroventral periventricular (AVPV) kisspeptin neurons, respectively. The work in this dissertation first demonstrated AVPV kisspeptin neurons were more excitable during positive feedback by performing electrophysiological recordings on cells from cycling and hormonal manipulated adult female mice. To test if the estradiol mediated excitability is due to estradiol action on estrogen receptor alpha (ERα) in kisspeptin neurons, kisspeptin specific ERα knockout mice (KERKO) and Clustered Regularly Interspaced Short Palindromic Repeats (CRISPR)/Cas9 based AAV vectors that target *Esr1* gene injected mice were used. The estradiol-induced increase in excitability of AVPV kisspeptin neurons was lost in cells from KERKO or AAV ERα knockdown mice. The comparable intrinsic excitability between two models suggests activational effects of estradiol can regulate firing activity. Besides intrinsic excitability, glutamatergic transmission to AVPV and arcuate kisspeptin neurons was characterized in cycling and hormonal manipulated adult female mice, as well as KERKO mice. This revealed that glutamatergic transmission to AVPV kisspeptin neurons is decreased during estradiol negative feedback whereas transmission to arcuate kisspeptin neurons is increased during negative feedback; frequency of glutamatergic transmission during positive feedback has the opposite pattern, being increased to AVPV and decreased to arcuate cells. Deletion of ERα in kisspeptin cells decreases glutamate transmission to AVPV neurons and markedly increases it to arcuate kisspeptin neurons, which also exhibits increased spontaneous firing rate. KERKO mice exhibit increased LH pulse

frequency, indicating loss of negative feedback. The CRISPR/Cas9 based AAV approach enables spatial- and temporal-specific gene editing in mice. This allows us to test the role of estradiol and ERα in AVPV and arcuate kisspeptin neurons plays to sense estradiol and orchestrate pulsatile and surge release of GnRH/LH and thus reproductive output.

Chapter 1 Introduction

The goal of this introduction is to review the state of the field at the beginning of the development of this dissertation project.

Significance

Reproductive function includes puberty onset and completion, reproductive cyclicity, gametogenesis, fertilization, pregnancy, lactation and senescence; all are indispensable to perpetuate species. As a window to overall health, reproductive health is vital for all stage of life. Fertility problems affect 20% of couples[1]; ovulatory disorders account for 25% of this total[2]. Beyond reproductive neuroendocrine and sex behavior systems, sex steroids act on many systems including nervous, cardiovascular, bone and skeletal system. These demonstrate the importance of understanding the reproductive system in physiological and pathological conditions. The advance of our knowledge in the field will help develop novel therapies for reproductive diseases in human patients, domestic animals, and endangered species.

The reproductive axis and estradiol feedback

Gonadotropin-releasing hormone (GnRH) neurons integrate central and peripheral cues, such as steroids, stress, metabolic status, circadian rhythms, and olfaction, to send the central output to regulate fertility[3]. Residing in the preoptic area (POA) and anterior hypothalamus and projecting to the median eminence, GnRH neurons release GnRH to the hypophyseal portal vasculature to stimulate the pituitary to produce and secrete gonadotropins [4,5]. High GnRH pulse frequency preferably stimulates luteinizing hormone (LH) release, whereas

low GnRH pulse frequency preferably promotes follicle-stimulating hormone (FSH) release[6]. The secretion of FSH and LH regulates gonadal gametogenesis and steroidogenesis[7]. The sex steroids including estradiol, progesterone and testosterone feed back on the brain to regulate GnRH release, and on the pituitary to regulate the responsiveness of gonadotropes to GnRH[8–11]. In males and during most of the female reproductive cycle, sex steroids suppress GnRH neuron activity and release[12,13]. During female preovulatory stage (late follicular phase or proestrus), a sustained elevation in estradiol causes a switch of estradiol action from negative to positive feedback and thus induces elevated GnRH neuronal activity, causing a preovulatory surge of GnRH and subsequent LH release, which triggers ovulation[14–16]. The investigation of the feedback regulation of hypothalamus has focused mainly on estradiol, as estradiol is the predominant signal to mediate positive feedback, a central focus of this dissertation project.

The physiological responses to estradiol in reproductive tissues and organs are known to be mediated by at least two subtypes of estrogen receptor, estrogen receptor α (ERα) and estrogen receptor β (ERβ), in distinct tissue or cell types[17,18]. In rodents and humans, these subtypes are encoded by different genes *Esr1* (human ESR1) and *Esr2* (human ESR2), respectively. Both ERα and ERβ belong to nuclear hormone receptor family and act as ligand-activated transcription factors[19]. The global knockout of ERα or ERβ, neither lethal, have different reproductive deficits. The ERαKO mice are infertile and exhibit disrupted reproductive tracks such as hypoplastic uteri, large hemorrhagic cysts and absence of corpora lutea in the ovaries, whereas ERβKO mice are fertile but have fewer and smaller litters [20,21]. Further, ERαKO but not βERKO female mice exhibit abnormally high serum LH after gonadectomy and estradiol replacement compared to normal control mice[22], demonstrating a necessity of ERα, but not ERβ in estradiol negative feedback. A neuron-specific ERα KO mouse model shares similar impaired negative feedback compared to the global KO model and impaired positive feedback marked as an absence of estradiol-induced LH surge

release[23]. These observations suggest that estradiol negative and positive feedback relies on estrogen signaling via ERα-expressing neurons.

Pulse and surge release of GnRH

As the GnRH release pattern is the central signal to regulate the pituitary reproductive function, it is critical to study how GnRH is released in physiological and pathological conditions. The challenges remain that long-term monitoring GnRH release can only be done in large animals like sheep and primates, from which GnRH can be measured in the extracellular space of the median eminence using techniques such as push-pull perfusion, in vivo microdialysis or direct sampling from pituitary stalk portal blood[24–26]. This cannot be done in small rodents due to their small body size and small hypothalamus and portal vasculature[27]. As the secretion of LH occurs highly correlated with GnRH secretion in large animals, LH is often used as a bioassay for central GnRH release in small rodents[28,29]. However, cases remain when LH pattern is not faithfully representing GnRH release pattern. One example is the high frequency of GnRH pulses in thyroidectomized ewes are not reflected by the less clear LH pulses[30]. This may because a shorter GnRH pulse interval does not provide time for the clearance of LH, which has a longer half-life compared to GnRH, thus the interpretation between GnRH and LH release patterns need to be carefully addressed[31]. Patterns of GnRH and LH secretion across female reproductive cycles have been descried as two release modes: pulsatile and surge release. These two patterns are modulated by the biphasic effect of estradiol, negative feedback and positive feedback, respectively.

The pulsatile release of GnRH/LH is characterized as discrete pulses separated by periods at basal levels. Lower levels of estradiol during the majority of the reproductive cycle exert negative feedback to decrease primarily GnRH pulse amplitude; estradiol also play a permissive role to facilitate the role of progesterone to decrease GnRH/LH pulse frequency[32]. This negative feedback is

critical for maintaining normal gonadotropin secretion, essential for normal pubertal process and maintaining reproductive cyclicity [33–36]. The patterns of GnRH release are critical for the regulation of gonadotropin secretion, demonstrated by a classic lesion/replacement study. In rhesus monkeys when the medial basal hypothalamus was lesioned to abolish the endogenous GnRH release, only those who received episodic but not continuous manner of GnRH reestablished pituitary gonadotropin secretion[37]. Abnormal GnRH secretion is involved in a number of reproductive disorders including polycystic ovary syndrome, and hypogonadotropic hypogonadism[38,39].

The switch of estradiol from negative to positive feedback at the end of follicular phase or proestrus triggers a sustained release of GnRH and LH. The surge release of GnRH occurs shortly prior to or coincidently with LH surge, and continues after the end of LH surge, denaturing from the pulsatile pattern[14]. There is some debate in higher primates about the necessity of the GnRH surge for ovulation, as LH surge occurs during an episodic release of free gonadotropin alpha subunit, a GnRH secretion marker, in women[40]. In rhesus monkeys that received hypothalamic lesion and unvarying GnRH pulse frequency replacement, LH surges also occurred, but could not be induced in the absence of GnRH replacement[41]. It is worth noting that monkeys do exhibit a GnRH surge along with the preovulatory or estradiol-induced LH surge[42,43]. In rodents and sheep, the preovulatory surge release of GnRH drives LH surge, which is crucial for ovulation[44,45].

GnRH central network

Given the scattered distribution of GnRH neurons in the forebrain, monitoring GnRH group-activity is particularly hard. A multi-unit recording study in the hypothalamic region of rhesus monkeys reveals an increased overall electrical activity correlated with LH pulses[46]. However, these results are difficult to interpret because of the lack of ability to distinguish the signals from GnRH vs

other neurons. The application of transgenic techniques really advanced the field by visualizing GnRH neurons with a reporter gene under its GnRH gene promotor[47,48]. This allows close examining of GnRH neurons, such as genetic profiling and individual GnRH neuronal activity monitoring[49]. Extracellular and whole-cell recordings have been applied to study GnRH neuronal activity. GnRH neurons exhibit spontaneous firing activity as well as periods of quiescence on brain slices via extracellular and whole-cell current-clamp recordings[50–52]. Burst firing, potentially facilitating hormone release[53], has also been found in GnRH neurons[50,54].

One critical aspect of GnRH electrophysiological properties is their manipulation by steroids. Several hormone manipulation paradigms have been used to mimic estradiol-induced LH surge to study estradiol positive feedback[55]. Here I will mainly review the paradigm that induces LH surge by constant elevated estradiol, as this is the model on which majority of the work in this dissertation has been done[12]. In this model, female mice are ovariectomized and an estradiol implant providing a constant physiological level of estradiol is placed at the time of surgery. This model produces a daily diurnal-timed LH surge occurring around time of lights off; in the morning, LH level remains low due to estradiol negative feedback. Correlated to the pituitary output, in this model GnRH neurons also exhibit low firing frequency in the morning as the consequence of negative feedback and high firing frequency due to positive feedback[12]. The fast-scan cyclic voltammetry (FSCV) technique has been adapted to measure the real-time release of GnRH in brain slices, attempting to correlate GnRH activity with the hormone release. GnRH release frequency at the median eminent correlates well with its firing frequency, low release during negative feedback and high release during positive feedback[13]. These estradiol-modulated changes may be attributable to GnRH intrinsic properties as well as fast synaptic inputs or the effects of neuromodulators [56–59].

Intrinsic properties include the ion channel expression profiles and their kinetics, as these can help sculpting the firing output of a neuron. Being closely influenced by estradiol signals, GnRH neurons do express ERβ and estrogen receptor GPR30[60,61]. The changes in intrinsic properties of GnRH neurons may be in part of attributable to these estrogen receptors that respond to acute rise of estradiol and potentially regulate the afterhyperpolarization (AHP) and the slow afterdepolarization (ADP) though voltage gated calcium channels, hyperpolarization-activated cation channels, and persistent sodium channels[57,58,62].

Fast synaptic transmission underlies a large proportion neuronal communication including the hypothalamic neurons[63,64]. Glutamate and/or gamma-aminobutyric acid (GABA) act via ionotropic receptors such as $GABA_A$, alpha-amino-3-hydroxy-5-methyl-4-isoxazole propionic acid (AMPA) and N-methyl-D-aspartate (NMDA) receptors. Both GABA and glutamate are excitatory to GnRH neurons[65,66]. GABAergic and glutamatergic transmission to GnRH neurons is increased during positive feedback compared to negative feedback[56,59]. The acutely application of ERα agonist PPT reduced the frequency of GABA transmission to GnRH neurons whereas ERβ agonist DPN increased frequency of GABA transmission[67]. These data show that estradiol can act rapidly or long-term to regulate GABAergic transmission to GnRH neurons in a receptor subtype-dependent manner. At least some of these GABAergic and glutamatergic GnRH-afferents are likely to express estrogen receptors.

In addition to the fast synaptic transmission, neuromodulators such as vasoactive intestinal peptide (VIP), orexin, and kisspeptin are also involved in GnRH regulation[68–72]. These suggest that GnRH neurons may receive endogenous released neuropeptide through the terminal of these peptidergic neurons. Both neurons in suprachiasmatic nucleus that synthesize VIP and orexin neurons in lateral hypothalamic area place fibers close to GnRH neurons[73,74]. The region and role of kisspeptin will be further discussed in the next section.

Kisspeptin signaling

The discovery of the link between KISS1 and KISS1R mutations and reproductive deficits including idiopathic hypothalamic hypogonadism, impaired pubertal maturation, and low-amplitude LH pulses in patients highlighted the role of kisspeptin (KISS1 product) and its receptor (KISS1R product) in puberty and fertility [75,76]. Transgenic mice that lack *Kiss1* and *Kiss1r* exhibit a similar hypothalamic hypogonadism phenotype, confirming the clinical observations[76,77]. Interestingly, *Kiss1* KO mice show a more variable and less severe of hypothalamic hypogonadism phenotypes compared to *Kiss1r* KO mice [78,79].

Identification the population of cells expressing *Kiss1r* is challenging due to the lack of antibody reliability. Both in situ hybridization studies and a *Kiss1r* promoter-driven *Lacz* knock-in mice show the expression of *Kiss1r* mRNA or its reporter protein in several brain regions including the preoptic area, where GnRH neurons are located[80,81]. Later, it was discovered that kisspeptin is a potent stimulator of GnRH neurons, as it induces cFos expression in GnRH neurons, a marker for recent increased activity[82]. The direct measurements of GnRH firing and release with kisspeptin treatment further demonstrated the stimulatory effect of kisspeptin on GnRH firing and release[13,72,83]. From a loss-of-function aspect, blockade of kisspeptin action by injecting an antibody or a specific antagonist decreases GnRH firing and release[84]. These studies demonstrate a strong functional link between kisspeptin and GnRH neurons.

Similar to the identification of *Kiss1r*, in situ hybridization studies and reporter transgenic mice have been used for identification of the expression pattern of *Kiss1*. In rodents, kisspeptin is found in two regions in the arcuate nucleus and the anteroventral periventricular nucleus (AVPV) of hypothalamus. The arcuate kisspeptin expression occurs in both sexes and AVPV kisspeptin expression is predominantly observed in females[84]. Kisspeptin fibers from AVPV exhibit direct

appositions to GnRH cell bodies and arcuate kisspeptin neurons to GnRH terminals[85,86], supporting a kisspeptin-GnRH direct connection from an anatomical perspective.

Both hypothalamic kisspeptin neuronal populations express ERα, ~70% in AVPV and ~99% in arcuate nucleus[87]. These two nuclei respond to elevated estradiol in a nucleus-specific manner, with increased kisspeptin mRNA in AVPV and decreased in arcuate nucleus[88,89]. This sets up the working hypothesis in the field that arcuate and AVPV kisspeptin neurons have distinct roles in mediating estradiol negative feedback and positive feedback, respectively. I will thus review the evidence to support their roles separately.

Arcuate kisspeptin neurons and negative feedback

The first evidence that suggest the link between arcuate nucleus neurons and LH pulse comes from early lesion studies: abolishing the arcuate nucleus abolishes LH pulses in rats and monkey[90,91]. Furthermore, the correlation of mediobasal hypothalamic (MBH) neuronal multi-unit activity with LH pulse release has been demonstrated in various animals[46,92,93], suggesting MBH neurons are involved in pulse generation. GnRH neurons in the brain are differently distributed in different animal models [94,95]. In rodents, GnRH neurons are rare in the MBH, but the correlated activity is still observed[93], indicating other neuronal populations are involved in pulse generation besides GnRH neurons. Although it is still arguable where the neuronal signals come from, arcuate kisspeptin neurons appear to be one reasonable source anatomically and functionally.

Besides kisspeptin, these arcuate neurons co-express neurokinin B (NKB) and dynorphin A (Dyn), thus they are called KNDy neurons [96–98]. Anatomical studies suggest these KNDy neurons may form an interconnected network; their cell bodies receive close apposition of contacts that express at least one of these three peptides[99]. Also, most KNDy neurons express NKB receptor NK3R and a smaller population of KNDy neurons express dynorphin-specific kappa-opioid receptor[98,100]. The functional role of NKB and Dyn has been demonstrated in

multi-unit activity (MUA) studies in goats and ewes: intracerebroventricular application of NKB or nor-binatorphimine (BNI), a kappa-opioid receptor antagonist, to the arcuate nucleus increases the frequency of electrical spikes and LH pulse frequency[101,102]. The application of dynorphin inhibits the MUA spikes as well as LH secretion[101]. Further, estradiol attenuates the stimulatory effect of NKB and inhibitory effect of dynorphin. Taken together, these suggest NKB plays an excitatory role and dynorphin plays an inhibitory role in LH pulse frequency. However, whether these neurons directly drive or only modulate LH pulses is still unknown.

KNDy neurons highly express ERα[87] and are sensitive to estradiol: they decrease kisspeptin, NKB and NKB receptor NK3R mRNA level when estradiol is elevated[88,89,98]. As both kisspeptin and NKB are stimulators of LH pulses, this suggests estradiol may directly attenuate activity of GnRH-afferent neurons including KNDy neurons, thus further reduce the firing in GnRH neurons and release of GnRH. Further evidence comes from examining a kisspeptin-specific ERα knockout mouse model. In this model, deletion of ERα from kisspeptin cells leads to precocious puberty onset and absence of reproductive maturation as these mice exhibited abnormal cyclicity[103]. This suggests ERα in kisspeptin cells is critical for reproductive function including puberty development and maintaining cyclicity. However, in this model, ERα is removed from both AVPV and arcuate kisspeptin neurons and other kisspeptin cell located centrally and peripherally, making the interpretation of the role of arcuate kisspeptin neurons not clear.

AVPV kisspeptin neurons and positive feedback

The AVPV region was associated with surge generation long before the discovery of kisspeptin. AVPV neurons are sexually dimorphic and exhibit increased cFos expression coincident with the elevated cFos in GnRH neuron during the surge[104,105]. Lesions of the AVPV block the natural occurring preovulatory as well estradiol-induced LH surge[106–108]. As a subgroup of neurons

in AVPV, kisspeptin neurons are also highly sexual dimorphic, with kisspeptin expressed far more abundantly in females than in males[85,109]. This suggests AVPV kisspeptin may play a female-specific role, further linking it to the female-specific preovulatory LH surge.

The majority of kisspeptin neurons in the AVPV express ERα (~70%) and can directly sense estradiol, supporting their roles in surge genration[110]. AVPV kisspeptin neurons are highly heterogeneous and coexpress various of neuron transmitter and neuropeptide including GABA (~75%), glutamate (~20%) and tyrosine hydroxylase (~70%)[87,111]. AVPV kisspeptin neurons form close contact with GnRH cell body and kisspeptin, glutamate and GABA are all excitatory to GnRH neurons. The role of tyrosine hydroxylase within kisspeptin neurons is less known. AVPV kisspeptin neurons and GnRH neurons both exhibit increased cFos expression that correlates with GnRH/LH surge onset[112,113], indicating elevated electrical activity during positive feedback. The functional roles of these neurons including how they fire action potentials to release neuropeptide and neurotransmitters to GnRH was not known back then and need to be tested.

Dissertation Project Preview

Before the studies presented in this dissertation, most of the research on AVPV and arcuate kisspeptin neurons are focused on either gene expressions or peptide effects on downstream GnRH and LH signal. There has been no direct test of the functional roles AVPV and arcuate kisspeptin neuron in negative and positive feedback, or estradiol actions on their electrophysiological properties. Chapter 2 focuses on how AVPV kisspeptin neurons are modulated by estrus cycle and estradiol. Chapter3 investigates on how estradiol and ERα in kisspeptin neurons mediate the presynaptic glutamatergic transmission to AVPV and arcuate kisspeptin neurons. This chapter also covers the role of ERα in kisspeptin neurons plays in arcuate kisspeptin neuronal firing and estradiol negative feedback. Chapter4 further tests how ERα in kisspeptin neurons

mediates the estradiol-induced shifts in their electrophysiological properties by deleting ERα either in early development or during adulthood. Chapter5 summarizes the work and proposes the next directions. Together these studies not only provide insights into the role of ERα in AVPV kisspeptin neurons in mediating estradiol-induced shifted excitability, but also demonstrate the distinct roles of ERα in AVPV and arcuate kisspeptin neurons.

Chapter 2 Excitability and Burst Generation of AVPV Kisspeptin Neurons Are Regulated by the Estrous Cycle via Multiple Conductances Modulated by Estradiol Action.

Luhong Wang, Richard A. DeFazio and Suzanne M. Moenter

This work was originally published in 2016 in the journal eNeuro 18 May 2016, 3 (3) ENEURO.0094-16.2016

Abstract

The preovulatory secretory surge of gonadotropin-releasing hormone (GnRH) is crucial for fertility and is regulated by a switch of estradiol feedback action from negative to positive. GnRH neurons likely receive estradiol feedback signals via ERα-expressing afferents. Kisspeptin neurons in anteroventral periventricular nucleus (AVPV) are thought to be critical for estradiol positive feedback induction of the GnRH surge. We examined the electrophysiological properties of GFP-identified AVPV kisspeptin neurons in brain slices from mice on the afternoon of diestrus (negative feedback) and proestrus (positive feedback, time of surge). Firing frequency and action potential bursts were increased on proestrus vs. diestrus in extracellular recordings. Whole-cell recordings were used to study intrinsic mechanisms of bursting. Upon depolarization, AVPV kisspeptin neurons exhibited tonic firing or depolarization-induced bursts (DIB). Both tonic and DIB cells exhibited bursts induced by rebound from hyperpolarization. DIB occurred similarly on both cycle stages, but rebound bursts were observed more often on proestrus. DIB and rebound bursts were both sensitive to Ni^{2+}, suggesting T-type Ca^{2+} currents (I_T) are involved. I_T current density was greater on proestrus vs.

diestrus. In addition to I_T, persistent sodium current, I_{NaP}, facilitated rebound bursting. On diestrus, 4-aminopyridine (4-AP)-sensitive potassium currents contributed to reduced rebound bursts in both tonic and DIB cells. Manipulation of specific sex steroids suggests estradiol induces the changes that enhance AVPV kisspeptin neuron excitability on proestrus. These observations indicate cycle-driven changes in circulating estradiol increased overall action potential generation and burst firing in AVPV kisspeptin neurons on proestrus vs. diestrus by regulating multiple currents

Significance Statement

The brain controls fertility via the hypothalamo-pituitary-gonadal axis. Gonadotropin-releasing hormone (GnRH) neurons form the final output pathway but are not directly sensitive to critical elements of gonadal steroid feedback. Kisspeptin neurons of the anteroventral periventricular nucleus may convey steroid feedback to GnRH neurons. We studied how action potential firing of kisspeptin neurons varies between two critical phases of the estrous cycle: diestrus when estradiol exerts negative feedback to suppress GnRH release, and proestrus when estradiol feedback activates GnRH neurons. Increased spontaneous and burst firing on proestrus were observed and attributable to estrous-cycle dependent changes in multiple ionic currents. These changes were specifically driven by estradiol. This estrous-cycle regulation of kisspeptin neuron excitability is likely a critical aspect of female fertility.

Introduction

GnRH neurons form the final common pathway for central regulation of reproduction. GnRH stimulates the pituitary to secrete follicle-stimulating hormone and luteinizing hormone (LH) to regulate gonadal functions. Gonadal steroids feed back to regulate GnRH release. In males and during most of the female reproductive cycle, sex steroids suppress GnRH neuron activity and

release[12,15,114,115]. In females, sustained elevations in estradiol during the follicular phase result in a switch of estradiol action from negative to positive feedback, inducing GnRH neuron activation, and a preovulatory surge of GnRH and LH release[116]. Although regulated by steroid feedback, GnRH neurons do not express detectable levels of most steroid receptors, including estrogen receptor alpha (ERα)[61,117], which mediates estradiol negative and positive feedback[118,119]. Steroid-sensitive afferents thus likely transmit feedback signals to GnRH neurons. Estradiol-sensitive kisspeptin-expressing neurons in the arcuate nucleus (ARC) and anteroventral periventricular (AVPV) nucleus may convey estradiol negative and positive feedback to GnRH neurons, respectively[110]. Kisspeptin is a potent stimulator of GnRH neuron activity and release[72,83]. AVPV kisspeptin neurons express ERα[88], as well as GABA and glutamate (Cravo et al., 2011), both of which also excite GnRH neurons[65,66]. AVPV kisspeptin neurons synapse on GnRH neurons[120,121] and express elevated cFos during the GnRH/LH surge[122]. Infusion of anti-kisspeptin antibodies into the preoptic area[123], or deletion of ERα specifically from kisspeptin neurons both block estradiol-induced LH surges[124]. Together these observations suggest a role for AVPV kisspeptin neurons in conveying estradiol positive feedback to GnRH neurons.

Given the evidence for a role for AVPV kisspeptin neurons in estradiol positive feedback, a fundamental question is how the firing activity of AVPV kisspeptin neurons shifts between estrous cycle stages to increase the release of kisspeptin, glutamate and/or GABA during positive feedback. AVPV kisspeptin neurons express several ionic conductances that may shape firing patterns[125–127], some of which are regulated by the reproductive cycle [125], but the mechanisms that underlie changes in AVPV kisspeptin neuron excitability are not fully understood. In particular, release of neuropeptides such as kisspeptin is classically linked with high frequency bursts of action potentials (van den Pol, 2012).

We examined spontaneous activity of AVPV kisspeptin neurons, and contributions of candidate currents to the firing properties of these cells during two estrous cycle stages: the afternoon of diestrus representing estradiol negative feedback and the afternoon of proestrus representing positive feedback[128,129]. We then determined the specific circulating steroids that mediate the cycle-dependent changes in firing patterns and how different ionic conductances contribute.

Material and Methods

Animals. Kiss1-hrGFP mice[130] mice were propagated in our colony. All mice were provided with water and Harlan 2916 chow *ad libitum* and were held on a 14L:10D light cycle with lights on at 0400 Eastern Standard Time. Mice were used during the diestrous or proestrous phases of the estrous cycle determined by monitoring vaginal cytology of female mice 60-90 days old for at least a week before experiments. Uterine mass was determined after brain slice preparation to confirm uteri on proestrus were >100mg, indicating exposure to high estradiol[131]. To examine the role of specific sex steroids, similarly aged adult female mice were ovariectomized (OVX) under isoflurane anesthesia (Abbott) and were either simultaneously implanted with a Silastic capsule (Dow-Corning) containing 0.625µg of estradiol suspended in sesame oil (OVX+E) or not treated further (OVX). Bupivacaine was provided local to the incisions as an analgesic. These mice were studied 2-3d post ovariectomy during the time of estradiol positive feedback[12]. On the day of study, some OVX+E mice received a sc injection at 0900-1000 Eastern Standard Time of progesterone (300 µg/20 g, OVX+E+P)[132], or sesame oil vehicle (OVX+E+V). All mice were killed at 1500-1600 Eastern Standard Time. There were no differences observed between OVX+E and OVX+E+V mice for firing patterns and burst generation; these data were combined for analyses and only OVX+E mice were included for further studies to reduce animal use. The Institutional Animal Care and Use Committee of the University of Michigan approved all procedures.

Slice preparation and cell identification. All chemicals were purchased from Sigma Chemical Co. unless noted. All solutions were bubbled with 95% O_2/5% CO_2 throughout the experiments and for at least 30 minutes before exposure to tissue. The brain was rapidly removed and placed in ice-cold sucrose saline solution containing (in mM): 250 sucrose, 3.5 KCl, 26 $NaHCO_3$, 10 D-glucose, 1.25 $NaHPO_4$, 1.2 $MgSO_4$, and 3.8 $MgCl_2$ (pH 7.6, 345 mOsm). Coronal (300 µm) slices were cut with a Leica VT1200S (Leica Biosystems). Slices were incubated in a 1:1 mixture of sucrose saline and artificial cerebrospinal fluid (ACSF) containing (in mM): 135 NaCl, 3.5 KCl, 26 $NaHCO_3$, 10 D-glucose, 1.25 Na_2HPO_4, 1.2 $MgSO_4$, 2.5 $CaCl_2$ (pH 7.4, 305 mOsm) for 30 min at room temperature (~21- 23 °C) and then transferred to 100% ACSF for additional 30-180 min at room temperature before recording. For recording, slices were placed into a chamber continuously perfused with ACSF at a rate of 3ml/min with oxygenated ACSF heated to 31 ± 1 °C with an inline-heating unit (Warner Instruments). GFP-positive AVPV kisspeptin neurons were identified by brief illumination at 488nm on an Olympus BX51WI microscope. Recorded cells were mapped to an atlas[133] to determine if any trends based on anatomical location emerged; no such trends were apparent in these data sets. Recordings were performed from 1 to 3 h after brain slice preparation. No more than three cells per animal were included for analysis of the same parameter, and at least 5 animals were tested per parameter.

Electrophysiological recording. Recording micropipettes were pulled from borosilicate capillary glass (type 7052, 1.65 mm outer diameter; 1.12 mm inner diameter; World Precision Instruments, Inc.) using a Flaming/Brown P-97 puller (Sutter Instruments) to obtain pipettes with a resistance of 3-5 MΩ for whole-cell recordings and 2-3 MΩ for targeted extracellular recordings when filled with the appropriate pipette solution. Recording pipettes were wrapped with Parafilm to reduce capacitive transients. Recordings were made with an EPC-10 dual patch clamp amplifier and Patchmaster software (HEKA Elektronik) running on a Macintosh computer.

Extracellular recordings Targeted extracellular recordings were made to obtain firing properties of cells under control conditions and with receptors for ionotropic $GABA_A$ and glutamate synaptic transmission antagonized with a combination of picrotoxin (100 μM), APV (D-(−)-2-amino-5-phosphonovaleric acid, 20 μM), and CNQX (6-cyano-7-nitroquinoxaline, 10 μM). This method was used as it maintains internal milieu and has minimal impact on the firing rate of neurons[134,135]. Recording pipettes were filled with HEPES-buffered solution containing (in mM): 150 NaCl, 10 HEPES, 10 glucose, 2.5 CaCl2, 1.3 MgCl2, and 3.5 KCl (pH=7.4, 310 mOsm), and low-resistance (22 ± 3 MΩ) seals were formed between the pipette and neuron after first exposing the pipette to the slice tissue in the absence of positive pressure. Recordings were made in voltage-clamp mode with a 0 mV pipette holding potential and signals acquired at 20 kHz and filtered at 10 kHz. Resistance of the loose seal was checked frequently during first 3 min of recordings to ensure a stable baseline, and also before and after a 10-min recording period; data were not use if seal resistance changed >30% or was >25 MΩ. The first 5 min of this 10-min recording were consistently stable among cells and were thus used for analysis of firing rate and burst properties.

Whole-cell recordings For whole-cell patch-clamp recording, two pipette solutions were used. Most recordings were done with a physiologic pipette solution containing (in mM): 135 K gluconate, 10 KCl, 10 HEPES, 5 EGTA, 0.1 $CaCl_2$, 4 MgATP and 0.4 NaGTP, pH 7.2 with NaOH, 305 mOsm. A cesium-based pipette solution, in which cesium gluconate replaced potassium gluconate, was used to reduce potassium currents and allow better isolation of calcium currents. All potentials reported were corrected online for liquid junction potential of -15.7 mV or -15.0 mV for the physiologic or Cs^+-based solution, respectively[136]. For all whole-cell recordings, ACSF contained picrotoxin, APV and CNQX as detailed above.

After achieving a minimum 1.6 GΩ seal and the whole-cell configuration, membrane potential was held at -70 mV between protocols during voltage-clamp recordings. Series resistance (R_s), input resistance (R_{in}), holding current (I_{hold})

and membrane capacitance (C_m) were frequently measured using a 5 mV hyperpolarizing step from -70 mV (mean of 16 repeats, 20 ms duration). Only recordings with R_{in} >500 MΩ, I_{hold} -40 to10 pA and R_S < 20 MΩ, and stable C_m were used for analysis. R_s was further evaluated for stability and any voltage-clamp recordings with ΔR_s >15% before and after the recording protocols were excluded from analysis; current-clamp recordings with ΔR_s >20% were excluded. There was no difference in I_{hold}, C_m, or R_s among any comparisons.

Current-clamp recordings Depolarizing and hyperpolarizing current injections (-50 pA to +50 pA for 500 ms, 5 pA steps) were applied to cells from an initial voltage of -71± 2 mV, close to their resting membrane potential -68.8 ± 1.9 mV[137]. In a small subset of experiments (n=12), the initial voltage was adjusted to -65 mV and -75 mV to test the voltage-dependence of depolarization-induced burst firing patterns. Tetrodotoxin (TTX, 1μM) was used to block action potentials and reveal underlying changes in membrane potential. $NiCl_2$ (100 μM), ZD7288 (50 μM) and 4-AP (5 mM) were applied to test the role of T-type calcium, hyperpolarization-activated mixed cation, and A-type potassium conductances (I_A) in generating bursts, respectively.

Voltage-clamp protocols for I_T ACSF containing antagonists of ionotropic $GABA_A$ and glutamate receptors with TTX (2 μM) and Cs-based internal solution were used for all recordings to isolate calcium-currents. Two voltage protocols were used to isolate I_T. First, total calcium current activation was examined. Inactivation was removed by hyperpolarizing the membrane potential to −110 mV for 350 ms (not shown in Figure 2-4 E). Next a 250 ms prepulse of -110 mV was given. Then membrane potential was varied in 10 mV increments for 250 ms from −110 mV to -30 mV. Finally, test pulse of -40 mV for 250 ms was given. From examination of the current during the test pulse, it was evident that no sustained (high-voltage activated) calcium current was activated at potentials more hyperpolarized than -40 mV. To remove HVA contamination from the step to -30 mV, a second protocol was used in which removal of inactivation (-110 mV, 350 ms) was followed by a 250 ms prepulse at -40 mV, then a step for 250 ms at -30 mV and finally a test pulse of -40 mV for 250 ms. I_T was isolated by

subtracting the trace following the -40 mV prepulse from those obtained after the -110 mV prepulse for the depolarized variable step to -30 mV; raw traces from the initial voltage protocol were used without subtraction for variable steps from -110 mV to -40 mV because of the lack of observed activation of HVA at these potentials. Activation of I_T was assessed from the resulting family of traces by peak current during the variable step phase. Inactivation of I_T was assessed from the peak current during the final -40 mV test pulse. For a subset of recordings (n=3 cells), $NiCl_2$ (100 μM) was used to block current generated to confirm it was I_T.

Voltage-clamp ramp protocols for I_{NaP}. Physiologic pipette solution was used for voltage-clamp ramp recordings. A voltage ramp from -80 mV to -20 mV at 10 mV/s was used under control conditions and following TTX (2 μM) application to characterize the voltage-dependence and magnitude of persistent TTX-sensitive sodium current, I_{NaP}. To test the relative role of I_{NaP} and I_A in cells that did not show rebound firing, current during the ramp was quantified under control conditions, then following I_A block with 4-AP (5 mM), followed by subsequent addition of TTX (2 μM).

Data Analysis. Data were analyzed offline using custom software written in IgorPro 6.31 (Wavemetrics) or MATLAB 8.4 (MathWorks, Inc.). For targeted extracellular recordings, mean firing rate in Hz was determined over 5 min of stable recording. Parameters for identification of bursts were chosen based on distributions of interspike intervals and were confirmed by measuring interspike interval of bursts that were identified manually using other criteria (upshift of baseline and progressive decrease of amplitude). Spikes were considered to form a burst if the interspike intervals were <105 ms. Spikes detected after an interval greater than 105 ms were considered to be the start of a new burst or single spike. Bursts were automatically detected and confirmed by eye with false-positive detection errors manually corrected[68].

Action potential parameters were quantified for the first action potential evoked in a firing train with minimal current injection (rheobase) from -70mV. First spike latency was the time from onset of current injection to the peak of first spike.

Rate of rise was the maximal slope (dV_m/dt) during the rising phase of the action potential. Action potential threshold was defined as the membrane potential at which the derivative exceeded 2 V/sec [138]. Full-width half maximum (FWHM) was the width of the spike at half-maximal spike amplitude from threshold. Afterhyperpolarization (AHP) amplitude was the difference between threshold and the most hyperpolarized potential after the spike. AHP time was the delay from threshold to the peak (most hyperpolarized) potential of the AHP.

In experiments examining I_T, the peak current amplitude at each step potential (V) was first converted to conductance using the calculated reversal potential of Ca^{2+} (E_{Ca}) and $G=I/(E_{Ca} - V)$, because driving force was linear over the range of voltages examined. The voltage dependencies of activation and steady-state inactivation were described with a single Boltzmann distribution: $G(V)= G_{max}/(1-\exp[(V_{1/2} - V_t)/k])$, where G_{max} is the maximal conductance, $V_{1/2}$ is the half-maximal voltage, and k is the voltage dependence (slope) of the distribution. Current density of I_T at each tested membrane potential was determined by dividing peak current by membrane capacitance.

To quantify the current density of I_{NaP}, 5 sweeps of the current induced by the ramp protocol were averaged and smoothed with a 10-point boxcar filter. A linear fit from -78mV to -70mV was made to correct the leak current for each trace. TTX-sensitive sodium current was obtained by subtracting the averaged trace recorded under TTX from that under control conditions[139]. The magnitude of I_{NaP} was measured at membrane potentials from -70 mV to -40 mV at 2.5 mV intervals. Current density as a function of membrane potential was calculated by dividing I_{NaP} determined at these intervals by membrane capacitance.

Statistics Data were analyzed using Prism 6 (GraphPad Software) and reported as mean ± SEM. The number of cells per group is indicated by n. Data were normally distributed and thus comparisons among groups were made by one-way ANOVA with Bonferroni *post hoc* analysis or two-way ANOVA with Bonferroni *post hoc* analysis. For repeated measurements, two-way repeated-measures (RM) ANOVA with Holm-Sidak *post hoc* analysis was used. For paired data, two-tailed paired Student's t test was used. For categorical data analysis,

Chi-square test of independence or Fisher's exact test of independence were used to test the null hypothesis that categorical variables have no correlation with each other. F-test was used to test the null hypothesis that the standard deviation for groups is equal. Linear regression was used to test the null hypothesis that slope is zero, and to measure the strength of the association (coefficient of determination, r^2) between two variables. The null hypothesis was rejected if $p<0.05$. $F_{DFn,DFd}$ values from one-way ANOVA, two-way ANOVA or two-way repeated-measures (RM) ANOVA are reported in Tables 2-1 to 2-3.

Results

AVPV kisspeptin neurons exhibit higher spontaneous firing rates and more burst firing on proestrus than diestrus.

Firing activity of GFP-identified kisspeptin neurons within the AVPV was monitored using targeted extracellular recordings in acutely-prepared brain slices. All cells studied were spontaneously active during the 5-min observation period under both control conditions and after blocking ionotropic $GABA_A$ and glutamate receptors. Figures 2-1A and B show representative firing patterns from each group. Figure 2-1C shows the average firing frequency of AVPV kisspeptin neurons on diestrus (di, representing negative feedback) and proestrus (pro, representing positive feedback) under control conditions (di, n=12; pro, n=11) or during antagonism of ionotropic receptors conveying GABAergic and glutamatergic fast synaptic transmission (di, n=12; pro, n=11). Consistent with a potential role in relaying estradiol positive feedback, the spontaneous firing rate of AVPV kisspeptin neurons was greater on the afternoon of proestrus than diestrus (Figure2-1C, two-way ANOVA/Bonferroni, $p<0.0001$). Antagonism of fast synaptic transmission via NMDA, AMPA, and $GABA_A$ receptors did not alter firing rate during either cycle stage ($p>0.9$). The cycle-dependent difference in firing frequency was maintained after blocking ionotropic receptors ($p=0.0019$).

Extracellular recordings were also used to evaluate burst vs. single spike firing. Bursts were defined as action potentials occurring within 105 ms of each other with progressively decreased amplitude and an upshift of baseline (black lines above traces, Figure 2-1B). AVPV kisspeptin neurons exhibit spontaneous burst firing during both diestrus (n=12) and proestrus (n=11), but the number of the burst events per 5 min was higher on proestrus (Figure 2-1D, two-way ANOVA/Bonferroni, p=0.005). The number of the burst events per 5 min was decreased on proestrus in the presence of ionotropic glutamate and $GABA_A$ receptor antagonists (di, n=14, pro, n=13, p=0.02) but was not changed on diestrus (p=0.14). Although it appears that the increase in number of bursts in 5 minutes on proestrus compared to diestrus was maintained when ionotropic receptors were blocked, the p-value was just short of that accepted for significance (Figure 2-1D, p=0.06).

We next analyzed the numbers of spikes per burst as a function of cycle stage (Figure 2-1E, two-way RM ANOVA/Holm-Sidak control, di, n=12, pro n=11; receptor antagonist, di=14, pro=13). Under control conditions, there were more bursts consisting of two spikes on proestrus than diestrus (p<0.0001). After blocking of ionotropic glutamate and $GABA_A$ receptors, the number of two-spike bursts was decreased on both cycle stages (di, p=0.01, pro, p<0.0001), but was still higher on proestrus than diestrus (p=0.005). No difference in number of bursts with ≥3 spikes was detected between cycle stages either with or without ionotropic receptor antagonists. Following addition of the receptor antagonists, however, no cell studied during diestrus (n=13) fired bursts with >2 spikes. This is in contrast to control conditions, under which 7 of 12 cells studied on diestrus firing bursts of ≥ 3 spikes. Cells studied on proestrus, in contrast, fired bursts with ≥3 spikes under control conditions as well as when ionotropic receptors were blocked. These observations suggest both intrinsic properties and fast synaptic transmission likely contribute to burst firing in AVPV kisspeptin neurons and that the relative contributions may change with cycle stage. We thus focused our remaining studies on intrinsic properties of these neurons.

Depolarization induces two firing patterns: tonic firing and depolarization-induced bursts (DIB).

To begin to understand the contributions of the intrinsic properties of AVPV kisspeptin neurons to burst firing, we performed whole-cell current-clamp recordings on brain slices in the presence of APV, CNQX and picrotoxin to antagonize effects attributable to activation of ionotropic glutamate and $GABA_A$ receptors. AVPV kisspeptin neurons exhibited two distinct firing patterns in response to similar magnitude depolarizing steady-state current injection (25 ± 5 pA, 0.5 s) initiated from -70 ± 2 mV. Representative examples under control conditions are shown in Figure 2-2A. Tonic firing was defined as a steady firing rate with a consistent instantaneous frequency (overall IF 22 ± 1 Hz, initial IF 29 ± 2 Hz vs. final IF 18 ± 1 Hz, paired t-test $p<0.0001$, standard deviation of IF 4 ± 1 Hz, n=25). Depolarization-induced bursting (DIB) cells exhibited an initial burst containing 3-4 spikes followed by mild frequency accommodation (overall IF 73 ± 3 Hz, initial IF 113 ± 4 Hz vs. final IF 13 ± 1 Hz, paired t-test initial vs. final $p<0.0001$; standard deviation of IF, 36 ± 2 Hz, n=16, F-test, tonic vs. DIB standard deviation, $p<0.0001$). Tonic and DIB firing patterns were observed to a similar extent on both cycle stages studied (tonic vs. DIB, di 64% vs. 36%, n=19; pro 59% vs. 41%, n=22, Fisher's exact test, $p>0.9$). We averaged instantaneous firing frequency of each cell type on each cycle stage and plotted this as a function of spike interval number (Figure 2-2 B, tonic, di, n=12; pro, n=13; DIB, di, n=7; pro, n=9). The initial IF of DIB cells was 4-fold larger than that in tonic cells on both cycle stages (Figure 2-2B, two-way RM ANOVA/Holm-Sidak, di, $p<0.0001$; pro, $p<0.0001$). The frequency plots did not show any difference between cycle stages in tonic or DIB cells ($p>0.1$).

We next examined action potential properties of tonic and DIB cells. In Figure 2-3A, the first action potential evoked by the minimum necessary depolarizing current injection is shown in tonic and DIB cells on diestrus (left) and proestrus (right). We measured and compared several action potential parameters between

cycle stages and cell types (tonic, di, n=12; pro, n=13; DIB, di, n=7; pro, n=9). As summarized in Figure 2-3 B-G, action potential threshold, amplitude and timing of the afterhyperpolarization potential (AHP) showed a cell firing-type-dependent but not cycle-dependent change (two-way ANOVA/Bonferroni, all post-hoc $p<0.001$). First spike latency, rate of rise, and full-width half-maximum (FWHM) of the action potential did not change among groups ($p>0.1$ for all post-hoc tests). The minimal necessary current injection (rheobase) itself was not different between cycle stages or cell types (di, tonic, 9.6 ± 1.0 pA, DIB 13.3 ± 2.2 pA; pro, tonic 10.8 ± 0.8 pA, DIB, 10.1 ± 1.1 pA; two-way ANOVA/Bonferroni, $p>0.1$ for all comparisons).

There was no difference in input resistance (R_{in}) of tonic firing cells on diestrus vs. proestrus (Figure 2-2C, two-way ANOVA/Bonferroni, p=0.47; di, n=12, pro, n=13), but R_{in} of DIB cells was greater on proestrus than diestrus (di, n=7, pro, n=9; p=0.04). Within a cycle stage, there was no firing pattern-dependent (tonic vs. DIB) difference in R_{in} (di, p=0.91; pro, p=0.22). The membrane capacitance was not different among groups (data not shown, $p>0.9$). When grouped by cycle stage, cells recorded on proestrus had a greater R_{in} compared to those recorded on diestrus (di, n=15, pro, n=15; p=0.01). This cycle-dependent difference in R_{in} was eliminated in recordings using a cesium-based pipette solution (Figure 2-2D, n=11 each, p=0.88). Because R_{in} exhibited a cycle-dependent difference between diestrus and proestrus, and only DIB cells showed a cycle-dependent difference, it is likely DIB cells contribute the difference in R_{in} under control conditions. The elimination of a difference in R_{in} with Cs^+ internal suggests a Cs^+-sensitive potassium conductance under estrous cycle regulation may contribute to the difference in R_{in}.

Termination of hyperpolarization: rebound bursts and their relationship to the firing pattern during depolarization.

In addition to depolarization-induced firing, many neurons exhibit firing upon termination of a hyperpolarizing stimulus[140,141]. We tested if AVPV kisspeptin

neurons exhibit so-called rebound bursts. Cells were injected with hyperpolarizing current to achieve a membrane potential of -105 ± 3 mV. After termination of hyperpolarization, most AVPV kisspeptin neurons exhibited rebound bursts (≥2 spikes), whereas the rest showed either single rebound spikes or no rebound as indicated in the representative examples in Figure 2-2A (control). The type of rebound events (bursts, single spike, or no spike) differed with cycle stage (Figure 2-2E, right, di, n=19, pro, n=22; Chi-square, $p<0.001$).

We next examined if there was a relationship between the observed firing patterns during depolarization and the rebound patterns following termination of hyperpolarization. Most cells (di, 8 of 12; pro, 10 of 13) that fired tonically upon depolarization had rebound bursts. The remaining cells studied on proestrus (3 of 13) fired a single spike rebound whereas most other cells studied on diestrus showed no rebound (3 of 12) and one cell showed single spike rebound. This distribution did not differ with cycle stage (Figure 2-2E, left, Chi-square, $p=0.1$). Strikingly, cells that fired DIB patterns only had rebound bursts on proestrus (Figure 2-2E, middle, di, n=7, pro, n=10).

We focused on rebound bursts (≥2 spikes) as they are more likely than single rebound spikes to achieve sufficient change in intracellular Ca^{2+} to influence neurosecretion and thus postsynaptic events[142]. We characterized rebound bursts by measuring the initial IF (between spikes 1 and 2) and overall frequency of rebound bursts (the number of spikes divided by the duration from the termination of hyperpolarization to the peak of the last rebound spike in the bursts). The initial IF and overall frequency of bursts in tonic and DIB cells showed a firing-pattern-dependent difference (Figure 2-2F, initial IF, tonic, di, n=8, pro, n=10; DIB, di, n=7; pro, n=9; Figure 2-2G, overall freq, tonic, di, n=9, pro=13; DIB, di, n=7, pro, n=9, two-way ANOVA/Bonferroni). On proestrus, initial IF and overall frequency was higher in DIB cells than tonic cells (IF, $p<0.0001$; overall, $p=0.03$). There was no cycle-dependent change of rebound burst frequency in tonic cells (both initial and overall, $p>0.9$), markedly different from

DIB cells, which did not exhibit rebound bursts on diestrus. Our observations thus indicate that DIB and tonic cells show different responses to the termination of hyperpolarization. The different firing signatures may be linked to differences in specific ionic currents.

Estrous cycle regulation of T-type calcium current properties and its role in depolarization and rebound firing patterns.

The observation that cells with different depolarization-induced firing patterns could exhibit different rebound patterns based on cycle stage led us to examine potential underlying mechanisms in greater detail. We first tested the membrane response to termination of hyperpolarization in the absence (to assess initial IF) and presence of TTX to assess the depolarizing membrane response (Figure 2-4A). After TTX application, marked membrane depolarization, often attributable to activation of T-type calcium channels[143,144], was observed following the termination of hyperpolarization in cells that fired rebound bursts but not in cells firing either single or no rebound spikes. This was not dependent on cycle stage but rather on pre TTX rebound profile. Figure 2-4B shows the correlation between rebound IF and amplitude of the depolarization. Rebound IF was positively correlated with rebound depolarization amplitude for tonic cells on both diestrus and proestrus (Figure 2-4B, di, r^2=0.47, p=0.045, n=9; pro, r^2=0.84, p=0.004, n=9). In contrast, there was no correlation between these properties for DIB cells on proestrus (n=7, r^2<0.001, p=0.98).

The above observations suggest that in addition to possible differences in currents driving action potential properties (Figure 2-3D, F, G), other ionic currents might contribute to the difference between tonic firing and DIB cells. In other neuron types, the amplitude of rebound depolarization directly correlates with the size of transient Ca^{2+} currents[143,144]. We tested the effect of Ni^{2+} (100 μM, a dose that is fairly specific for T-type channels[145]) on depolarization-induced firing patterns and hyperpolarization-induced rebound bursts. Ni^{2+} decreased the initial IF of the depolarization-induced bursts to roughly half (Figure 2-2A,

summary data Figure 2-4G, n=8, paired t-test, p=0.0002). The initial IF after Ni^{2+} application was still higher in DIB cells than that in tonic cells under control (no Ni^{2+}) conditions (p=0.006). The initial IF of tonic cells also decreased after Ni^{2+} application (Figure 2-4G, n=11, paired t-test, p=0.049), but to a lesser extent (decreased 19 ± 7% in tonic vs. 54 ± 6% in DIB cells, Student's t-test, p=0.001). Since T-type channels are voltage-dependent, we altered the initial membrane potential to -65, -70 or -75 mV, and then applied current injection of 25 ± 5 pA to depolarize the membrane to generate n ± 2 action potential spikes (n, action potential numbers generated at -70mV, with 25 ± 5 pA current injection, Figure 2-4C). The IF of DIB cells was decreased as initial membrane potential was depolarized from -75 to -70 to -65 mV (Figure 2-4D, tonic, n=5, DIB n=6, two-way RM ANOVA/Holm-Sidak, all post-hoc in DIB, p<0.0001). No change in IF of tonic cells was observed (p>0.1). Rebound bursts were eliminated after Ni^{2+} application in majority of cells recorded on both cycle stages (di, 7 out of 8; pro, 6 out of 7). The rebound bursts that Ni^{2+} did not block were reduced from 3-4 spikes per bursts to a single spike. Together these observations suggest a substantial role for Ni^{2+}-sensitive currents, perhaps I_T, in both depolarization-induced and rebound firing patterns.

Persistence of single rebound spikes could be attributable to 100 μM Ni^{2+} not being sufficient to block all channels carrying I_T. Alternatively, but not exclusively, other channels might affect the occurrence of the rebound bursts. We first measured T-type current properties in AVPV kisspeptin neurons. To facilitate the isolation of I_T, a Cs^+-based pipette solution was used to reduce potassium conductances and TTX was bath-applied to block fast voltage-dependent sodium channels. All cells recorded on diestrus and proestrus exhibited I_T based on voltage dependence of the observed current. Figure 2-4E shows the representative whole-cell voltage-clamp traces of I_T triggered by the voltage protocol described in the materials and methods. Application of 100 μM Ni^{2+} blocked a majority of the current (73.1 ± 0.4%, n=4) evoked at test pulse of -40

mV from -110 mV (Figure 2-4F). This suggests the currents observed are I_T and that most, but not all, of the current is sensitive to 100 μM Ni^{2+}.

The conductance-voltage relationship was fit with a Boltzmann function. Neither the slope factor k nor the voltage-dependence of activation or inactivation were different between cycle stages (Figure 2-4H, n=11 each, activation, $V_{1/2}$, di, -54.5 ± 1.3 mV, pro -53.5± 1.3mV, p=0.59, slope factor k, di, 5.1 ± 0.4, pro 5.5 ± 0.4, p=0.59; inactivation, n=12 each, $V_{1/2}$, di, -66.4 ± 1.6 mV, pro -67.6± 1.5mV, p=0.56, slope factor k, di, -3.2 ± 0.1, pro 3.0 ± 0.1, p=0.11, Student's t-test). The current density, however, was greater on proestrus than diestrus at membrane potentials between -50 mV and -30 mV (Figure 2-4I, n=11, two-way RM ANOVA/Holm-Sidak, p<0.01). The change in current density was not attributable to a difference in either membrane capacitance or series resistance between groups.

Other voltage-dependent currents modifying rebound bursts: persistent sodium current (I_{NaP}) and A-type potassium current (I_A).

The generation of rebound bursts can be a complex interplay of multiple channel types that pass currents in inward and outward directions. Since rebound firing is Ni^{2+}-sensitive, I_T likely plays a dominant role in generating rebound bursts. The lower likelihood of firing rebound bursts on diestrus vs. proestrus may be attributable to estrous cycle regulation of other currents that either facilitate or inhibit rebound burst generation. One candidate for a facilitating current is the persistent sodium current, I_{NaP}, as it activates at membrane potentials in the subthreshold range.

We characterized I_{NaP} in AVPV kisspeptin neurons on diestrus and proestrus using slow (10 mV/s) voltage ramps from -80 to -20 mV (Figure 2-5A, top). Ramp-induced current was linear from -80 mV to approximately -65 mV (Figure 2-5A, bottom). At membrane potentials more depolarized than -65 mV, we observed a persistent inward current that peaked near -40 mV. This current was

blocked by TTX, suggesting the net current is I_{NaP} (Figure 2-5B). The current density of I_{NaP} was higher on proestrus than diestrus from -55 to -47.5 mV (Figure 2-5C, D, n=12 each, two-way RM ANOVA/Holm-Sidak, -55 mV, p=0.057, -52.5 mV, p=0.002, -50 mV, p=0.01, -47.5 mV, p=0.045).

Because I_{NaP} appears to be regulated by the estrous cycle, we tested if it facilitates rebound burst generation. We divided cells on diestrus into those exhibiting rebound bursts (≥ 2 spikes) vs. those not exhibiting any rebound spikes, and compared I_{NaP} current density of these two groups with that of cells on proestrus (all of which had rebound bursts with ≥2 spikes). Figure 2-5C shows a representative I_{NaP} for each group, and Figure 2-5E shows the quantitative current density comparison among groups. I_{NaP} current density was lower in cells on diestrus that do not fire rebound bursts (n=11) than in those that fire rebound bursts (n=9) at membrane potentials between -52.5 and -42.5 mV (two-way RM ANOVA/Holm-Sidak, $p<0.05$). I_{NaP} current density between cells exhibiting rebound bursts on diestrus (n=9) and proestrus (n=11) was not different ($p>0.6$). This suggests that cells that do not fire rebound spikes likely account for the lower I_{NaP} current density on diestrus vs. proestrus.

We also considered the possibility that an outward current counteracts inward current from I_{NaP} and I_T to decrease the burst occurrence on diestrus. Because Cs^+-sensitive potassium channels likely contribute to the decreased R_{in} on diestrus vs. proestrus, we hypothesized potassium currents may contribute to silencing of bursts on diestrus for both tonic and DIB cells. In particular we examined the 4-AP-sensitive A-type potassium current (I_A) because it can be activated at relatively hyperpolarized potentials and is thus more likely to play a role in modifying spike initiation [138,146,147]. We performed current-clamp recordings to identify the tonic or DIB cells that did not exhibit rebound spikes on diestrus, then treated these cells with 4-AP (5 mM). Of the 12 cells we tested, five exhibited rebound during 4-AP treatment (four cells had one rebound spike and one cell had a 2-spike burst) (Figure 2-6B, right). These were referred to as

4-AP-sensitive cells. The remaining seven cells did not initiate spikes upon rebound following 4-AP treatment (4-AP-insensitive). Figure 2-6A shows the representative tonic and DIB cells that were 4-AP-sensitive (left) and insensitive (right). Figure 2-6B shows that half of the tonic cells (left, n=6) and one third of DIB cells (middle, n=6) were 4-AP sensitive. We then compared I_{NaP} in cells that were 4-AP sensitive (n=5) and insensitive (n=7) and found that current density was greater in 4-AP-sensitive group (Figure 2-6C, D, two-way RM ANOVA/Holm-Sidak, -47.5mV, p=0.04; -45mV,p=0.02). R_{in} of the tested cells increased after 4-AP treatment, consistent with the above change when Cs^+-based pipette solution was used (paired t-test, n=11, control vs. 4-AP, 858 ± 72 vs. 1044 ± 98 MΩ, p=0.005). This suggests that for a subset of neurons, potassium channels may play an active role to prevent burst generation that may be independent from the regulation of I_{NaP} and I_T.

Some AVPV kisspeptin neurons are known to express hyperpolarization-activated non-selective cation channels (HCN) and exhibit a sag in membrane potential during current-clamp typical of cells exhibiting I_h[125]. We observed that after achieving a hyperpolarized membrane potential of -105 ± 3 mV, 70% of AVPV kisspeptin neurons showed sag potential (> 2 mV) on diestrus (n=29, 3.8 ± 0.5 mV) and 95% on proestrus (n=20, 7.3 ± 0.7 mV). Our results confirmed that sag potential is cycle-dependent (Figure 2-6F, Student's t-test, p=0.0002). To examine the role of I_h in generating rebound bursts, we blocked HCN channels using ZD7288 (50 μM, Figure 2-6E). This eliminated the sag potential but did not affect the number of spikes per rebound burst for cells tested on either stage (di, n=5; pro, n=4), consistent with previous findings[126]. This suggests that although I_h is regulated by the estrous cycle, it may play a little or no role in generating rebound bursts under our experimental conditions.

Estrous cycle regulation of burst properties is attributable to circulating estradiol, not progesterone.

The cycle-dependent changes in burst properties observed above are most likely attributed to estrous-cycle dependent changes in circulating levels of ovarian sex steroids, in particular estradiol and/or progesterone. To determine the role of specific gonadal steroids in these biophysical properties, we set up four groups of mice: OVX, OVX+E, OVX+E+P, and OVX+E+V to rule out the potential effects induced by injection-associated stress in OVX+E+P mice. OVX+P alone was not tested as a single-cell real-time PCR scan[148] of AVPV kisspeptin neurons harvested from OVX mice indicated only 2 of 10 of these cells expressed the estrogen-dependent progesterone receptor 3 days after ovariectomy, vs 7 of 9 cells in OVX+E from OVX+E mice (not shown).

Short-term firing patterns of AVPV kisspeptin neurons were monitored (as in Figure 1) in all four groups (OVX, OVX+E, OVX+E+V, OVX+E+P) via extracellular recordings with AMPA, NMDA, and $GABA_A$ receptors antagonized. There were no differences in firing rate or bursts between OVX+E and OVX+E+V mice when we compared all four groups (one-way ANOVA/Bonferroni, $p>0.99$), indicating that injection alone causes no detectable change in firing properties in AVPV kisspeptin neurons. OVX+E and OVX+E+V cells were thus combined for burst analyses and are reported as OVX+E in Figure 2-7B, C; vehicle-treated animals were not included in further studies. Firing frequency in OVX+E, OVX+E+P was increased compared to OVX ($p<0.0001$, $p<0.02$, respectively), whereas no difference was observed between OVX+E+P vs. OVX+E (Figure 2-7A, B one-way ANOVA/Bonferroni). Spontaneous bursting events were increased in cell from OVX+E vs. OVX mice (Figure 2-7C one-way ANOVA/Bonferroni, $p=0.04$). Number of bursts in cells from OVX+E+P mice was intermediate to and not different from either that in cells from OVX and OVX+E mice. These observations suggest estradiol alters the firing frequency and pattern of AVPV kisspeptin neurons, and that addition of progesterone does not appear to further shift these parameters.

To examine steroid effects on action potential properties, whole-cell recordings were used to capture the firing signature of AVPV kisspeptin neurons in OVX, OVX+E and OVX+E+P groups in response to depolarization and removal of hyperpolarization (Figure 2-7E). Most cells in from OVX+E mice (64%, n= 7 of 11) and OVX+E+P mice (67%, 6 of 9) exhibit depolarization-induced bursts (DIB). In contrast, DIB was not observed in cells from OVX mice and all cells from these mice fired in a tonic manner upon depolarization (Figure 2-7D, n=10, Chi-square, p=0.003). In response to the removal of hyperpolarization, more cells fire rebound bursts in OVX+E and OVX+E+P groups than OVX group: only 30% of OVX cells (3 of 10) fire rebound bursts, whereas ~90% OVX+E (10 of 11) and OVX+E+P (8 of 9) cells fire rebound bursts (Chi-square p=0.003). The number of spikes in rebound bursts was increased in cells from OVX+E (4.7 ± 0.9, n=11) compared to OVX (0.9 ± 0.3, n=10, one-way ANOVA/Bonferroni OVX vs OVX+E p=0.0007). This parameter had an intermediate value in cells from OVX+E+P mice (2.9 ± 0.5, n=9). The latency to the first spike was decreased in cells from OVX+E vs OVX mice (p=0.02); again this parameter had an intermediate value in cells from OVX+E+P mice (Figure 2-7F). FWHM, and afterhyperpolarization (AHP) amplitude was increased in cells from both OVX+E and OVX+E+P mice compared to observed in OVX mice (Figure 2-7G, H, see Table 2-3).

We also examined effects of estradiol on modulation of I_T and I_{NaP} as detailed above. Estradiol increased I_T current density (Figure 2-8A, C, OVX, n=10, OVX+E n=10, two-way RM ANOVA/Holm-Sidak, -50mV p=0.04; -40mV p<0.001; -30mV p<0.001) as well as I_{NaP} current density (Figure 2-8D, E, OVX=10, OVX+E=11, two-way RM ANOVA/Holm-Sidak, -50mV p=0.02; -45mV p=0.01; -40mV p=0.01). Similar to the lack of change in voltage-dependent activation and inactivation of I_T between diestrous and proestrous phases of the estrous cycle, estradiol did not affect these parameters (Figure 2-8B n=10 each, activation, $V_{1/2}$, OVX, -55.3 ± 1.2, OVX+E, -54.0 ± 1.0, p=0.41, slope factor k, OVX, 5.6 ± 0.5, OVX+E, 5.3 ± 0.4, p=0.51; inactivation, n=10 each, $V_{1/2}$, OVX, -66.3 ± 1.3, OVX+E, -69.1 ± 1.5,

p=0.09, slope factor k, OVX, -3.3 ± 0.2, OVX+E, -3.3 ± 0.2 p=0.80, Student's t-test). The sag potential, which represent the activation of HCN channel at hyperpolarized potential, was increased in cells in OVX+E and OVX+E+P groups compared to that observed in the OVX group (Figure 2-8F one-way ANOVA/Bonferroni, OVX+E vs OVX and OVX+E+P vs OVX, $p<0.0001$). These observations suggest most cycle-dependent effects on AVPV kisspeptin neuron firing and associated currents are attributable to estradiol.

Discussion

Steroid milieu and other cues are integrated to generate a GnRH release pattern as the central signal controlling fertility. In most vertebrates, estradiol positive feedback induces a surge of GnRH release crucial for ovulation[14,116]. GnRH neurons receive estradiol feedback mainly via steroid-sensitive afferents including AVPV kisspeptin neurons[149]. We demonstrated AVPV kisspeptin neurons increase overall and burst firing rate on proestrus vs. diestrus, and revealed the estrous cycle regulates interactions of multiple conductances contributing to burst generation primarily via cycle-dependent changes in circulating estradiol levels (Figure 2-9).

Burst firing is implicated in increasing reliability of neural information processing, synaptic plasticity, and neuropeptide/neuroendocrine secretion[53,150]. For the latter, increased cytoplasmic calcium induced by bursts may enhance dense core vesicle fusion with the plasma membrane[151,152]. Shifts towards increased AVPV kisspeptin neuron firing frequency and burst events may thus indicate increased neurosecretion.

The increased activity of AVPV kisspeptin neurons from proestrous and OVX+E mice is consistent with elevated cFos expression in this cell population during the preovulatory or estradiol-induced LH surge[112,122]. Of note, other studies found no cycle-dependent shift in the spontaneous firing rate of AVPV kisspeptin neurons,

with reports of trends towards either increased or decreased activity on proestrus[153–155]. This contrast may in part be attributable to methodological differences including slice thickness, recording duration and time-of-day of experiment. Activity of the reproductive neuroendocrine circuitry, particularly that involved in estradiol positive feedback, is regulated by time of day[116]. Slices in the present study were prepared at Zeitgeber time (ZT) 10-11, at the peak of the reported increase in expression of cFos in AVPV kisspeptin neurons in OVX+E mice (ZT9-12)[113,156], whereas previous studies were conducted from ZT4-6. Notably, firing frequency of AVPV kisspeptin neurons in the present study increased by ~20-30% after an 8-10 min stable recording, limiting confidence in analysis of longer-term firing patterns. Of note, we did not observe quiesecen cells in our extracellular recordings, suggesting AVPV kisspeptin neurons keep a certain firing pace during diesturs, when negative feedback is dominent.
Burst firing may be attributable to intrinsic mechanisms and/or synaptic inputs. AVPV kisspeptin neurons receive glutamate and GABA synaptic inputs[157], the latter of which is known to be regulated by both time of day and estradiol[137]. Blocking fast synaptic transmission reduced but did not eliminate burst firing in the present study, suggesting intrinsic mechanisms contribute to bursts. Although a role for other transmitters/peptides in AVPV kisspeptin neuron burst generation cannot be eliminated, we focused on the intrinsic ionic conductances underlying firing and burst generation.

AVPV kisspeptin neurons were classified as tonic or DIB neurons based on depolarization-evoked firing patterns from their resting membrane potential. Both tonic and DIB cells exhibited rebound bursts induced by hyperpolarization termination. The percentage of cells exhibiting DIB and rebound bursts was increased by estradiol (OVX vs OVX+E), with rebound bursts also increasing on proestrus vs. diestrus. This increase in elicited bursts agreed with increased spontaneous firing during both experimentally-induced or cycle-dependent elevation of estradiol. Together, these studies suggest depolarization and release from hyperpolarization as two possible mechanisms for generating spontaneous

bursts observed in extracellular recordings. DIB was not observed in the absence of estradiol, indicating a critical role for this steroid in generating closely spaced spikes upon depolarization. Of interest, the percentage of cells that fire DIB (~70%) is similar to that expressing ERα[87,121]. Our results add new, functional parameters to classify AVPV kisspeptin neurons. Future studies will focus on combining the electrophysiological properties with molecular signatures to uncover specific roles each cellular subtype may perform.

The distinct action potential signatures of tonic and DIB patterns suggest that they may have different channel types contributing to action potential firing [158]. We next began to decipher the ionic conductances underlying firing properties in tonic and DIB cells. The presence of currents at sub-threshold membrane potentials can enhance or retard spike generation to influence the overall firing patterns in many brain regions[58,138,139,159,160] including AVPV kisspeptin neurons[126,127]. In the present studies, the sensitivity of depolarization-induced bursting to Ni^{2+} and initial membrane potential further suggests this firing pattern may arise from conductances that are voltage-dependent and/or Ni^{2+}-sensitive. Rebound bursts were also Ni^{2+}-sensitive. Further, the positive correlation between rebound depolarization when firing was blocked and instantaneous frequency of rebound bursts further suggests I_T may also be important to rebound burst generation. Of note, no such correlation was observed in DIB cells; this may be attribute to a higher potassium conductance near the baseline potential opposing the action of I_T.

Because Ni^{2+} is not a complete or exclusive blocker of I_T and it is difficult to attribute the role of a specific conductance to observations in current-clamp recordings, voltage-clamp was used to isolate I_T. The increased current density on proestrus and in cells from OVX+E mice in the absence of shifts in voltage-dependence suggests that increased channels in the membrane may contribute to increased bursting. Interestingly, the current density differed at physiologically-relevant membrane potentials critical for spike generation. Questions remain if

tonic and DIB cells have distinct I_T current density because firing properties are difficult to quantify with the Cs^+-based pipette solution used to quantify I_T. However, we did not see the voltage-dependence differ between OVX (all tonic) vs OVX+E (70% DIB), suggesting these parameters may be less likely to contribute to the different burst patterns.

Interestingly, all the cells tested on diestrus exhibited I_T, raising the question why only half of these cells exhibit rebound bursts. The latter may be attributable to a decreased depolarizing conductance and/or an increased hyperpolarizing conductance in cells without rebound bursts. We targeted I_{NaP} and I_A to test this postulate because of their activation at subthreshold membrane potentials. We found both of these currents may sculpt burst firing in AVPV kisspeptin neurons. Cells that did not fire rebound bursts had decreased I_{NaP} relative to cells that fired rebound bursts in diestrous mice. Furthermore, blocking I_A permitted rebound spikes in half of the cells recorded on diestrus regardless of their depolarization-evoked firing pattern. Interestingly, I_{NaP} was also different between 4-AP sensitive vs. insensitive cells near action potential threshold, suggesting the possibility that a smaller I_{NaP} makes restoration of bursts by blocking I_A less likely. The lack of specific I_{NaP} blockers precludes parsing its role vs. that of I_T in generating rebound bursts, but its upregulation upon specific manipulation of estradiol suggests this steroid plays a role in the cycle-dependent changes observed.

These observations are consistent with the increasing understanding through experimental and computational studies that different interactions among ionic conductances can generate the same firing properties in many neurons across species[159,161]. Neurons can achieve similar firing output by adding, deleting or modulating different conductances[162,163]. In AVPV kisspeptin neurons, the present results indicate bursts can be generated via depolarization or release of hyperpolarization, both of which may recruit multiple ionic conductances. Bursts may be triggered and facilitated by increased I_T, I_{NaP} or decreased I_A; and they may be silenced or reduced (number of events, frequency) with a combination of

decreased I_T, I_{NaP} and increased I_A. In a cell type likely critical to reproduction, the ability to produce the appropriate output via a variety of scenarios is pertinent to survival of the species.

Another question is which cycle-dependent cues are responsible for regulation of multiple ionic conductances. In the present study, we recorded at a consistent time of day to control the diurnal input to AVPV kisspeptin neurons. One prominent difference between cycle stages is sex steroid milieu, especially estradiol, which regulates kisspeptin mRNA and cFos expression[122]. Specific steroid manipulations suggest a dominant role for estradiol in increased current density of I_T, I_h and I_{NaP}, adding strong mechanistic support for estradiol regulation of AVPV kisspeptin neuron firing[121]. Estradiol may act through genomic mechanisms to change ion channel expression or function, or via membrane-associated mechanisms to effect posttranslational modifications of ion channels or insertion into the membrane[164,165]. Recently, a genetic tracing approach suggested only AVPV kisspeptin neurons expressing ERα synapse on GnRH neurons[121], further supporting the postulate of an estradiol-kisspeptin-GnRH feedback loop.

In summary, our findings demonstrate that increased firing rate and burst events in AVPV kisspeptin neurons on proestrus vs. diestrus likely result from cycle-dependent changes in estradiol modifying multiple conductances. Burst generation may be attributed to the interplay of intrinsic properties with both excitatory input and release from inhibition. Our results support previous observations and extend these by focusing on regulation of the interactions among intrinsic properties in generating the electrophysiological output of AVPV kisspeptin neurons. The changes in this output associated with the shift between estradiol negative and positive feedback actions likely play an important role in female fertility.

Figures and Legends

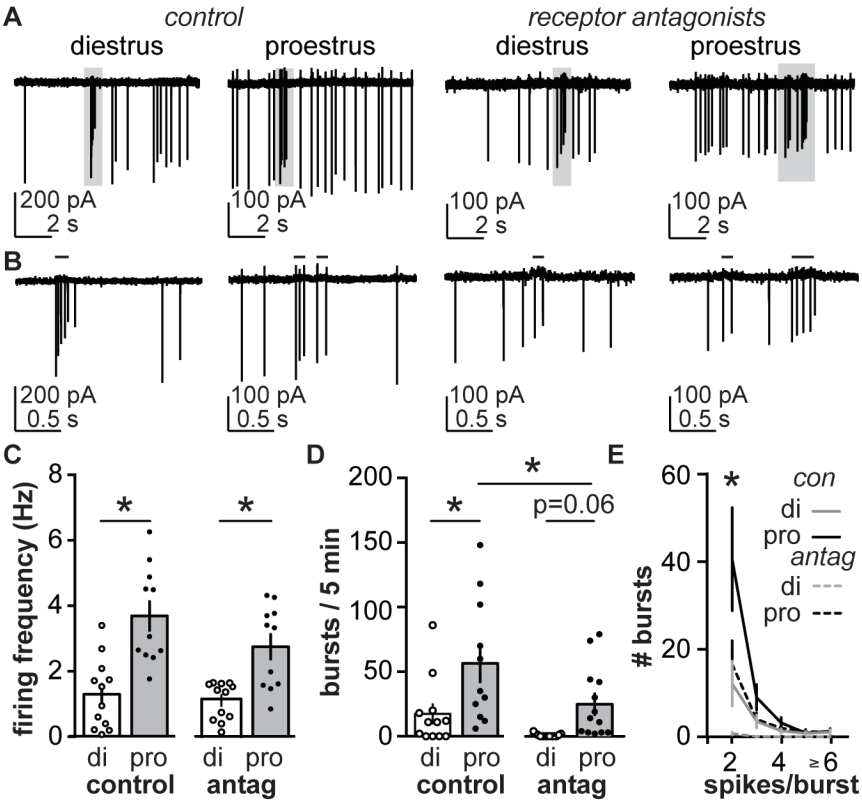

Figure 2-1 Extracelular firing rate of AVPV kisspeptin neurons.

A. Representative extracellular recordings of AVPV kisspeptin neurons on diestrus (di) and proestrus (pro) under control conditions (left) and with AMPA, NMDA, and GABAA receptors antagonized (right). B. Areas in grey boxes expanded from A. Black lines over traces in B indicate identified bursts. C-D, Mean ± SEM firing frequency (C) and number of burst events (D). E, The number of burst events plotted as a function of number of spike per burst on diestrus (grey) and proestrus (black) under control conditions (solid line) and with receptor antagonists (dashed line). Antag, antagonists of ionotropic GABA and glutamate receptors. * $p<0.05$ calculated by two-way ANOVA/Bonferroni or two-way RM ANOVA/Holm-Sidak test.

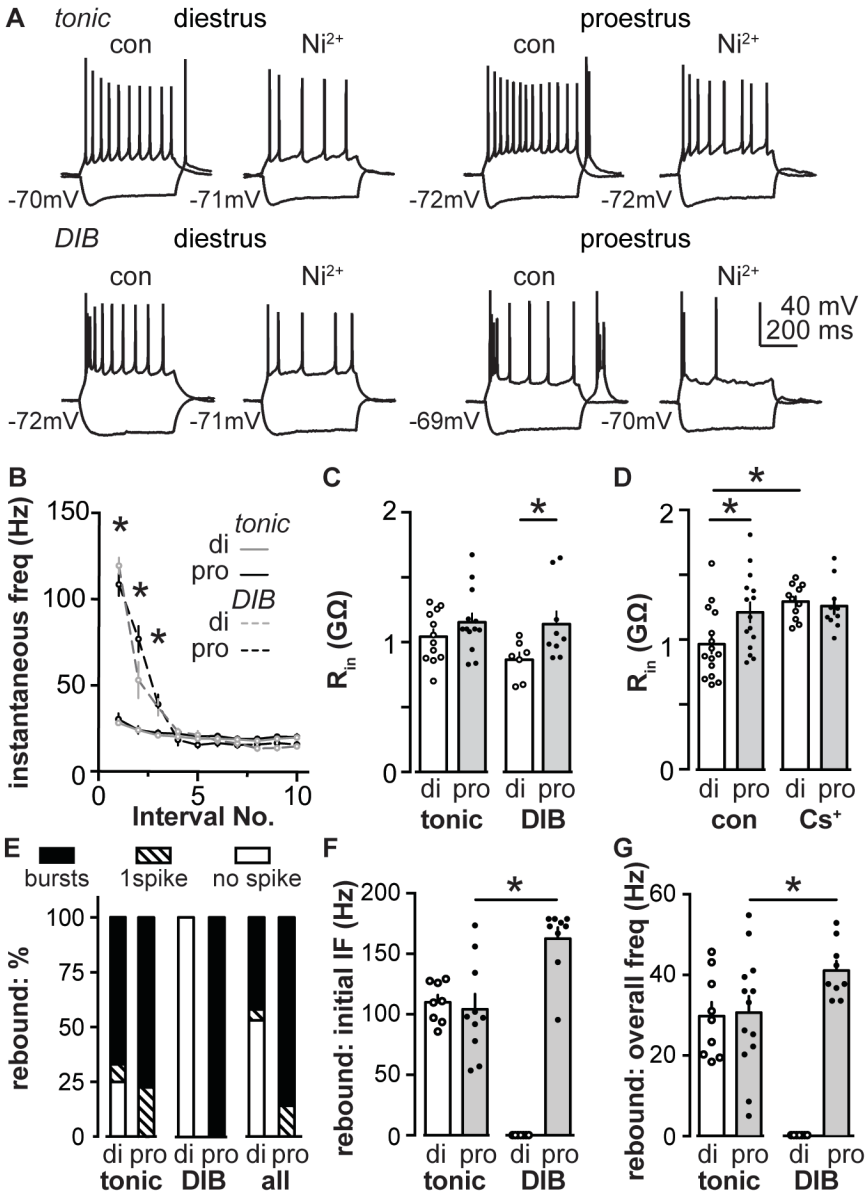

Figure 2-2 Depolarization and removal of hyperpolarization both induce distinct firing properties.

A, Representative firing properties of tonic and DIB cells on diestrus and proestrus under control conditions and during treatment with Ni2+ (100 μM). B, Mean ± SEM instantaneous frequency (IF) of tonic (solid line) and DIB (dash line) cells on diestrus (di, grey) and proestrus (pro, black) plotted as a function of spike interval number. C, Input resistance (Rin) for tonic and DIB cells on diestrus and proestrus. D, Rin for cells on diestrus and proestrus assessed using physiological (con) and Cs+-based pipette solution. E, Distribution of cells that generated rebound bursts (black bar), one rebound spike (hatched bar), or no rebound spikes (white bar) on diestrus and proestrus for tonic, DIB, and all cells combined. F-G, Initial IF (F) and overall frequency (G) of rebound bursts in tonic and DIB cells on diestrus and proestrus. * $p<0.05$ calculated by two-way ANOVA/Bonferroni or two-way RM ANOVA/Holm-Sidak test.

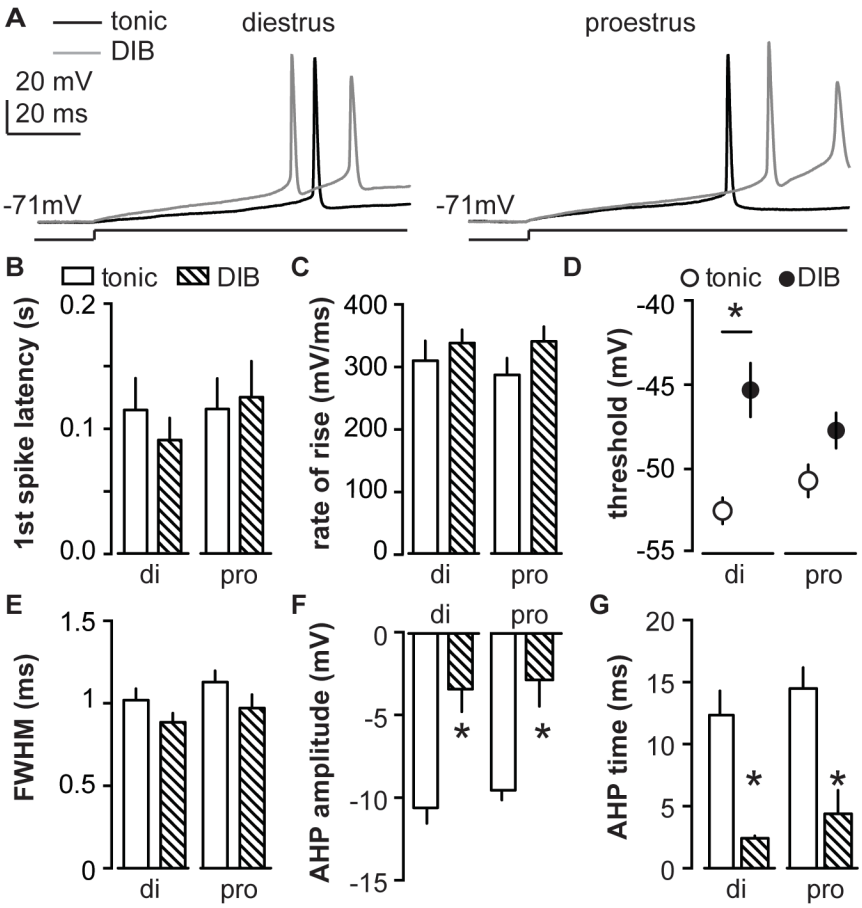

Figure 2-3 Action potential properties of AVPV kisspeptin neurons depend on firing pattern during depolarization but not cycle stage.

A, Representative first action potential evoked via minimal necessary depolarizing current in tonic (black) and DIB (grey) cells on diestrus (left) and proestrus (right). The line under the action potentials indicate timing of current injection (10pA for examples shown except 15pA for the DIB cell on proestrus). **B-F**, Mean ± SEM action potential parameters in tonic cells (open bar for **B-C** and **E-G**; open circle for **D**) and DIB cells (hatched bar for **B-C** and **E-G**; black circle for **D**) on diestrus (di) and proestrus (pro), including (**B**) 1st spike latency, (**C**) action potential rate of rise, (**D**) threshold, (**E**) full-width half-maximum (FWHM), (**F**) afterhyperpolarization potential (AHP) amplitude and (**G**) AHP time on diestrus and proestrus. * $p<0.05$ calculated by two-way ANOVA/Bonferroni test tonic vs. DIB.

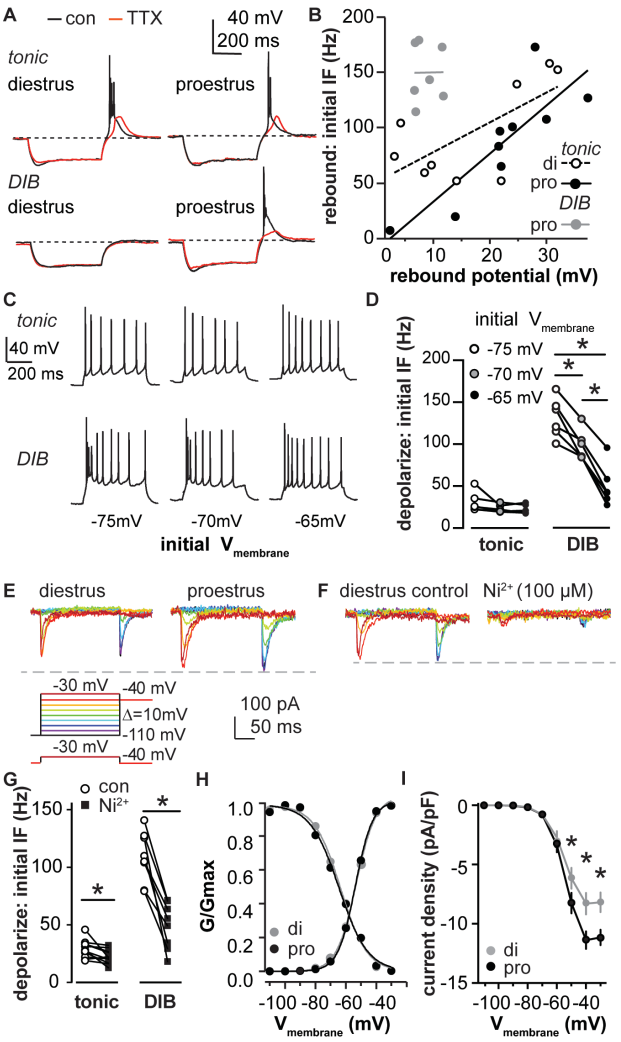

Figure 2-4 Ni^{2+}-sensitive current is critical for bursting patterns and is under estrous cycle regulation.

A, Representative examples for rebound potential of tonic and DIB cells on diestrus and proestrus under control conditions (black) and then tested with TTX (1μM) application (red). Dashed lines indicate -70mV. **B**, Positive correlation between rebound depolarization and initial instantaneous frequency (IF) was observed in tonic cells on diestrus (di, open circle fitted with dashed line) and proestrus (pro, black circle fitted with solid black line) but not in DIB cells on proestrus (grey circle fitted with grey line). **C**, Representative examples of depolarization-induced firing pattern of tonic and DIB cells initiated at -65, -70 and -75 mV. **D**, IF was dependent on preceding membrane potential in tonic and DIB cells, each line connects values from the same cells at different membrane potentials. **E**, Voltage protocols for I_T isolation; bottom protocol was subtracted from top to remove HVA contamination from step -30 mV (bottom, left). Representative isolated I_T on diestrus (top, left) and proestrus (top,right), each color represents a tested voltage. **F**, Isolated I_T was blocked by Ni^{2+} (100 μM). **G**, Initial IF of depolarization induced firing for tonic and DIB cells under control conditions and with Ni^{2+} (100 μM) application, paired. **H**, Activation and inactivation of I_T conductance was plotted and fit with Boltzmann function to derive $V_{1/2}$ and k value on diestrus (grey dots fitted with grey line) and proestrus (black dots fitted with black line). **I**, Mean ± SEM current density of I_T on diestrus and proestrus. * $p<0.05$ calculated by two-way RM ANOVA/Holm-Sidak test.

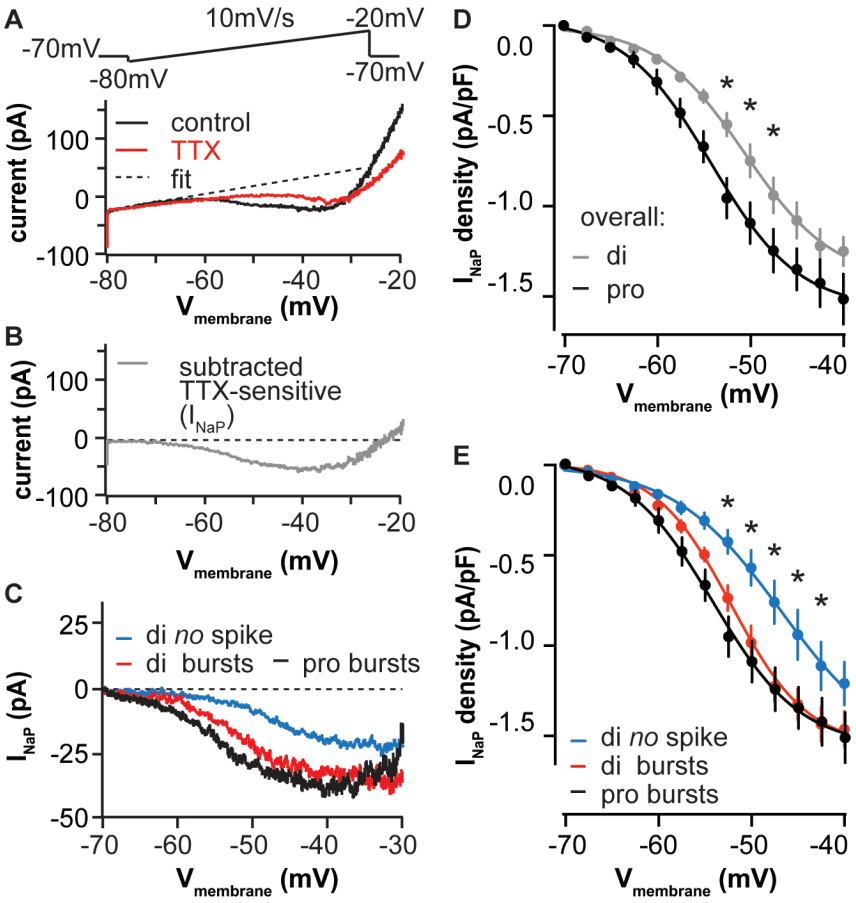

Figure 2-5 Persistent sodium conductance (I_{NaP}) facilitates rebound burst generation and is regulated by the estrous cycle.

A (top) ramp protocol, (bottom) and representative raw currents under control conditions (black) and after application of TTX (red). Dashed line indicates the linear fit to correct for leak current. **B**, Representative TTX-sensitive I_{NaP} obtained by subtracting the TTX trace from the control trace in **A** after linear fit of each. **C**, Representative I_{NaP} in cells that exhibit rebound bursts (red) or no rebound spikes (blue) on diestrus and those that exhibited rebound bursts on proestrus (black). **D-E**, Mean ± SEM I_{NaP} current density on diestrus (di) vs. proestrus (pro) (**D**) and with cells parsed by cycle stage and rebound firing (**E**). * $p<0.05$ calculated by two-way RM ANOVA/Holm-Sidak test.

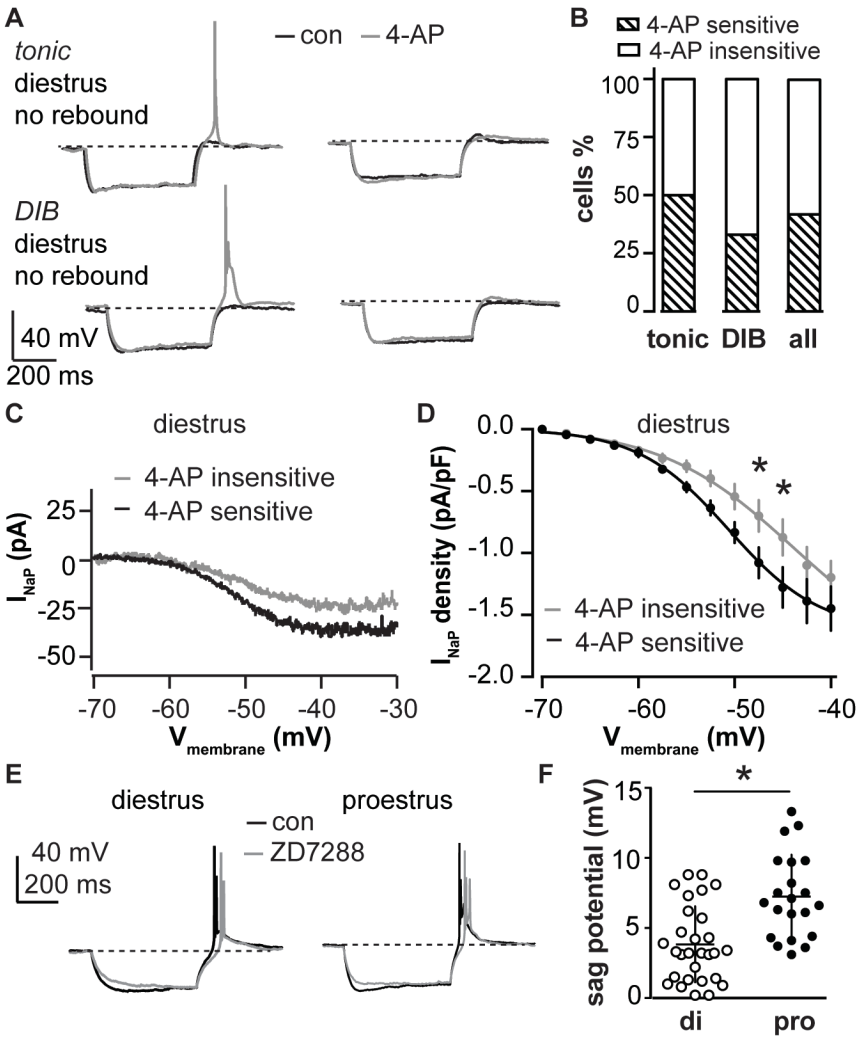

Figure 2-6 Subpopulations of cells that exhibit no rebound spikes on diestrus have restored ability to generate rebound spike(s) after blocking I_A.

A, Representative firing properties of tonic and DIB cells on diestrus that did not exhibit rebound spikes under control conditions (black): 4-AP (5 mM) treatment (grey) restored rebound spike(s) in some cells (left) but not others (right). **B**, Percentage of cells with 4-AP-sensitive (hatched bar) or 4-AP-insensitive rebound firing (open bar) for tonic, DIB and all cells combined on diestrus. **C**, Representative I_{NaP} in 4-AP-sensitive (black) and 4-AP-insensitive (grey) cells tested on diestrus. **D**, Mean ± SEM I_{NaP} current density for 4-AP-sensitive (black) and 4-AP-insensitive (grey) cells tested on diestrus. * $p<0.05$ calculated by two-way RM ANOVA/Holm-Sidak test. **E**, Representative cells on diestrus and proestrus preserved rebound bursts but not sag potential after ZD7288 (50μM) application. **F**, sag potential was increased on proestrus compared to diestrus. * $p<0.05$ Student's t-test.

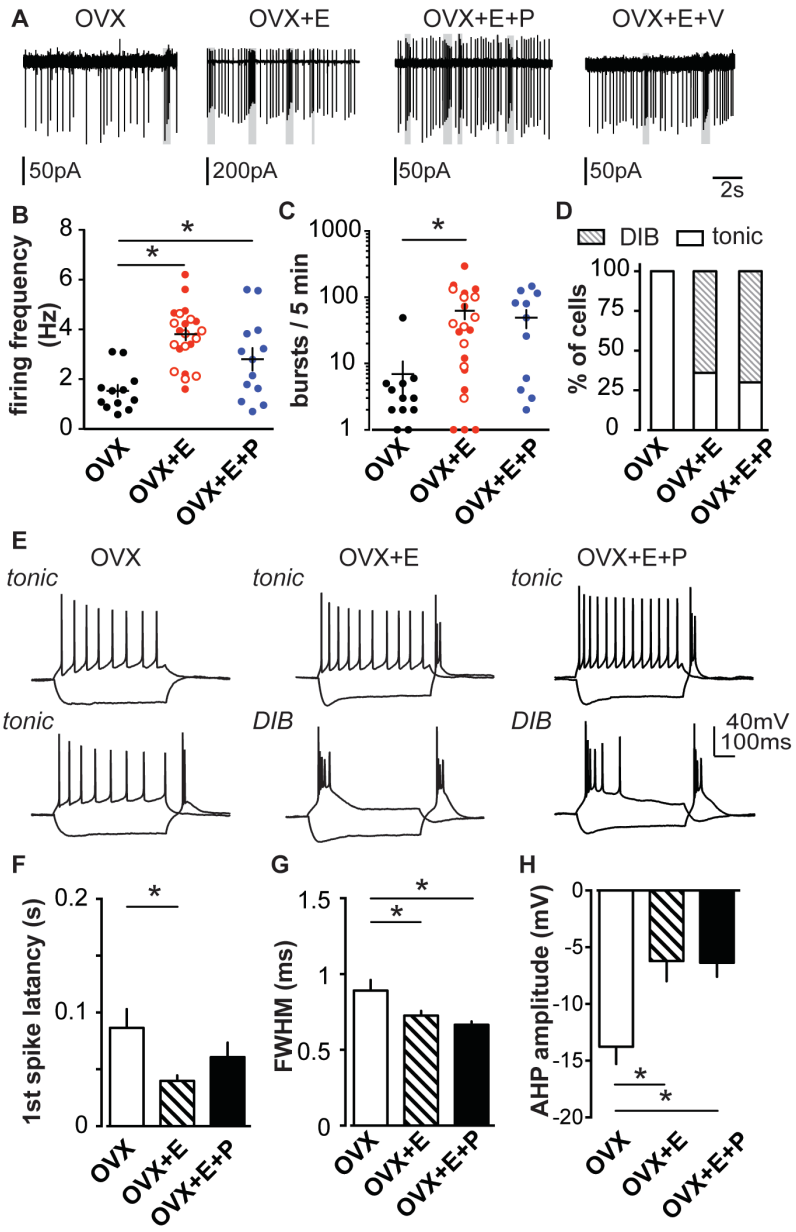

Figure 2-7 Estradiol but not progesterone increases overall excitability and burst events in AVPV kisspeptin neurons.

A, Representative extracellular recordings of OVX, OVX+E (E, estradiol), OVX+E+P (P, progesterone), and OVX+E+V (V, vehicle) with AMPA, NMDA, and GABAA receptors antagonized. Grey boxes indicate bursts. **B-C**, Mean ± SEM firing frequency (**B**) and number of burst events (**C**) of OVX (black circles), OVX+E (solid red circles), OVX+E+V (open red circles), OVX+E+P (blue). **D**, Percentage of cells that fire depolarization-induced bursts (DIB) or tonic patterns on OVX, OVX+E and OVX+E+P groups. **E**, Representative firing properties of tonic (top) and DIB (bottom, except OVX) cells in OVX, OVX+E, and OVX+E+P groups. **F-H**, Mean ± SEM of action potential parameters in OVX (white), OVX+E (hatched) and OVX+E+P (black) groups: latency to first spike (**F**), action potential full-width half-maximum (FWHM) (**G**), and afterhyperpolarization potential (AHP amplitude) (H). * $p<0.05$ calculated by one-way ANOVA/Bonferroni test.

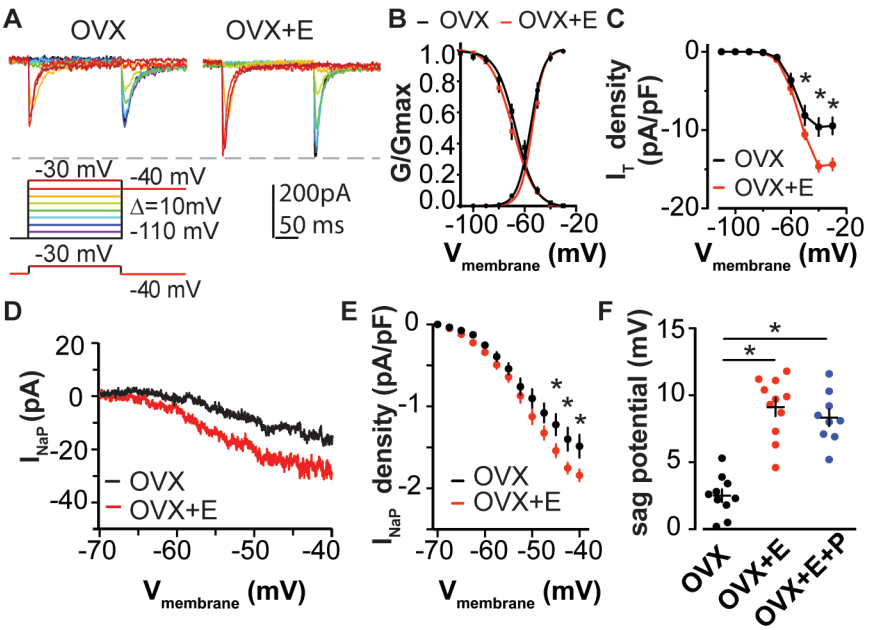

Figure 2-8 Estradiol increases I_T and I_{NaP} current density density in AVPV kisspeptin neurons.

A, Voltage protocol (bottom) and representative subtraction-isolated I_T in OVX (top left) and OVX+E groups (top right). **B,** Activation and inactivation of I_T conductance was plotted and fit with a Boltzmann function to derive $V_{1/2}$ and k value in OVX (black) and OVX+E (red). **C**, Mean ± SEM current density of I_T in OVX (black) and OVX+E (red). **D**, Representative I_{NaP} in OVX (black) and OVX+E (red) groups. **E**, Mean ± SEM I_{NaP} density in OVX (black) vs. OVX+E (red) groups. **F**, Mean ± SEM of sag potential induced by hyperpolarization. * $p<0.05$ calculated by two-way RM ANOVA/Holm-Sidak test for **D**, **E**; * $p<0.05$ calculated by one-way ANOVA/Bonferroni test for **F**

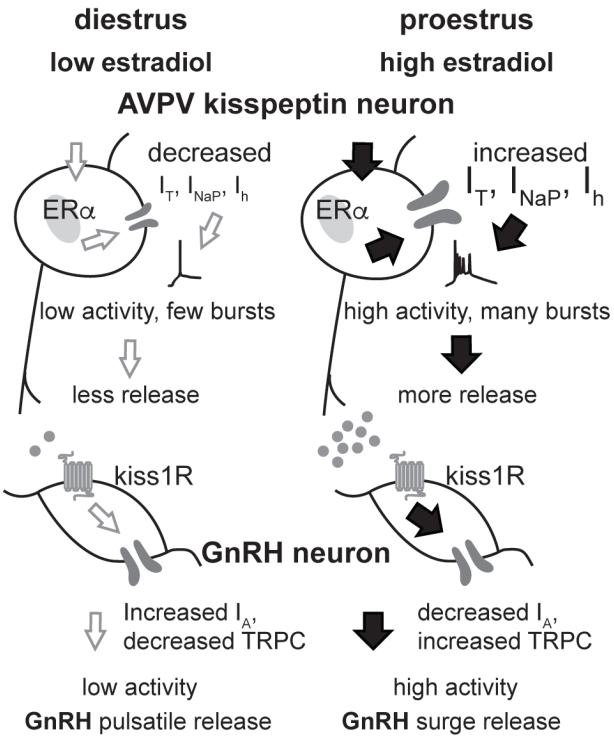

Figure 2-9 Schematic model of cyclic regulation of the AVPV kisspeptin-GnRH circuitry.

On diestrus, low estradiol levels exert negative feedback and AVPV kisspeptin neurons exhibit low $I_{T,}$ I_{NaP} and I_h. This contributes to reduced overall and burst firing, thus lower release of kisspeptin, GABA and glutamate. GnRH neurons exhibit low activity and a pulsatile release pattern. On proestrus, high levels of estradiol exert positive feedback action, increasing $I_{T,}$ I_{NaP} and $I_{h,}$ facilitate increased overall excitability and, for the former two currents, increased burst firing. This increases neurosecretion from these neurons, increasing excitatory drive to GnRH neurons via kisspeptin, GABA and glutamate, and also increasing GnRH neuron activity via kisspeptin-mediated reduction of I_A [71] and increase in TRPC conductance [166]. Together the intrinsic changes and increased excitatory drive provoke increased release of GnRH [13].

Tables

Table 2-1 Two-way ANOVA parameters for comparison among groups: cells from diestrus vs. proestrus mice

Extracellular recordings

Parameter (figure)	Estrous cycle stage	Antagonists	Interaction
Firing frequency (Figure 1C)	F(1, 42)=37.3 ***	F(1,42)=3.0	F(1,42)=1.2
Bursts/5min (Figure 1D)	F(1, 46)=14.8 ***	F(1,46)=8.4**	F(1,46)=0.8

Whole-cell recordings

Parameter (figure)	Estrous cycle stage	Cesium	Interaction
Input resistance (Figure 2D)	F(1,47)=2.3	F(1,47)=7.5 **	F(1,47)=4.2 *
Parameter (figure)	**Estrous cycle stage**	**Tonic vs DIB**	**Interaction**
Input resistance (Figure 2C)	F(1,37)=1.7	F(1,37)=6.7*	F(1,37)=1.2
Rebound: initial IF (Figure2F)	F(1,30)=69.3***	F(1,30)=7.0*	F(1,30)=80.3***
Rebound: overall freq (Figure 2G)	F(1,34)=34.8***	F(1,34)=7.3*	F(1,34)=32.0 ***
1st spike latency (Figure 3B)	F(1,37)=0.8	F(1,37)=0.4	F(1,37)=0.3
Rate of rise (Figure 3C)	F(1,37)=0.6	F(1,37)=0.7	F(1,37)=0.01
Threshold (Figure 3D)	F(1,37)=0.1	F(1,37)=22.6***	F(1,37)=3.8
FWHM (Figure 3E)	F(1,37)=2.1	F(1,37)=2.8	F(1,37)=0.2
AHP amplitude (Figure 3F)	F(1,37)=0.7	F(1,37)=35.3***	F(1,37)=0.1
AHP time (Figure 3G)	F(1,37)=1.6	F(1,37)=26.2***	F(1,37)=0.1

*p < 0.05; **p < 0.01; ***p < 0.001.

Table 2-2 Two-way repeated-measures ANOVA for whole-cell comparison among groups: cells from diestrus vs. proestrus mice

Parameter (figure)	Estrous cycle stage	Interaction	Matching
Control: spike/burst (Figure1E)	F(1, 21)=5.6*	F(4, 84)=6.7***	F(21, 84)=2.3**
Antagonists: spike/burst (Figure1E)	F(1, 25)=11.6**	F(4, 100)=11.4***	F(25, 100)=2.8***
I_T density (Figure 4I)	F(1, 20)=4.4*	F(8, 160)=4.3***	F(20, 160)=4.7***
I_{NaP} density (Figure 5D)	F(1, 22)=5.4*	F(22, 264)=3.6***	F(12, 264)=15.7 ***

Parameter (figure)	Tonic vs DIB	Interaction	Matching
Diestrus: tonic vs DIB (Figure 2B)	F(1, 16)=84.5***	F(6, 96)=82.6***	F(16, 96)=2**
Proestrus: tonic vs DIB (Figure 2B)	F(1, 17)=42.2***	F(5, 85)=88.1*	F(17, 85)=5.1***
Depolarize: IF (Figure 4D)	F(1, 9)=46.1***	F(2, 18)=52.2***	F(9, 18)=11.2***

Parameter (figure)	Diestrus: rebound vs no rebound	Interaction	Matching
I_{NaP} density (Figure 5E)	F(1, 16)=7.3*	F(12, 192)=5.7***	F(16, 192)=12.7***

Parameter (figure)	Rebound: diestrus vs proestrus	Interaction	Matching
I_{NaP} density (Figure 5E)	F(1, 18)=0.8	F(12, 216)=1.2	F(18, 216)=17.8***

Parameter (figure)	4-AP sensitive vs insensitive	Interaction	Matching
I_{NaP} density (Figure 6D)	F(1, 10)=3.5	F(12, 120)=2.3**	F(10, 120)=10.2***

*p < 0.05; **p < 0.01; ***p < 0.001.

Table 2-3 One-way and two-way ANOVA parameters

Extracellular recording

Parameter (figure)	OVX, OVX+E and OVX+E+P
Firing frequency (Figure 7B)	F(2, 45)=12.7 ***
Bursts/5min (Figure 7C)	F(2, 45)=3.3 *

Whole-cell Recordings

Parameter (figure)	OVX, OVX+E and OVX+E+P
1st spike latency (Figure 7F)	F(2, 27)=3.9 *
FWHM (Figure 7G)	F(2, 27)=6.3**
AHP amplitude (Figure 7H)	F(2, 27)=7.6**
Sag potential (Figure 8F)	F(2, 27)=35.9***

Two-way repeated-measures ANOVA for comparison among groups: OVX and OVX+E

Parameter (figure)	OVX vs OVX+E	Interaction	Matching
I_T (Figure 8C)	F(1, 18)=8.0*	F(8, 144)=8.3***	F(18, 144)=4.9***
I_{NaP} (Figure 8E)	F(1, 19)=5.8*	F(12, 228)=4.3***	F(19, 228)=12.5***

*p < 0.05; **p < 0.01; ***p < 0.001.

Chapter 3 Glutamatergic Transmission to Hypothalamic Kisspeptin Neurons Is Differentially Regulated by Estradiol through Estrogen Receptor α in Adult Female Mice.

Luhong Wang, Laura L. Burger, Megan L. Greenwald-Yarnell, Martin G. Myers, Jr., and Suzanne M. Moenter

This work was originally published in 2018 in the *Journal of Neuroscience* 31 January 2018, 38 (5) 1061-1072

Abstract

Estradiol feedback regulates gonadotropin-releasing hormone (GnRH) neurons and subsequent luteinizing hormone (LH) release. Estradiol acts through estrogen receptor α (ERα)-expressing afferents of GnRH neurons including kisspeptin neurons in the anteroventral periventricular (AVPV) and arcuate nuclei, providing homeostatic feedback on episodic GnRH/LH release as well as positive feedback to control ovulation. Ionotropic glutamate receptors are important for estradiol feedback but it is not known where they fit in the circuitry. Estradiol negative feedback decreased glutamatergic transmission to AVPV and increased it to arcuate kisspeptin neurons; positive feedback had the opposite effect. Deletion of ERα in kisspeptin cells decreased glutamate transmission to AVPV neurons and markedly increased it to arcuate kisspeptin neurons, which also exhibited increased spontaneous firing rate. KERKO mice had increased LH pulse frequency, indicating loss of negative feedback. These observations indicate ERα in kisspeptin cells is required for appropriate differential regulation of these neurons and neuroendocrine output by estradiol.

Significance Statement

The brain regulates fertility through gonadotropin-releasing hormone (GnRH) neurons. Ovarian estradiol regulates the pattern of GnRH (negative feedback) and initiate a surge of release that triggers ovulation (positive feedback). GnRH neurons do not express the estrogen receptor needed for feedback (ERα); kisspeptin neurons in the arcuate and anteroventral periventricular nuclei are postulated to mediate negative and positive feedback, respectively. Here we extend the network through which feedback is mediated by demonstrating that glutamatergic transmission to these kisspeptin populations is differentially regulated during the reproductive cycle and by estradiol. Electrophysiological and in vivo hormone profile experiments on kisspeptin-specific ERα knockout mice demonstrate ERα in kisspeptin cells is required for appropriate differential regulation of these neurons and for neuroendocrine output.

Introduction

Gonadotropin-releasing hormone (GnRH) neurons form the final common pathway for central regulation of fertility. GnRH stimulates the pituitary to secrete the gonadotropins, follicle-stimulating hormone and luteinizing hormone (LH), which regulate gonadal functions. Gonadal steroids feed back to regulate GnRH release. Estradiol, via estrogen receptor alpha (ERα), plays crucial roles in providing both negative and positive feedback to GnRH/LH release [13,15,119]. In females, low estradiol levels through most of the reproductive cycle provide negative feedback, whereas when estradiol levels are high during the preovulatory phase of the cycle, estradiol feedback action switches to positive to initiate a surge of GnRH/LH release, ultimately causing ovulation [116]. As GnRH neurons typically do not express detectable ERα[61], estradiol feedback is likely transmitted to these cells by ERα-expressing afferents.

Kisspeptin-producing neurons in the anteroventral periventricular (AVPV) and arcuate nucleus are estradiol-sensitive GnRH afferents [96,120,121]. Kisspeptin is a potent stimulator of GnRH neurons, and its expression is differentially regulated in these nuclei by estradiol [69,72,83,88]. AVPV kisspeptin neurons were postulated as positive feedback mediators as kisspeptin expression is increased [88]. Subsequent studies demonstrated these neurons are more excitable during positive feedback compared to negative feedback, a shift mediated by estradiol [126,167]. ERα in kisspeptin cells is required for positive feedback, as kisspeptin-specific ERα knockout (KERKO) mice do not exhibit estradiol-induced LH surges [103,124,168]. Arcuate kisspeptin neurons are also known as KNDy neurons because of their coexpression of neurokinin B (NKB) and dynorphin [96]. NKB and dynorphin, respectively, increase and decrease firing rate of these cells [148,169]. KNDy neurons have been postulated to generate episodic GnRH release and to mediate steroid negative feedback on GnRH release frequency [96,170]. The mechanisms through which these two populations of kisspeptin neurons are differentially regulated by estradiol are not fully understood.

In this regard, the network upstream of the kisspeptin-to-GnRH neuron link is largely unstudied Activation of ionotropic glutamate receptors is needed to generate both pulse and surge modes of LH release [171–173]. GnRH neurons, however, appear to receive limited ionotropic glutamate input [59,174], suggesting GnRH afferents may be the recipients of the transmission involved in estradiol feedback. Estradiol increases expression of ionotropic glutamate receptor mRNA in AVPV neurons [175] and glutamatergic projections from the AVPV to GnRH neurons [176]. Glutamate also regulates several processes in the arcuate nucleus [177], where KNDy neurons reside. We thus hypothesized that ionotropic glutamatergic transmission to these two kisspeptin populations is differentially regulated via cycle-dependent changes in circulating estradiol levels. KNDy neurons use glutamate as a co-transmitter [87] and form a complex network as they synapse on each other, as well as on AVPV kisspeptin neurons [120,169]. We thus further tested if glutamatergic transmission to kisspeptin neurons, firing rate

of these neurons and in vivo output of the reproductive neuroendocrine system are disrupted in mice lacking ERα in kisspeptin cells (KERKO).

Materials and Methods

All chemicals were purchased from Sigma Chemical Company (St Louis, MO) unless noted.

Animals. Adult female mice aged 60-120 days were used for these studies. All mice were provided with water and Harlan 2916 chow (VetOne) *ad libitum* and were held on a 14L:10D light cycle with lights on at 0400 Eastern Standard Time. To delete ERα specifically from kisspeptin cells, mice with *Cre* recombinase gene knocked-in after the *Kiss1* promoter (*Kiss1*-Cre mice) were crossed with mice with a floxed *Esr1* gene, which encodes ERα (ERα floxed mice)[168]. The expression of Cre recombinase mediates deletion of ERα in all kisspeptin cells (KERKO mice). To visualize kisspeptin neurons for recording, mice heterozygous for both Kiss-Cre and floxed ERα were crossed with Cre-inducible YFP mice. Crossing mice heterozygous for all three alleles yielded litters that contained some mice that were homozygous for floxed ERα and at least heterozygous for both *Kiss1*-Cre and YFP; these were used as KERKO mice. Littermates of KERKO mice with wild type *Esr1, Kiss1*-Cre YFP or *Kiss1*-hrGFP mice [87] were used as controls; no differences were observed among these controls and they were combined. The University of Michigan Institutional Animal Care and Use Committee approved all procedures.

To study the role of naturally fluctuating ovarian steroids, Kiss1-hrGFP mice were used during the diestrous, proestrous or estrous phases of the estrous cycle as determined by monitoring vaginal cytology for at least a week before experiments. Uterine mass was determined to confirm uteri on proestrus were >100mg, indicating exposure to high endogenous estradiol [131]. Ovary-intact KERKO mice have disrupted estrous cycles with persistent cornified vaginal cytology typical of estrus; we thus used females in estrus as controls. To examine the role of ovarian estradiol, mice were ovariectomized (OVX) under

isoflurane anesthesia (Abbott) and were either simultaneously implanted with a Silastic (Dow-Corning) capsule containing 0.625µg of estradiol suspended in sesame oil (OVX+E) or not treated further (OVX)[12]. Bupivacaine (0.25%, APP Pharmaceuticals) was provided local to the incisions as an analgesic. These mice were studied 2-3d post ovariectomy in the late afternoon, which is the time of estradiol positive feedback[12].

Slice preparation and cell identification. All solutions were bubbled with 95% O2/5% CO2 throughout the experiments and for at least 30min before exposure to tissue. The brain was rapidly removed (1500-1600 Eastern Standard Time; Zeitgeber time 10-11) and placed in ice-cold sucrose saline solution containing (in mM): 250 sucrose, 3.5 KCl, 26 $NaHCO_3$, 10 D-glucose, 1.25 Na_2HPO_4, 1.2 $MgSO_4$, and 3.8 $MgCl_2$ (pH 7.6, 345 mOsm). Coronal (300 µm) slices were cut with a Leica VT1200S (Leica Biosystems). Slices were incubated in a 1:1 mixture of sucrose saline and artificial cerebrospinal fluid (ACSF) containing (in mM): 135 NaCl, 3.5 KCl, 26 $NaHCO_3$, 10 D-glucose, 1.25 Na_2HPO_4, 1.2 $MgSO_4$, 2.5 $CaCl_2$ (pH 7.4, 310 mOsm) for 30min at room temperature (~21-23 °C) and then transferred to 100% ACSF for additional 30-180min at room temperature before recording. For recording, slices were placed into a chamber continuously perfused with ACSF at a rate of 3ml/min with oxygenated ACSF heated to 30-31 °C with an inline-heating unit (Warner Instruments). GFP-positive kisspeptin neurons were identified by brief illumination at 488nm on an Olympus BX51WI microscope. Recorded cells were mapped to an atlas[133] to determine if any trends based on anatomical location emerged; no such trends were apparent in these data sets. Recordings were performed from 1 to 3 h after brain slice preparation except for KERKO mice (up to 6h). No more than three cells per animal were included for analysis of the same parameter, and at least five animals were tested per parameter. Values towards both ends of the data distribution were observed within the same animal, and the variance of the data was no smaller within an animal than among animals.

Electrophysiological recordings. Recording micropipettes were pulled from borosilicate capillary glass (type 7052, 1.65mm outer diameter; 1.12mm inner

diameter; World Precision Instruments, Inc.) using a Flaming/Brown P-97 puller (Sutter Instruments) to obtain pipettes with a resistance of 3-4 MΩ for extracellular and whole-cell recordings when filled with the appropriate pipette solution. Recording pipettes were wrapped with Parafilm to reduce capacitive transients; remaining transients were electronically cancelled. Recordings were made with an EPC-10 dual patch clamp amplifier and Patchmaster software (HEKA Elektronik) running on a Macintosh computer.

Extracellular recordings. Targeted extracellular recordings were made to obtain firing properties of cells without any receptor or channel blockers. This method was used as it maintains internal milieu and has minimal impact on the firing rate of neurons[134,135]. Recording pipettes were filled with HEPES-buffered solution containing (in mM): 150 NaCl, 10 HEPES, 10 glucose, 2.5 $CaCl_2$, 1.3 $MgCl_2$, and 3.5 KCl (pH=7.4, 310 mOsm), and low-resistance (<20MΩ) seals were formed between the pipette and neuron after first exposing the pipette to the slice tissue in the absence of positive pressure. Recordings were made in voltage-clamp mode with a 0mV pipette holding potential for 20min and signals acquired at 10kHz and filtered at 5kHz. Resistance of the loose seal was checked every 5min during the 20min recordings; data were not use if seal resistance changed >30% or was >20MΩ. The first and last 5-min recording is to determine if seal resistance is stable (<20% change). We used the middle 10min of recording to determine the spontaneous firing frequency.

Whole-cell recordings. All recordings were done with a physiologic pipette solution containing (in mM): 135 K gluconate, 10 KCl, 10 HEPES, 5 EGTA, 0.1 $CaCl_2$, 4 MgATP and 0.4 NaGTP, pH 7.3 with NaOH, 300 mOsm. All potentials reported were corrected online for liquid junction potential of -15.7mV. After achieving a minimum 2.5 GΩ seal and then the whole-cell configuration, membrane potential was held at -70mV between protocols during voltage-clamp recordings. Series resistance (<20MΩ, <20% change during the recording period) and the passive properties of the neuron (input resistance >400MΩ, membrane capacitance stable, and holding current absolute value <50pA) were monitored every 2min from the current resulting from a 5mV hyperpolarizing

voltage step from −70mV (mean of 16 repeats, 20ms duration); our algorithm for determining passive properties and series resistance discards traces with synaptic activity during this protocol. There was no difference in I_{hold}, C_m, or R_s among any comparisons. As reported[167], R_{in} is in AVPV kisspeptin neurons is lower on diestrus that proestrus (diestrus, R=739 ± 82, proestrus, R=1136 ± 83, p=0.003). No differences in R_{in} were observed in arcuate kisspeptin neurons among groups.

To record spontaneous AMPA-mediated excitatory postsynaptic currents (EPSCs), membrane potential was held at -68mV, the calculated reversal potential of Cl^- based on Cl^- concentration in pipette solution vs ACSF, Cl^- activity coefficient[137] and the recording temperature. We did not use picrotoxin or other $GABA_A$ receptor blockers to avoid disinhibitory effects on the circuitry that is preserved within the slices. No PSCs were observed at a holding potential of -65 to -70mV after 10μM CNQX application to block AMPA receptors; outward $GABA_A$ receptor-mediated PSCs were observed when membrane potential was depolarized beyond -60mV and inward $GABA_A$ receptor-mediated PSCs were observed membrane potential was hyperpolarized beyond -70mV (n=4 for both AVPV and arcuate). For recording AMPA receptor-mediated miniature excitatory postsynaptic currents (mEPSCs), membrane potential was held at -68mV and ACSF contained picrotoxin (100μM), APV (D-(−)-2-amino-5-phosphonovaleric acid, 20μM) and tetrodotoxin (TTX, 1μM). In this case, TTX blockade of action potentials eliminates concerns regarding disinhibition.

Arcuate kisspeptin neurons are a potential source of glutamate transmission to one another [87] as well as to AVPV neurons[169]; projections among arcuate kisspeptin neurons are more likely to be preserved in a slice. Dynorphin can inhibit firing activity of arcuate kisspeptin neurons[148], we thus tested the effect of dynorphin on spontaneous and miniature EPSCs of arcuate kisspeptin neurons. Dynorphin A (1μM, Bio-techne) was bath-applied to the brain slices from control OVX female and KERKO OVX and OVX+E female for 5min. Both spontaneous and miniature EPSCs were recorded as above before and during dynorphin treatment, and during subsequent washout.

Tail-tip blood collection All adult female mice were ovary-intact and handled more than two weeks before experiments. Vaginal cytology of control and KERKO mice was determined for more than 10 days prior to sampling. As KERKO mice exhibit prolonged cornification typical of estrus, control mice displaying regular 4- or 5-day cycles were sampled during estrus. Repetitive tail-tip blood collecting was preformed as described (n=6 each control and KERKO)[178]. After the excision of the very tip of the tail, mice were put on a cage top and tail blood (6µl) was collected every 6min for 2h from 1300 to 1500. Each time the tail was wiped clean and then massaged for about 10s until 6µl blood sample was collected with a pipette tip. Whole blood was immediately diluted in 54µL of 0.1M PBS with 0.05% Tween 20 and homogenized and then kept on ice. Samples were stored at −20°C for a subsequent ultrasensitive LH assay. Intra-assay %CV is 2.2%. Interassay coefficients of variation were 7.3% (low QC, 0.13 ng/ml), 5.0% (medium QC, 0.8 ng/ml) and 6.5% (high QC, 2.3ng/ml). Functional sensitivity is 0.016ng/ml[179].

Kisspeptin and GnRH challenge. At the end of the frequent sampling period, mice received a single intraperitoneal injection of kisspeptin (65.1µg/kg)[180]. Blood was collected before and 15min after injection. GnRH (150µg/kg) was injected 40-45min after kisspeptin, with blood collected immediately before and 15min after injection.

Pituitary RNA extraction and gene expression. Ovary intact control (estrous stage of the cycle) and KERKO female mice were used. Pituitaries were collected from these animals; a further set of six pituitaries was collected from animals used in recording experiments; these were preserved in RNALater (ThermoFisher) at -20C until processing. No differences were observed between these and freshly processed pituitaries and they were combined for analyses. Tissues were homogenized in Qiagen RLT using pellet pestles (BioMasher II, Kimble Chase). RNA was extracted (with on-column DNasing) using RNeasy spin columns (Qiagen). Sample RNAs (500 ng) and a standard curve of pooled mouse pituitary RNAs (1000, 200, 40, and 8ng) were reverse transcribed using Superscript III (20µl reaction volume, ThermoFisher) [148]. All cDNA was assayed in duplicate for

candidate gene messenger RNAs (mRNAs) by hydrolysis probe-based quantitative PCR chemistry (TaqMan, ThermoFisher). A final concentration of 1ng/µl cDNA for unknowns was used for all genes except Fst and Npffr1, which required 10ng/µl. The standard curves were similarly diluted. TaqMan primer-probes for mRNAs of pituitary genes (*Kiss1r, Gnrhr, Lhb, Fshb, Cga, Egr1, Fst, Npffr1)* and housekeeping mRNAs *Gapdh and Actb* were purchased from Integrative DNA Technologies (Table 3-1).

Primer-probes were resuspended in Tris-EDTA to 20× (5 µm each primer, 10 µm probe) as recommended. qPCR was performed using cDNA as described[148]. In brief, 5 µl of diluted cDNA (10 or 1ng/µl) were run in duplicate using TaqMan Gene Expression Master Mix (Applied Biosystems) for 40 cycles as indicated by the manufacturer. Linearity and parallelism of the amplification was confirmed. Amplicon size was confirmed by agarose gel electrophoresis and sequencing for custom primer-probe sets.

Data Analysis. Events (PSCs or action currents) were detected and visually confirmed using custom software written in Igor Pro (Wavemetrics)[137,181]. Frequency is reported as the total number of confirmed events divided by the duration of recording. Superimposed events were measured from each event's baseline for amplitude; such events were excluded from analysis of event kinetics including full-width at half-maximum FWHM (ms), an average 10–90% decay time (ms), and rise time (ms). LH pulses were detected by a version of Cluster[182] transferred to IgorPro using cluster sizes of two points for both peak and nadir and t-scores of two for detection of increases and decreases. Normalized relative gene expression was determined by the ΔΔCt method[183]. *Gapdh* gene expression was regulated between control and KERKO, thus relative gene expression was normalized to *Actb*. To avoid intra-assay variability all samples were assayed within the same assay.

Experimental design and statistical analysis. Only adult female mice were used for these studies as only females exhibit estradiol positive feedback. Our objective was to understand the switch between estradiol negative and positive feedback regulation in female reproduction. The sample size for each individual

experiment is listed in the result session. Data were analyzed using Prism **7** (GraphPad Software), and are reported as mean ± SEM. The number of cells per group is indicated by n. Normality tests were performed using the Shapiro-Wilk normality test. Data were compared as dictated by distribution and experimental design; tests are specified in the results. All two group comparisons were two-tailed. Significance was set at $p<0.05$, all p values <0.1 are indicated in text and figures and all p values <0.2 are mentioned in the text. P value for any comparison made for which a specific p value is not given was ≥ 0.2. Parameters for all statistical comparisons are reported in Tables 3-2 and 3-3 or in the legends.

Results

Ionotropic AMPA-mediated glutamatergic transmission to AVPV kisspeptin neurons is increased during positive feedback (proestrus) compared to negative feedback (diestrus and estrus).

Whole-cell recordings of AMPA-mediated spontaneous excitatory postsynaptic currents (sEPSCs) were made in the late afternoon from AVPV kisspeptin neurons in brain slices from ovary-intact control mice in different stages of the estrous cycle (diestrus, proestrus, estrus), and KERKO mice (persistent cornified vaginal cytology similar to estrus; high circulating estradiol similar to proestrus[168]). sEPSCs include both action potential-dependent and action-potential-independent glutamate release. Representative recordings from each cycle stage studied are shown in Figure 3-1A. Frequency of sEPSCs was higher on proestrus compared diestrus or estrus in AVPV kisspeptin neurons (Figure 3-1C, n=11 each, Kruskal-Wallis/Dunn's test, diestrus vs proestrus, $p=0.006$; proestrus vs estrus, $p=0.002$; diestrus vs estrus, $p>0.99$).

To determine if increased sEPSC frequency was attributable to increased presynaptic activity and/or increased synaptic release sites, miniature EPSCs were recorded (Figure 3-1B). Miniature EPSCs (mEPSCs) arise from the

postsynaptic response to activity-independent vesicle fusion and transmitter release from the presynaptic neuron. Their frequency is proportional to a combination of the number of functional release sites and/or release probability, whereas amplitude reflects amount of glutamate release and/or postsynaptic AMPA receptor expression[184]. Frequency of mEPSCs was higher on proestrus compared to diestrus or estrus, suggesting increases in release sites and/or probability during estradiol positive feedback. On proestrus but not diestrus or estrus, mEPSC frequency was lower than that of sEPSCs (sEPSCs 4.5±0.5Hz, mEPSCs, 2.3±0.4Hz, two-way ANOVA/Holm-Sidak, p=0.0006). This suggests at least some afferents of AVPV kisspeptin cells are preserved within the slices, and that the activity of these afferents is increased on proestrus by the hormonal changes of the estrous cycle. No changes of amplitude (Figure 3-1D) or kinetics of sEPSCs or mEPSCs were observed among groups (Table 3-4).

Estradiol increases glutamatergic transmission to AVPV kisspeptin neurons.

To test if changes observed in spontaneous and miniature EPSC frequency in AVPV kisspeptin neurons observed on proestrus are mediated by circulating estradiol, we compared sEPSC and mEPSC frequency in AVPV kisspeptin neurons from OVX and OVX+E mice; recordings were done in the late afternoon at the time of estradiol-induced positive feedback in OVX+E and proestrous mice. Increased frequency of both sEPSCs and mEPSCs (Figure 3-2A-C) was observed in cells from OVX+E vs OVX mice (sEPSCs, n=11 each, two-way ANOVA/Holm-Sidak, p=0.009; mEPSCs, n=11 each, two-way ANOVA/Holm-Sidak, p=0.04), suggesting estradiol plays a role in activating afferents of AVPV kisspeptin neurons as well as remodeling synaptic release sites. No changes of amplitude (Figure 3-2D) or kinetics of EPSCs were observed among groups (Table 3-4)

ERα expression in kisspeptin cells is required for regulation of glutamatergic transmission to AVPV kisspeptin neurons during the estrous cycle and by estradiol.

To test the role of ERα expression in kisspeptin cells in glutamatergic transmission to AVPV kisspeptin neurons, we examined EPSC frequency in cells from KERKO mice. KERKO mice have persistent vaginal cornification and enlarged uteri, indicative of prolonged exposure to elevated estradiol[168]. Nonetheless, sEPSC frequency in AVPV kisspeptin neurons from KERKO mice was lower than that observed on proestrus (estradiol peak during the cycle, Figure 3-1A, C n=11 for KERKO, one-way ANOVA/Holm-Sidak, p=0.02). Frequency of mEPSCs in cells from KERKO mice, however, did not differ from that of diestrous or estrous mice (Figure 3-1B, C, n=9 for KERKO, one-way ANOVA/Holm-Sidak, p>0.6 for all comparisons). Deletion of ERα from kisspeptin cells may thus alter the activity of their primary afferents but appears to have minimal effect on synaptic release sites.

To investigate if loss of ERα in kisspeptin cells alters estradiol regulation of glutamatergic transmission in KERKO mice, we examined EPSCs in AVPV kisspeptin neurons from OVX and OVX+E KERKO mice. In KERKO mice, estradiol failed to increase sEPSC and mEPSC frequency it did in control mice (Figure 3-2A, C, n=9 for KERKO OVX and OVX+E, two-way ANOVA/Holm-Sidak, control OVX+E vs KERKO OVX+E). Further, in AVPV cells from KERKO mice neither frequency nor amplitude of sEPSCs or mEPSCs were regulated by estradiol. No changes of amplitude (Figure 3-2D) or kinetics of EPSCs were observed among all groups (Table 3-4). This suggests ERα in kisspeptin cells is required for estradiol-dependent regulation of ionotropic glutamatergic afferents to AVPV kisspeptin neurons during the estrous cycle.

Ionotropic AMPA-mediated glutamatergic transmission to arcuate KNDy neurons is decreased during positive feedback (proestrus) compared to negative feedback (diestrus or estrus).

Estradiol differentially regulates the expression of kisspeptin in arcuate and AVPV kisspeptin neurons[88]. To examine if this differential regulation extends to physiologic properties, we monitored EPSCs in arcuate KNDy neurons. In contrast to AVPV kisspeptin neurons, sEPSC frequency in arcuate KNDy neurons was reduced on proestrus compared to diestrus or estrus (Figure 3-3A, C, n=13 for diestrus and proestrus, n=12 for estrus, n=9 for KERKO, Kruskal-Wallis/Dunn's test, diestrus vs proestrus, p=0.03; proestrus vs estrus, p=0.04 diestrus vs estrus, p>0.9). The frequency of mEPSCs was increased on estrus compared to proestrus. No difference was detected between diestrus and either proestrus or estrus (Figure 3-3B, C, diestrus n=12, proestrus and estrus n=11 each one-way ANOVA/ Holm-Sidak; proestrus vs estrus, p=0.02), suggesting the number of release sites and/or release probability may increase on estrus. Altered sEPSC frequency in KNDy neurons is thus likely mediated by changes in afferent activity. No changes of amplitude (Figure 3-3D) or kinetics of EPSCs were observed among all groups (Table 3-4).

Estradiol decreases glutamatergic transmission to arcuate KNDy neurons.

To test if cycle-mediated changes observed in glutamatergic transmission to arcuate KNDy neurons are mediated by estradiol, we compared sEPSC and mEPSC frequency in KNDy neurons from OVX vs OVX+E mice. Frequency of sEPSCs was lower in OVX+E than OVX mice (Figure 3-4A, C, n=12 each, two-way ANOVA/Holm-Sidak, p=0.04). No changes were observed in mEPSC frequency (Figure 3-4 B, C, n=11 each, two-way ANOVA/Holm-Sidak). This suggests the cycle-dependent changes observed above are mostly mediated by estradiol modulation of afferent neuron firing. No changes of amplitude (Figure 3-4D) or kinetics of EPSCs were observed among groups (Table 3-4).

ERα expression in kisspeptin cells is required for regulation of glutamatergic transmission to arcuate KNDy neurons during the estrous cycle and by estradiol.

To test the role of ERα expression in kisspeptin cells in glutamatergic transmission to KNDy neurons, we examined sEPSC and mEPSC frequency in arcuate kisspeptin neurons from KERKO mice. Strikingly, the frequency of sEPSCs in cells from KERKO mice was markedly increased compared to proestrus; the p values for comparisons to cells from estrous and diestrous mice approached the level set for significance (Figure 3-3A, C, n=9 for KERKO, Kruskal-Wallis/Dunn's, KERKO vs proestrus, $p<0.001$; KERKO vs diestrus, $p=0.07$; KERKO vs estrus, $p=0.08$). Frequency of mEPSCs in KNDy neurons from KERKO mice was greater than in cells from ovary-intact mice during any cycle stage (Figure 3-3B, C n=9 for KERKO, one-way ANOVA/Holm-Sidak, KERKO $p<0.001$ vs proestrus, diestrus and estrus). These observations suggest that the lack of ERα in kisspeptin cells may increase glutamate release sites and/or probability.

We then tested if estradiol regulation of glutamatergic transmission to arcuate kisspeptin neurons is altered in KERKO mice. Frequency of sEPSCs was higher in cells from OVX+E KERKO than control mice (Figure 3-4A, C, KERKO, n=9 each, two-way ANOVA/Holm-Sidak, $p<0.001$), but did not differ between cells from OVX control and KERKO mice ($p=0.15$). This suggests estradiol regulation of glutamatergic transmission to arcuate kisspeptin neurons is lost in KERKO mice. Frequency of mEPSCs in cells from KERKO mice was increased compared to controls in both OVX and OVX+E groups (Figure 3-4B, C, KERKO, n=9 each, two-way ANOV/Holm-Sidak, OVX, $p=0.04$, OVX+E, $p=0.006$). These findings suggest estradiol suppresses presynaptic activity to decrease sEPSC frequency during positive feedback. In contrast, in KERKO mice estradiol primarily increases synaptic release sites and/or release probability.

Glutamatergic transmission to arcuate KNDy neurons was suppressed by dynorphin.

Previous research suggests that arcuate KNDy neurons synapse on each other[120,169]. This is of interest because most KNDy neurons are also glutamatergic[87] and may thus serve as glutamatergic inputs to one another[169]. Dynorphin suppresses the activity of KNDy neurons[148], as well as arcuate POMC neurons[185], a subpopulation of which (~30%) are also glutamatergic[186,187]. We hypothesized dynorphin decreases glutamatergic transmission to KNDy neurons. Bath application of dynorphin A (1μM) suppressed the frequency of both sEPSCs and mEPSCs to KNDy neurons within 5min, similar to the time required for it to suppress the firing rate of KNDy neurons [148]; this effect was reversible and EPSC frequency was restored to control values within a 15-min washout period (Figure 3-5 A, D, sEPSCs, n=7, one-way repeated-measures Friedman/Dunn's, control vs treatment, p=0.007; Figure 3-5B, E, mEPSCs, n=6, one-way repeated-measures ANOVA/Holm-Sidak, control vs treatment, p=0.02, control vs washout, p=0.08). To test if EPSC frequency changed with duration of recording, we performed mock treatments; in these cells EPSC frequency remained constant over a similar time period (Figure 3-5A, D, mock vs control, sEPSCs, n=5, paired Student's *t*-test). Since EPSC frequency and amplitude were not different between cells from OVX and OVX+E KERKO mice, we combined cells from both groups to test the effects of dynorphin. As in control mice, dynorphin reduced glutamatergic transmission to arcuate KNDy neurons from KERKO mice (Figure 3-5C, E n=5, one-way repeated-measures Friedman/Dunn's, control vs dynorphin, p=0.02, control vs washout p=0.06). Dynorphin may act on presynaptic neurons to decrease the activity-dependent glutamate release, and on presynaptic sites to suppress the release of stored glutamate. This modulation did not require ERα expression by kisspeptin cells.

The short-term firing frequency of KNDy neurons was not influenced by estradiol but is increased in KERKO mice.

Glutamatergic transmission to KNDy neurons is increased when either estradiol or kisspeptin-specific ERα expression are removed. The suppression of EPSC frequency in these neurons by dynorphin suggests these EPSCs may arise at least in part from KNDy-to-KNDy connections. We thus hypothesized that KNDy neuronal activity is modulated by estradiol and ERα expression within kisspeptin cells. We monitored the spontaneous firing frequency of arcuate kisspeptin neurons in OVX and OVX+E control and KERKO mice. KNDy neurons from control mice were either quiescent, or exhibited irregular firing. Interestingly, neither the short-term firing frequency (Figure 3-6A, B two-way ANOVA/Holm-Sidak) nor the percentage of firing cells (firing rate $\geq$ 0.01Hz) was different between OVX and OVX+E control mice (OVX vs OVX+E, Fisher's exact test). Firing rate in KNDy neurons from OVX+E KERKO mice was increased compared to controls ($p=0.008$) and approached the value set for significance in cells from OVX mice ($p=0.06$). Estradiol did not affect the firing activity of KNDy neurons from KERKO mice (Figure 3-6A, B). Further, a higher percentage of cells fired action potentials in KERKO compared to control mice (Figure 3-6C, Chi-square, $p=0.01$). In addition to increasing firing rate, the pattern of firing in cells from KERKO mice was shifted in a subgroup of cells. Specifically, 3 of 17 cells exhibited a distinct and consistent burst pattern throughout the entire 10-min observation window (Figure 3-6D); this was not observed in control mice under any steroid condition tested, or in any of our previous studies of firing in KNDy neurons[148,170,188]. The loss of ERα in kisspeptin cells thus elevated firing and triggered bursting in KNDy neurons; this may contribute to the increased EPSC frequency in KNDy neurons and disrupted estradiol negative feedback regulation in KERKO mice.

ERα in kisspeptin cells is required for pulsatile release of LH and pituitary response to kisspeptin.

Previous work in KERKO mice has shown elevated LH levels during development but not in adults[103,168]. Further, although ERα in kisspeptin cells was needed for estradiol positive feedback, ERα was not required for estradiol negative feedback[124]. These studies evaluated LH in single samples. While typical in mice because of low blood volume, this method cannot detect differences in the pattern of LH release, which is reflective under most physiologic circumstances of GnRH release. We utilized a recently-developed[179] assay that allows measurement of LH in small quantities of tail blood to assess LH pulse frequency over two hours in KERKO mice and their littermate controls on estrus. Representative pulse patterns are shown in Figure 3-7A. Similar to previous measures using single-time-point assessment, KERKO mice exhibited similar LH-pulse amplitude and baseline compared to control mice (Figure 3-7A, B, D) and there was no difference in mean LH between groups (control n=6, 0.5±0.1ng/μl vs KERKO n=6, 0.5±0.1ng/μl). LH-pulse frequency, however, was higher in KERKO mice compared to controls (Figure 3-7C). After the 2h sampling period, mice were challenged with kisspeptin and ~0.8h later with GnRH. KERKO mice did not exhibit an increase in serum LH after kisspeptin and had a reduced respond to GnRH vs controls (Figure3- 7E, F).

To gain insight into possible mechanisms underlying the blunted LH response to kisspeptin and GnRH in KERKO mice, we examined gene expression in the pituitary from separate groups of estrous control and KERKO mice that had not undergone blood (control n=7, KERKO n=8, Figure 3-7G). Steady-state mRNA levels of selected genes were determined using quantitative real-time PCR (two-tailed Student's *t* test unless specified). βactin (*Actb*) was selected as the housekeeping gene as *Gapdh* is known to be regulated by estradiol and age[189,190], and was differently regulated in pituitaries (p=0.008). *Kiss1r* (p=0.048) but not *Gnrhr* was decreased in the pituitaries from KERKO mice. *Fshb* (Mann-Whitney U test) and *Cga* were unchanged, whereas *Lhb* was decreased in

KERKO vs control mice (Mann-Whitney U test, p=0.02). For *Egr1*, a gene activated by GnRH and kisspeptin[191], the p-value approached significance for a decrease in KERKO mice (p=0.07). *Fst* expression is typically upregulated by high-frequency GnRH pulses[192] and was increased in pituitaries from KERKO mice (p=0.048). The gene encoding the gonadotropin-inhibitory hormone (GnIH) receptor, *Npffr1*, was decreased in pituitaries from KERKO mice (Mann-Whitney U test, p=0.01).

Discussion

GnRH neurons form the final common pathway for control of reproduction and receive regulatory input from many sources. Estradiol feedback appears to be indirect via ERα-expressing cells, including two hypothalamic kisspeptin populations[96,110]. Similarly, low-frequency activation of ionotropic glutamate receptors in GnRH neurons points to an indirect effect of glutamate[119,174]. We extended the estradiol feedback network to include glutamatergic afferents of kisspeptin neurons (Figure 3-8). ERα is required in kisspeptin cells for estradiol regulation of glutamatergic transmission to kisspeptin neurons, and for regulation of LH release *in vivo*. Estradiol thus acts on multiple nodes of a broad neuroendocrine network.

AVPV kisspeptin neurons help mediate estradiol induction of the GnRH/LH surge[110]. During positive feedback (proestrus, OVX+E PM), intrinsic excitability of these neurons is increased[126,167]. The present work supports and extends these observations, demonstrating estradiol positive feedback increases glutamate transmission to AVPV kisspeptin neurons. Estradiol positive feedback also suppresses hyperpolarizing GABAergic transmission to these cells[137], indicating that during positive feedback, estradiol tilts the balance toward excitatory inputs. Coupled with estradiol upregulation of intrinsic conductances underlying bursting firing[167], AVPV kisspeptin neurons are poised to increase output during positive feedback to drive the GnRH/LH surge.

The estradiol-induced increase in excitatory glutamatergic drive to AVPV kisspeptin neurons is attributable to at least two mechanisms: elevated presynaptic activity and changes in release sites. Activity-dependent glutamate release likely arises from cells preserved within the slice. Estradiol sensitivity of these afferents may come from their expression of estrogen receptors and/or through modifications induced by additional layer(s) of estradiol-sensitive afferents. Nearby neurons co-expressing ERα and vesicular glutamate transporter-2[193] are candidates for direct estradiol regulation. Few AVPV kisspeptin neurons are glutamatergic[87], and interconnections have not been reported among these cells[120,121], suggesting they are unlikely to be a major source of glutamatergic drive to one another. Many AVPV kisspeptin neurons are GABAergic[87]; the concomitant increased activity of and decreased GABAergic transmission to these cells during positive feedback provides a functional argument against interconnections[137,167]. The AVPV contains GABA/glutamate dual-labeled neurons; in some of these cells, the relative abundance of GABA decreases during positive feedback[176]. The shift towards increased glutamate and reduced GABA input to AVPV kisspeptin neurons during positive feedback could thus arise from one population utilizing both primary fast synaptic transmitters in a differential manner dependent upon estradiol feedback state.

In the AVPV, increased mEPSC frequency during positive feedback suggests estradiol increases connectivity and/or release probability[184]. In other regions, estradiol increases dendritic spine density, typically associated with glutamatergic synapses[194,195]. Estradiol also increases AMPA receptor subunit expression in unidentified AVPV neurons[175]; the lack of change in EPSC amplitude or kinetics suggest these changes may occur in non-kisspeptin cells. Also of interest are preoptic glutamatergic neuronal nitric oxide synthase (nNOS) neurons, which project to AVPV kisspeptin neurons and are regulated by kisspeptin and estradiol[180]. Nitric oxide regulation of presynaptic glutamate release may contribute to increased glutamatergic transmission to AVPV kisspeptin neurons. KNDy neurons also release glutamate onto AVPV kisspeptin

neurons[169] and may contribute to increased mEPSCs, but not activity-dependent changes as typically only processes from KNDy neurons are preserved in AVPV slices.

In contrast to AVPV kisspeptin neurons, KNDy neurons are postulated to mediate estradiol negative feedback[96]. In females, estradiol regulation of spontaneous firing of KNDy neurons is debated[154,196]. In short-term recordings, we observed no estradiol-induced change in firing frequency. Steroid feedback may primarily affect long-term activity patterns of these cells as in males[170]. Estradiol did, however, suppress glutamatergic transmission to KNDy neurons, reducing sEPSC frequency. Of interest, mEPSC frequency in KNDy neurons was not regulated by estradiol (OVX vs OVX+E) but was increased on estrus compared to proestrus. This change in mEPSC frequency may arise from cyclic changes ovarian progesterone, which rises after the LH surge, or to other cycle-dependent factors. This suggests estradiol positive feedback reduces activity-dependent glutamate release but has minimal effects on connectivity and/or release probability.

KNDy neuron firing is modulated by two of its neuropeptide products: NKB and dynorphin[148]. Here, dynorphin potently and reversibly suppressed glutamatergic transmission to KNDy neurons, likely attributable in part to an inhibitory effect of dynorphin on presynaptic activity. Within the arcuate, KNDy (~90%) and POMC (~30%) neurons are glutamatergic and express κ-opioid receptors[87,148,197]. Dynorphin suppresses firing of both of these populations[148,185]. The observations that dynorphin suppresses activity of these cells and EPSC frequency in KNDy neurons suggests POMC and KNDy neurons as glutamatergic afferents of KNDy neurons. KNDy neurons synapse on each other[120,169] and interconnect bidirectionally with POMC neurons [198,199]. During proestrus however, POMC neurons have elevated cFos expression[196], suggesting they may be activated by estradiol and potentially release more glutamate. If POMC neurons were major afferents of KNDy neurons, one would expect transmission to increase rather

than decrease during positive feedback. The dynorphin-induced decrease in mEPSC frequency in KNDy neurons suggests dynorphin may also act as a retrograde messenger to inhibit activity-independent neurotransmitter release[200,201] in addition to possible effects on afferent activity.

ERα within kisspeptin is important for regulation of reproduction. Positive feedback is disrupted in KERKO mice[124] and kisspeptin expression is decreased in the AVPV and increased in the arcuate[103,168]. Estradiol-mediated changes in glutamatergic drive to both populations were abolished in KERKO mice. Deletion of ERα from kisspeptin cells may alter glutamatergic inputs to AVPV and arcuate kisspeptin neurons through organizational and/or activational mechanisms. ERα is deleted as soon as *Kiss1* is expressed, before birth in KNDy neurons and before puberty in AVPV kisspeptin neurons[202,203]. This may cause developmental changes in the circuitry of these cells. Loss of ERα as a transcriptional factor may also alter expression of synapse-related genes and signaling pathways. From an activational perspective, the failure of estradiol to increase glutamatergic transmission to AVPV kisspeptin neurons in KERKO mice may indicate glutamate afferents receive cues from kisspeptin cells through local feedback circuits. In the arcuate, both spontaneous firing frequency of, and glutamate transmission to, KNDy neurons are increased in cells from KERKO mice. These correlative observations further indicate KNDy neurons provide glutamatergic transmission to themselves. Developmental changes subsequent to ERα deletion in kisspeptin cells may alter activity and thus activity-dependent synaptogenesis among KNDy neurons. The observed increase in mEPSC frequency in KNDy neurons from KERKO mice is consistent with this postulate. Alternatively, but not exclusively, increased glutamate release from KNDy neurons may result in overall increased KNDy neuron firing frequency and, in some cases, acquisition of a burst firing pattern.

Ultimately, changes in hypothalamic kisspeptin neurons may affect GnRH neuron activity and pituitary LH release. The increase in LH pulse frequency in KERKO

vs control mice is consistent with increased neuroendocrine drive, possibly due to increased frequency GnRH release triggered by a KNDy network lacking negative feedback. Importantly, LH release reports the integrated output of the reproductive neuroendocrine system. The same objective criteria were used for pulse detection in both groups; subjectively, LH pulse quality looks poorer in KERKO mice. Similar degradation of LH pulse patterns occurs when GnRH frequency is high[31,204]. *Fst* and *Lhb* are typically up-regulated by high GnRH-pulse frequencies[189,192]. In pituitaries from KERKO mice, *Fst* is elevated whereas *Lhb* suppressed, perhaps because supraphysiological GnRH pulse frequencies reduce *Lhb* expression[205]. Deletion of ERα from kisspeptin cells and/or altered feedback from other ovarian factors may also affect pituitary gene expression. The attenuated response of pituitaries from KERKO mice to kisspeptin and GnRH may be explained by decreased *Kiss1r* expression in pituitary as well. The increased LH pulse frequency and altered pituitary gene expression suggest ERα in kisspeptin cells play a vital role in negative feedback regulation.

These studies extend the network for estradiol negative and positive feedback beyond kisspeptin neurons, demonstrating glutamatergic transmission to hypothalamic kisspeptin neurons is a critical component these responses. ERα in kisspeptin cells modulates the glutamatergic network upstream of these two kisspeptin populations and sculpts central reproductive neuroendocrine output within the animal.

Figures and Legends

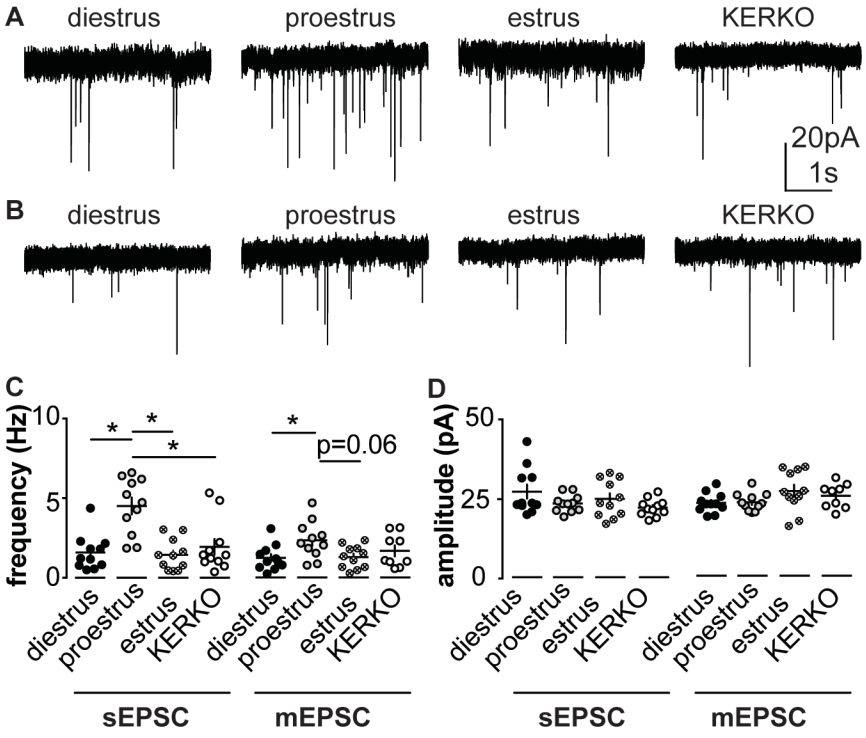

Figure 3-1 Estrous-cycle dependent regulation of glutamatergic transmission to AVPV kisspeptin neurons requires ERα in kisspeptin cells.

A and B, representative spontaneous (A) and miniature (B) post-synaptic currents in AVPV kisspeptin neurons in ovary-intact control mice on diestrus, proestrus and estrus and KERKO mice. C, Individual values and mean ± SEM sEPSC (left) and mEPSC (right) frequency. D, Individual values and mean ± SEM sEPSC (left) and mEPSC (right) amplitude. * $p<0.05$ calculated by Kruskal-Wallis/Dunn's (C) or one-way ANOVA/Holm-Sidak (D)

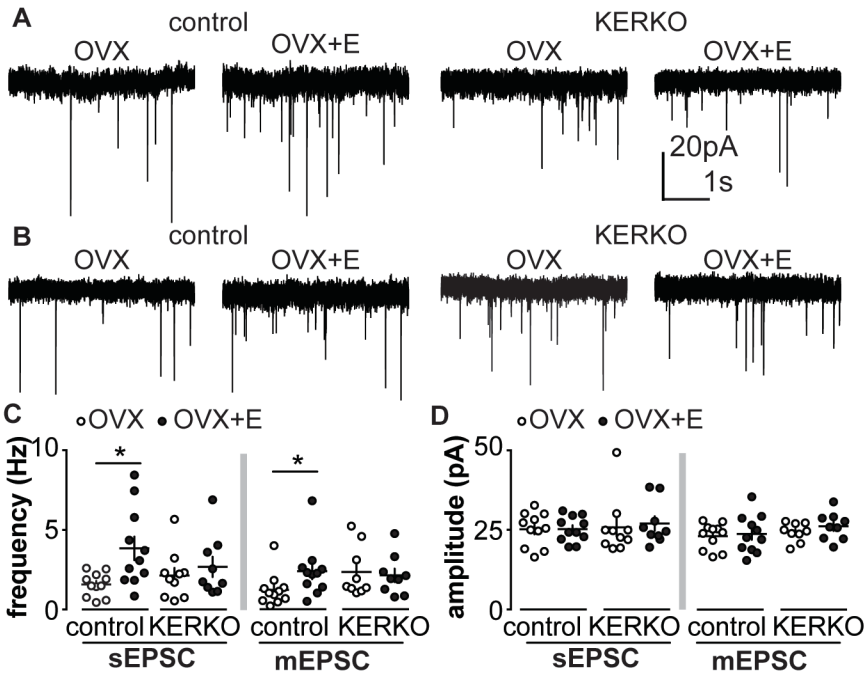

Figure 3-2 Estradiol does not modulate glutamatergic transmission to AVPV kisspeptin neurons from KERKO mice.

A and B, representative spontaneous (A) and miniature (B) post-synaptic currents in AVPV kisspeptin neurons in OVX and OVX+E groups in control and KERKO mice. C, Individual values and mean ± SEM sEPSC (left) and mEPSC (right) frequency. D, Individual values and mean ± SEM sEPSC (left) and mEPSC (right) amplitude. * $p<0.05$ calculated by two-way ANOVA/Holm-Sidak.

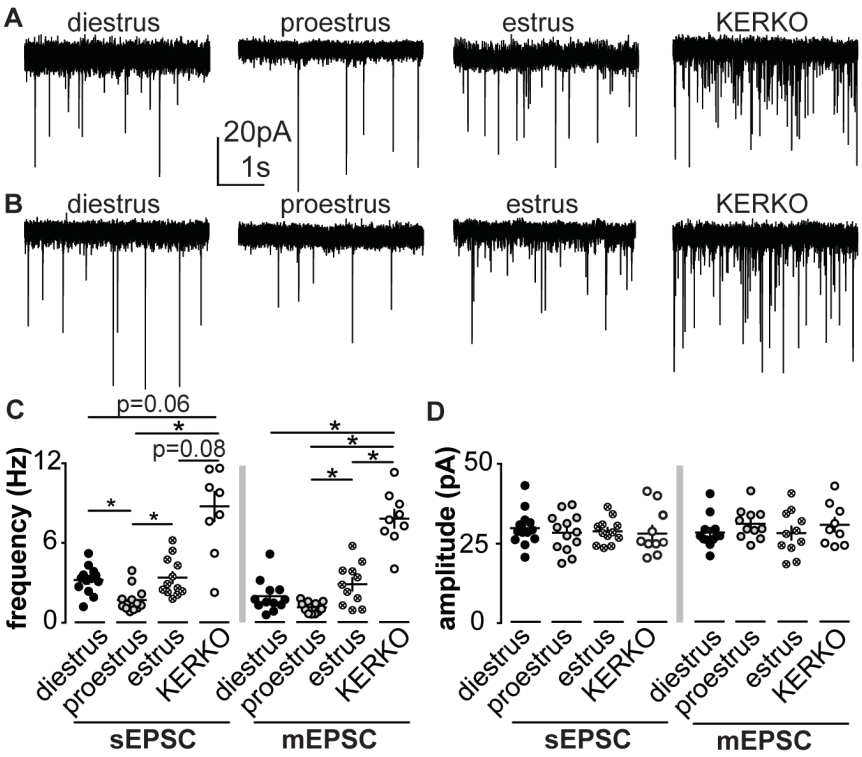

Figure 3-3 Estrous-cycle dependent regulation of glutamatergic transmission to arcuate kisspeptin neurons requires ERα in kisspeptin cells.

A and B, representative spontaneous (A) and miniature (B) post-synaptic currents in arcuate kisspeptin neurons in ovary-intact control mice on diestrus, proestrus and estrus and KERKO mice. C, Individual values and mean ± SEM sEPSC (left) and mEPSC (right) frequency. D, Individual values and mean ± SEM sEPSC (left) and mEPSC (right) amplitude. * $p<0.05$ calculated by Kruskal-Wallis/Dunn's (C, left) or one-way ANOVA/Holm-Sidak (the rest).

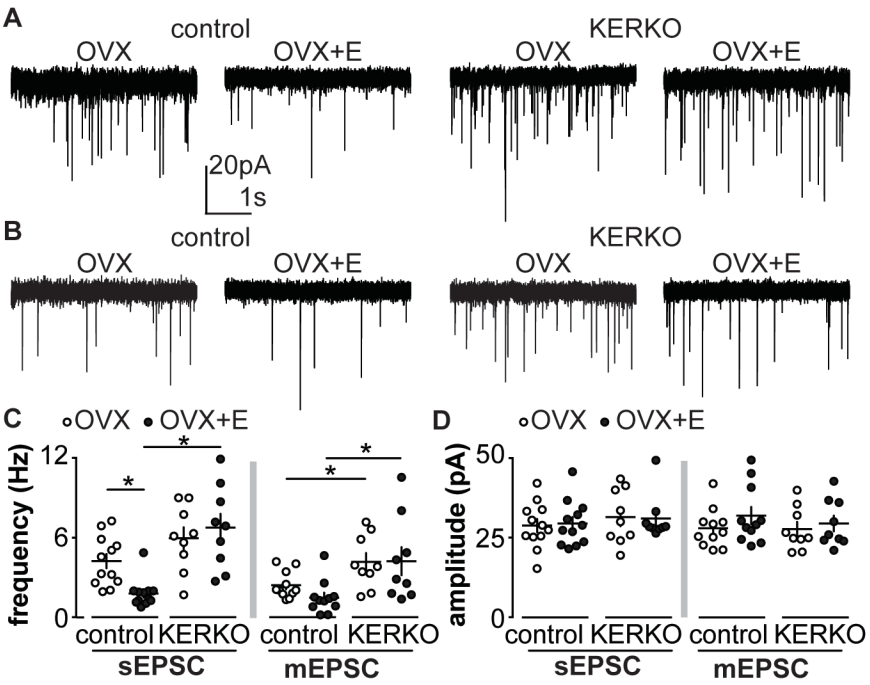

Figure 3-4 Estradiol does not modulate glutamatergic transmission to arcuate kisspeptin neurons from KERKO mice.

A and B, representative spontaneous (A) and miniature (B) post-synaptic currents in arcuate kisspeptin neurons in OVX and OVX+E groups in control and KERKO mice. C, Individual values and mean ± SEM sEPSC (left) and mEPSC (right) frequency. D, Individual values and mean ± SEM sEPSC (left) and mEPSC (right) amplitude. * $p<0.05$ calculated by two-way ANOVA/Holm-Sidak.

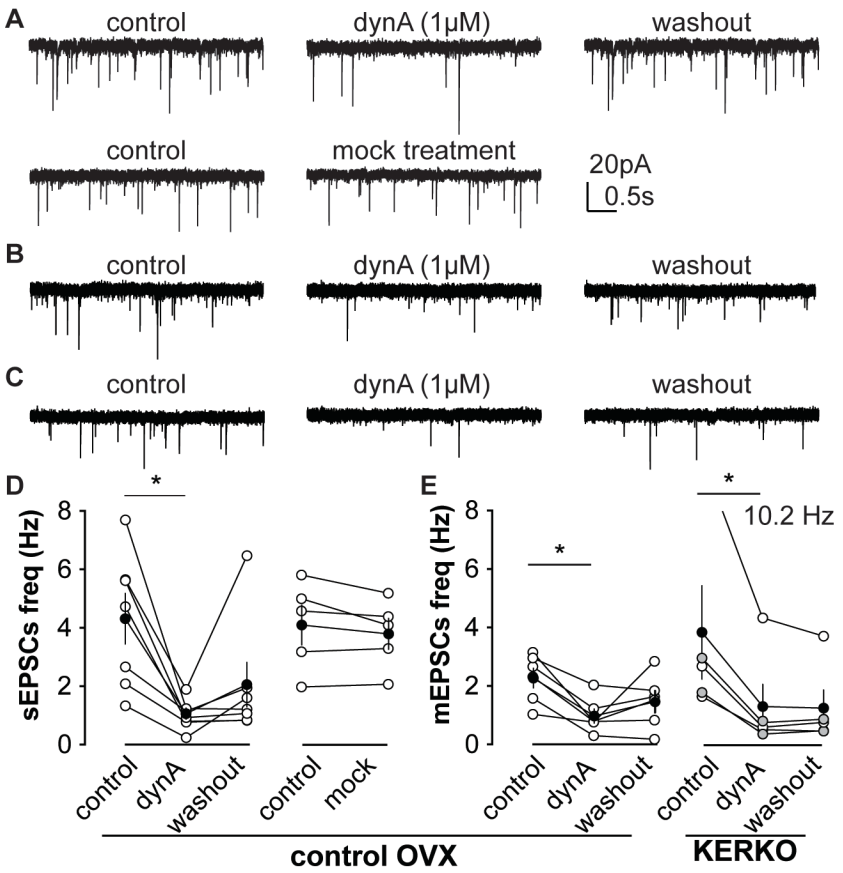

Figure 3-5 Dynorphin suppresses both sEPSC and mEPSCs frequency in arcuate kisspeptin neurons.

A, representative sEPSCs in arcuate kisspeptin neurons in OVX mice during control, dynA treatment and washout period (upper) and during control and mock treatment (lower). B and C, representative mEPSCs during control, dynA treatment and washout period in arcuate kisspeptin neurons in OVX control mice (B) and in OVX KERKO mice (C). D, Individual values (white) and mean ± SEM (black) and sEPSC frequency in arcuate during control, treatment and washout (left) and during control and mock treatment (right). One data point that was out of range of the axes is indicated in text (10.2Hz). For dynA treatment (left), Friedman statistic=8.9; for mock treatment (right), t statistic=1.5, degrees of freedom (df) =4. E, Individual values (white OVX, grey OVX+E) and mean ± SEM (black) mEPSC frequency during control, treatment and washout in OVX control mice (left, one-way ANOVA, treatment, $F(2,10)=4.9$; individual, $F(5,10)=1.5$) and in KERKO mice (right, Friedman statistic, 7.6). * $p<0.05$.

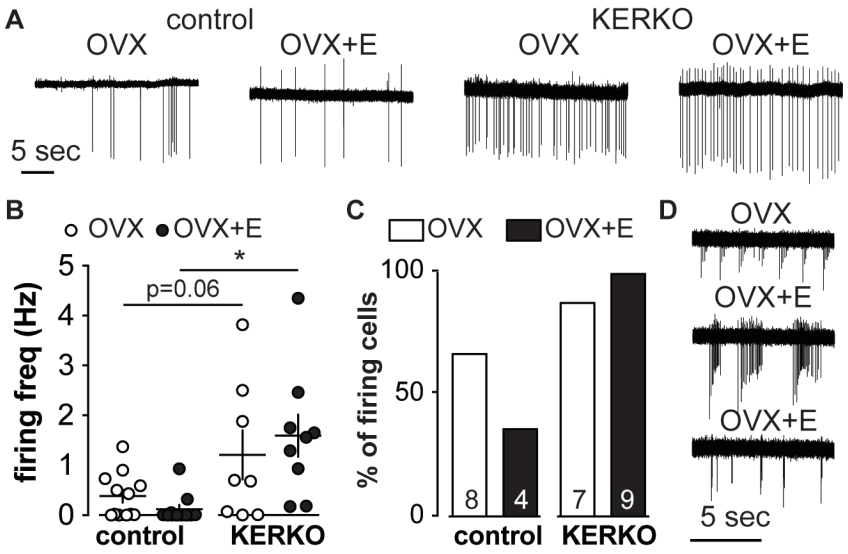

Figure 3-6 The short-term firing frequency of KNDy neurons was not modulated by estradiol, but was elevated in cells from KERKO mice.

A, representative extracellular recordings from each group. B, individual values and mean ± SEM firing frequency in OVX and OVX+E control and KERKO mice. C, percentage of spontaneously active cells in each group; number in bar is total number of cells. D, all bursting cells recorded in KERKO group. * $p<0.05$ calculated by two-way ANOVA/Holm-Sidak. Note difference in timescale between A and D.

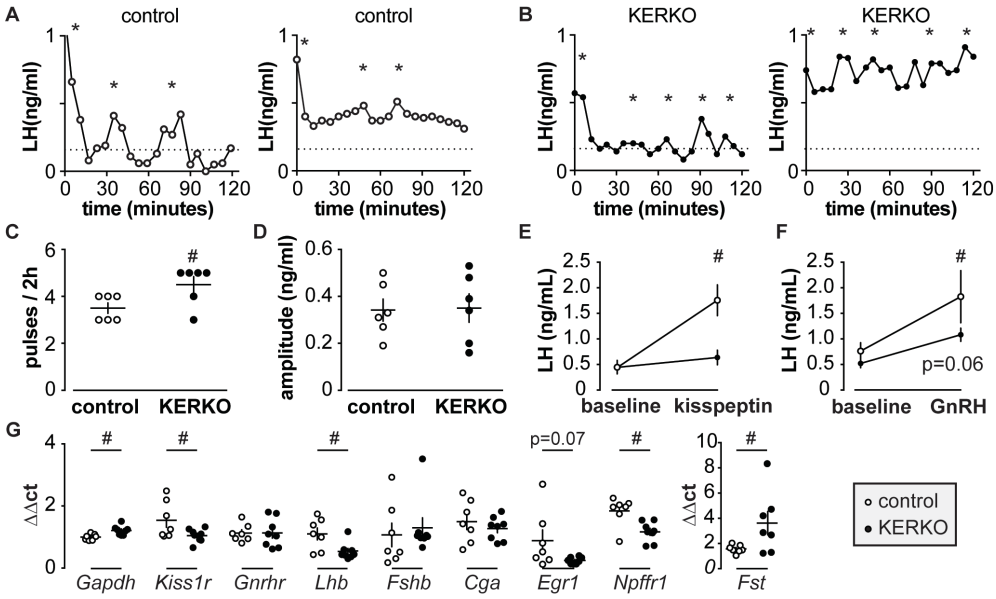

Figure 3-7 ERα in kisspeptin cells is required for estradiol negative feedback regulation of LH pulse frequency and pituitary response to kisspeptin.

A and B, representative LH patterns over 2h in ovary-intact estrous control (A) and KERKO (B) adult mice. * indicates LH pulses detected with Cluster. C and D, individual values and mean ± SEM LH pulse frequency (C) and amplitude (D); # $p<0.05$ unpaired Student's t test. Statistical parameters: C, degrees of freedom (df)=10, t statistic=2.5; D, df=10, t statistic=0.1. E and F, mean ± SEM LH before and after IP injection of kisspeptin (E) or GnRH (F); # $p<0.05$ two-way repeated measures ANOVA/Holm-Sidak; statistical parameters: E, treatment, $F(1,10)=40.2$*, genotype, $F(1,10)=5.3$*, interaction, $F(1,10)=23.4$*; F, treatment, $F(1,10)=18.3$*, genotype, $F(1,10)=2.0$, interaction, $F(1,10)=1.8$; *$p < 0.05$. G, Individual values and mean ± SEM normalized relative expression ($\Delta\Delta$ct) of genes in pituitary. All gene expression was normalized to βactin gene (Actb). # $p<0.05$ calculated by unpaired two-tailed Student's t-test, except Lhb, Fshb and Npffr1 for which two-tailed Mann-Whitney U test was used. Statistical parameters: df=13 (except Fst, df=12); t statistics, Gapdh, 3.2; Kiss1r, 2.2; Gnrhr, 0.02; Cga, 0.8; Egr1, 2.0; Fst, 2.2; Mann-Whitney U value, Lhb, 8.5; Fshb, 20; Npffr1, 6.

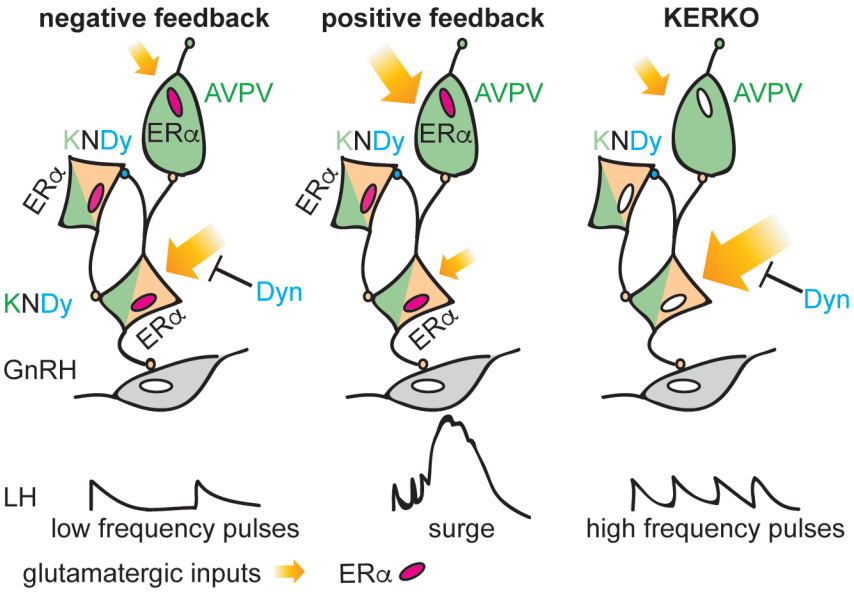

Figure 3-8 Schematic diagrams.

Schematic of estradiol feedback regulation of glutamatergic transmission to AVPV and arcuate kisspeptin neurons during negative feedback (left), positive feedback (middle) and KERKO mice (right, loss of feedback). The deletion of ERα from kisspeptin cells disrupts glutamatergic transmission to kisspeptin neurons and the negative feedback regulation on LH pulses.

Tables

Table 3-1 Integrative DNA technologies qPCR assays for pituitary gene expression

Gene	IDT assay ID	Ref Seq No.	Exons	Amplicon size, bp	Amplicon location, bp
Gapdh	Mm.PT.39.1	NM_008084	2-3	140	250-389
Actb	Mm.PT.39a.22214843.g	NM_007393	5-6	147	1057-1203
Kiss1r	Mm.PT.49a.16255718.g	NM_053244	5-5	76	2626-2701
Gnrhr	Mm.PT.45.16240237	NM_010323	1-2	93	573-665
Npffr1	Mm.PT.49a.12363343	NM_001177511	3-4	128	342–469
Lhb	Mm.PT.45.5612498	NM_008497	2-3	91	137–227
Fshb	Mm.PT.45.17694677	NM_008045	1-2	104	2–105
Cga	Mm.PT.58.31855537	NM_009889	1-2	109	33-141
Egr1	Mm.PT.45.13313108	NM_007913	1-2	115	523–637
Fst	Mm.PT.45.6344184	NM_008046	5-6	88	1295–1382

Table 3-2 Statistical parameters for one-way ANOVA or Kruskal-Wallis test parameters for comparison among groups.

	Parameter (figure)	Diestrus, proestrus, estrus and KERKO
AVPV	sEPSC frequency (Figure 1C)	Kruskal-Wallis statistic = 16.8***
	sEPSC amplitude (Figure 1D)	Kruskal-Wallis statistic = 3.9
	mEPSC frequency (Figure 1C)	F (3,38) = 3.259*
	mEPSC amplitude (Figure 1D)	F (3,38) = 1.85
arcuate nucleus	sEPSC frequency (Figure 3C)	Kruskal-Wallis statistic = 25.8****
	sEPSC amplitude (Figure 3D)	F (3,43) = 0.2087
	mEPSC frequency (Figure 3C)	F (3,39) = 43.5****
	mEPSC amplitude (Figure 3D)	F (3,39) = 0.7656

*p < 0.05; **p < 0.01; ***p < 0.001.

Table 3-3 Statistical parameters for two-way ANOVA test parameters for comparison among groups: OVX and OVX+E treatment of control and KERKO mice.

Parameter (figure)	Estradiol	Genotype	Interaction
AVPV			
sEPSC frequency (Figure 2C)	F(1,37)=6.4*	F(1,37)=0.2	F(1,37)=2.5
sEPSC amplitude (Figure 2D)	F(1,37)=0.1	F(1,37)=0.3	F(1,37)=0.1
mEPSC frequency (Figure 2C)	F(1,36)=1.8	F(1,36)=0.4	F(1,36)=3.4
mEPSC amplitude (Figure 2D)	F(1,36)=1.1	F(1,36)=2.2	F(1,36)=0.03
arcuate nucleus			
sEPSC frequency (Figure 4C)	F(1,38)=1.1	F(1,38)=24.7***	F(1,38)=5.8*
sEPSC amplitude (Figure 4D)	F(1,38)=0.2	F(1,38)=1.9	F(1,38)=0.4
mEPSC frequency (Figure 4C)	F(1,36)<0.01	F(1,36)=19.2***	F(1,36)<0.01
mEPSC amplitude (Figure 4D)	F(1,36)=1.0	F(1,36)=0.5	F(1,36)=0.07
extracellular			
firing frequency (Figure 6B)	F(1,36)=0.01	F(1,36)=14.8***	F(1,36)=1.0

*p < 0.05; **p < 0.01; ***p < 0.001.

Table 3-4 Kinetics of sEPSCs and mEPSCs in AVPV and arcuate kisspeptin neurons; no statistic difference noticed

		Rise time (ms)	FWHM (ms)	Decay (ms)
AVPV sEPSCs				
Ovary-intact	diestrus	0.25±0.02	2.3±0.1	3.6±0.2
	proestrus	0.25±0.01	2.0±0.1	3.2±0.1
	estrus	0.28±0.04	2.3±0.1	3.6±0.3
	KERKO	0.27±0.04	2.0±0.1	3.0±0.3
control	OVX	0.26±0.03	2.3±0.1	3.6±0.2
	OVX+E	0.25±0.03	2.1±0.1	3.3±0.2
KERKO	OVX	0.23±0.03	2.0±0.2	3.5±0.2
	OVX+E	0.23±0.03	2.1±0.2	3.8±0.4
AVPV mEPSCs				
Ovary-intact	diestrus	0.28±0.02	2.7±0.2	3.5±0.3
	proestrus	0.27±0.02	2.5±0.2	3.3±0.3
	estrus	0.21±0.03	2.0±0.1	3.2±0.2
	KERKO	0.24±0.02	2.1±0.2	3.3±0.4
control	OVX	0.28±0.04	2.7±0.1	3.9±0.3
	OVX+E	0.30±0.05	2.1±0.1	2.9±0.2
KERKO	OVX	0.24±0.01	2.1±0.1	3.7±0.3
	OVX+E	0.26±0.03	2.2±0.4	3.7±0.2
arcuate sEPSCs				
Ovary-intact	diestrus	0.21±0.03	2.5±0.2	3.6±0.3
	proestrus	0.19±0.03	2.1±0.1	3.7±0.2
	estrus	0.18±0.03	2.0±0.1	4.0±0.2
	KERKO	0.20±0.04	2.3±0.2	3.6±0.3
control	OVX	0.25±0.03	2.1±0.1	3.4±0.2
	OVX+E	0.21±0.03	2.1±0.1	4.3±0.2
KERKO	OVX	0.17±0.03	2.0±0.2	3.8±0.6
	OVX+E	0.22±0.03	2.0±0.1	3.3±0.2
arcuate mEPSCs				
Ovary-intact	diestrus	0.23±0.02	2.2±0.1	3.6±0.3
	proestrus	0.19±0.02	2.2±0.1	4.0±0.2
	estrus	0.18±0.02	2.0±0.1	3.8±0.2
	KERKO	0.18±0.02	2.4±0.2	3.8±0.4
control	OVX	0.24±0.04	2.1±0.2	3.6±0.2
	OVX+E	0.22±0.04	2.2±0.2	4.4±0.3
KERKO	OVX	0.24±0.03	2.1±0.2	3.6±0.3
	OVX+E	0.21±0.03	1.9±0.2	3.0±0.2

Chapter 4 CRISPR-Cas9 Mediated Deletion of ERα in AVPV Kisspeptin Neurons in Adulthood

Abstract

The brain regulates fertility through gonadotropin-releasing hormone (GnRH) neurons. Estradiol induces negative feedback on pulsatile GnRH release and positive feedback generating GnRH/luteinizing hormone (LH) surges. Negative and positive feedback are postulated to be mediated by kisspeptin neurons in arcuate and anteroventral periventricular (AVPV) kisspeptin neurons, respectively. Kisspeptin-specific ERα knockout (KERKO) mice exhibit disrupted pulse patterns and lack an LH surge. Here we show the estradiol-induced increase in excitability of AVPV kisspeptin neurons is lost in KERKO mice. We further tested organizational vs activational roles of ERα specifically in AVPV kisspeptin neurons by deleting ERα from only this region in adulthood. AAV vectors were designed to mediate CRISPR/Cas9 target *Esr1* gene deletion only in AVPV kisspeptin cells. Firing signatures of AVPV kisspeptin neurons that lost ERα in adulthood were comparable to those in KERKO mice, suggesting activational effects of estradiol can regulate firing activity.

Introduction

Infertility is a common clinical problem affecting 15% of couples; ovulatory disorders account for 25% of this total[206]. The hypothalamic-pituitary-gonadal (HPG) axis controls reproduction and malfunction of the HPG axis can cause ovulatory disorders and/or other disturbances of the reproductive cycle[7,207].

Gonadotropin-releasing hormone (GnRH) neurons form the final common pathway for regulation of reproduction by the hypothalamic component. GnRH stimulates the pituitary to secrete follicle-stimulating hormone and luteinizing hormone (LH), which regulate gonadal steroid production. Estradiol, via estrogen receptor alpha (ERα), plays crucial roles in both homeostatic negative feedback and positive feedback to GnRH/LH release[13,15,119]. In female, low estradiol levels suppress GnRH neuron activity and release, whereas sustained elevations in estradiol during the late follicular phase of the cycle cause a switch of estradiol action from negative to positive feedback, inducing elevated GnRH/LH release and triggering ovulation[116]. As GnRH neurons typically do not express detectable ERα[61], estradiol feedback is likely transmitted to GnRH neurons by ERα-expressing afferents.

Kisspeptin neurons in the arcuate and anteroventral periventricular (AVPV) regions are estradiol-sensitive GnRH afferents that are postulated to mediate estradiol negative and positive feedback, respectively. Kisspeptin potently stimulates GnRH neurons and *Kiss1* mRNA is differentially regulated in these nuclei by estradiol[69,72,83,88,96,120,121]. AVPV kisspeptin neurons increase cFos expression during positive feedback[88] and, in brain slices, these neurons are more excitable during positive feedback compared to negative feedback, a shift mediated by estradiol[126,167]. Estradiol also alters fast synaptic transmission to these cells, increasing glutamatergic inputs on proestrus and reducing GABAergic transmission[137,208]. It is thus not known if the shifted excitability in AVPV kisspeptin neurons requires ERα in kisspeptin cells or is derived from altered neuromodulatory input.

ERα in kisspeptin cells is critical for estradiol negative and positive feedback, as kisspeptin-specific ERα knockout (KERKO) mice exhibit higher frequency LH pulses and fail to exhibit an estradiol-induced LH surge[103,124,168,208]. Although informative, the KERKO model has several caveats that limit interpretation. First, ERα is deleted as soon as *Kiss1* is expressed, before birth in KNDy neurons and

before puberty in AVPV kisspeptin neurons [202,203]. This may cause developmental changes in these cells. Second, ERα is deleted from all kisspeptin cells, thus making it impossible to assess independently the role of AVPV and arcuate kisspeptin neurons. Combining CRISPR-Cas9 with targeted viral vector injection allows deletion of ERα in a nucleus-specific and temporally-controlled manner to address the above caveats[209]. We designed cre-dependent AAV vectors that carry single guide RNAs (sgRNAs) that target *Esr1* (encoding ERα) or *Lacz* and delivered these vectors to the AVPV of adult female mice that express Cas9 in kisspeptin cells. We compared the reproductive phenotypes as well as kisspeptin neuronal excitability Cas9-AAV targeted mice with KERKO and control mice.

Materials and Methods

All chemicals were purchased from Sigma Chemical Company (St Louis, MO) unless noted.

Animals. The University of Michigan Institutional Animal Care and Use Committee approved all procedures. Adult female mice aged 60-150 days were used for these studies. All mice were provided with water and Harlan 2916 chow (VetOne) *ad libitum* and were held on a 14L:10D light cycle with lights on at 0400 Eastern Standard Time. To delete ERα specifically from kisspeptin cells, as previously reported[208], mice with the *Cre* recombinase gene knocked-in after the *Kiss1* promoter (Kiss-Cre mice) were crossed with mice with a floxed *Esr1* gene, which encodes ERα (ERα floxed mice)[168]. The expression of Cre recombinase mediates deletion of ERα in all kisspeptin cells (KERKO mice). To visualize kisspeptin neurons for recording, mice heterozygous for both Kiss-Cre and floxed ERα were crossed with Cre-inducible YFP mice. Crossing mice heterozygous for all three alleles yielded litters that contained some mice that were homozygous for floxed ERα and at least heterozygous for both Kiss-Cre and YFP; these were used as KERKO mice. Littermates of KERKO mice with wild type *Esr1,* Kiss-Cre YFP were used as controls; no differences were observed among these controls

and they were combined. To generate kisspeptin-specific Cas9 expressing mice, mice with *Cre* recombinase gene knocked-in after the *Kiss1* promoter (*Kiss1*-Cre mice) were crossed with mice that have Cre recombinase-dependent expression of CRISPR associated protein 9 (Cas9) endonuclease, a 3X-FLAG epitope tag and EGFP directed by a CAG promoter. Ovary-intact KERKO mice have disrupted estrous cycles with persistent cornified vaginal cytology typical of estrus; we thus used females in estrus as controls; estrous cycle stage was determined by vaginal lavage. To examine the role of circulating estradiol, mice were ovariectomized (OVX) under isoflurane anesthesia (Abbott) and were either simultaneously implanted with a Silastic (Dow-Corning) capsule containing 0.625µg of estradiol suspended in sesame oil (OVX+E) or not treated further (OVX)[12]. Bupivacaine (0.25%, APP Pharmaceuticals) was provided local to the incisions as an analgesic. These mice were studied 2-3d post-surgery. Mice for electrophysiological studies were sacrificed in the late afternoon which is the time of estradiol positive feedback[12]; for free-floating immunochemistry staining, mice were sacrificed at 1700 EST 2-3d post OVX+E surgery, when the pick of estradiol induced LH surge was expected.

sgRNA design. For spCas9 targets selection and generation of single guide RNA (sgRNA), 20-nt target sequences were selected to precede a 5'NGG protospacer-adjacent motif (PAM) sequence. To minimize off-targeting effects and maximize sgRNA activity, two CRISPR design tools were used to evaluate the sgRNAs[210,211] that target mouse gene *Esr1* exon1 sequences. The two best candidate sgRNAs were selected based on predicted lowest off-target effects and highest activity. The 1st sgRNA target sequence is 5'-CACTGTGTTCAACTACCCCG-3' and the 2nd sgRNA target sequence is 3'-CTCGGGGTAGTTGAACACAG-5'. Control sgRNA sequence was designed to target *Lacz* gene from *Escherichia coli* (target sequence: 5'-TGCGCAGCCTGAATGGCGAA -3').

In vitro validation of sgRNAs. C2C12 mouse myoblast cells (a generous gift of Dr. Daniel Michele, University of Michigan) were grown in DMEM (Dulbecco's Modified Eagle Medium, Thermo Fisher) containing 10% FBS (Thermo Fisher) at

37°C in a 5% CO2 atmosphere. Each individual sgRNA was introduced to BsmBI site of the lentiCRISPRv2 construct. Cells were transiently co-transfected with one of the lentiCRISPRv2 plasmids containing sgRNAs and a standard GFP plasmid construct[212] using Lipofectamine 3000 (Invitrogen) according to the manufacturer's instructions. Cells were selected for more than 3 weeks with 1 µg/ml puromycin. Cells were harvested, and DNA was isolated using the Qiagen DNA Extraction Kit (Qiagen, Valencia, CA) and sequenced by the sequencing core at the University of Michigan.

AAV vector production. To construct the AAV plasmid, a mCherry-U6 promoter-sgRNA scaffold segment was synthesized by IDT. After PCR amplification, the ligation product containing mCherry-U6 promoter-sgRNA scaffold was cloned in reverse orientation into a Cre-inducible AAV vector backbone[213]. The individual sgRNAs were then inserted into the designed SapI site between U6 promoter and sgRNA scaffold component. The AAV8 viral stocks were prepared at University of North Carolina (UNC) Vector Core (Chapel Hill, North Carolina, USA).

Stereotaxic injections. Kiss1Cre/Cas9-GFP female animals at least two months of age were selected, and estrous cycles monitored for >10days before surgery; only mice with normal cycles were used further. Mice were anesthetized with 1.5%–2% isoflurane in preparation for craniotomy. The skull was exposed, bregma and lambda were leveled, a hole was drilled, and 100 nl virus injected bilaterally via a pulled pipette at the target coordinates at ~5 nl/min. For the AVPV region, the coordinates were anteroposterior (AP) +0.98, mediolateral (ML) ± <0.2 and dorsoventral (DV) -4.7 to -4.8. The pipette was left in place for 5 min after injection to allow the virus to diffuse into the brain, then the pipette was slowly removed. Carprofen (Rimadyl, 5 mg/kg) were given to the mice before and 24hrs after the surgery to alleviate postsurgical pain. During a 4wk postsurgical recovery, estrous cycles were monitored daily.

Perfusion and free-floating immunohistochemistry. Mice were anesthetized with isoflurane and then transcardial perfused with PBS followed by 10% neutral-buffered formalin for 10min (~50mL). Brains were removed and placed into the

same fixative overnight, followed by 30% sucrose for at least 24h for cryoprotection. Brains were cut into 30µm sections on using a cryostat (Leica CM3050S) in four series and stored at -20°C in antifreeze solution (25% ethylene glycol, 25% glycerol). For staining, sections were washed with PBS and then treated with 0.1% hydrogen peroxide. Sections were then placed in blocking solution (PBS containing 0.1% Triton X-100, 4% normal goat serum) for 1h, then incubated with rabbit anti-ERα (#06-935，Millipore, 1:10000 in blocking solution) for 48h at 4°C . The sections were washed then incubated with biotinylated anti-rabbit antibody (Jackson Immunoresearch, 1:500) followed by ABC amplification (Vector Laboratories, 1:500) and nickel-enhanced diaminobenzidine (Thermo Scientific) reaction (4.5 min). Sections were washed with PBS and incubated overnight with chicken anti-GFP (ab13970, Abcam, 1:2000) and rat anti-mCherry (# M11217, Invitrogen, 1:5000) in blocking solution. The next day, sections were washed and incubated with Alexa 594-conjugated anti-rat and Alexa 488-conjugated anti-chicken antibodies for 1hr at room temperature (Molecular Probes, 1:500). Sections were mounted and coverslipped (VWR International No. 48393 251). Images were collected on a Zeiss AXIO Imager M2 microscope, and the number of immunoreactive GFP alone, GFP/mCherry, and GFP/mCherry/ERα cells were counted in AVPV region. The arcuate region in the hypothalamus was examined and no infection of kisspeptin cell bodies was observed.

Extracellular recordings. All recordings were made with receptors for ionotropic $GABA_A$ and glutamate synaptic transmission antagonized with a combination of picrotoxin (100µM), APV (D-(−)-2-amino-5-phosphonovaleric acid, 20µM), and CNQX (6-cyano-7-nitroquinoxaline, 10µM). Extracellular recordings were made as it maintains internal milieu and has minimal impact on the firing rate of neurons [134,135]. Recording pipettes were filled with HEPES-buffered solution containing (in mM): 150 NaCl, 10 HEPES, 10 D-glucose, 2.5 $CaCl_2$, 1.3 MgCl2, and 3.5 KCl (pH=7.4, 310 mOsm), and low-resistance (22±3 MΩ) seals were formed between the pipette and neuron after first exposing the pipette to the slice tissue in the absence of positive pressure. Recordings were made in voltage-

clamp mode with a 0 mV pipette holding potential and signals acquired at 20 kHz and filtered at 10 kHz. Resistance of the loose seal was checked frequently during first 3 min of recordings to ensure a stable baseline, and also before and after a 10-min recording period; data were not use if seal resistance changed >30% or was >25 MΩ. The first 5 min of this 10-min recording were consistently stable among cells and were thus used for analysis of firing rate and burst properties.

Whole-cell recordings. For whole-cell patch-clamp recording, three pipette solutions were used. Most recordings were done with a physiologic pipette solution containing (in mM): 135 K gluconate, 10 KCl, 10 HEPES, 5 EGTA, 0.1 $CaCl_2$, 4 MgATP and 0.4 NaGTP, pH 7.2 with NaOH, 305 mOsm. A neurobiotin-contained solution was made and adjusted to similar Osmolarity containing (in mM): 35 K gluconate, 10 KCl, 10 HEPES, 5 EGTA, 0.1 $CaCl_2$, 4 MgATP and 0.4 NaGTP, pH 7.2 with NaOH, 10 neurobiotin (Vector laboratories). A cesium-based pipette solution, in which cesium gluconate replaced potassium gluconate, was used to reduce potassium currents and allow better isolation of calcium currents. All potentials reported were corrected online for liquid junction potential of -15.7 mV for the K-gluconate solutions with or without neurobiotin or -15.2 mV for the Cs^+-based solution[136].

After achieving a minimum 1.6 GΩ seal and the whole-cell configuration, membrane potential was held at -70 mV between protocols during voltage-clamp recordings. Series resistance (R_s), input resistance (R_{in}), holding current (I_{hold}) and membrane capacitance (C_m) were frequently measured using a 5 mV hyperpolarizing step from -70 mV (mean of 16 repeats, 20 ms duration). Only recordings with R_{in} >500 MΩ, I_{hold} -40 to10 pA and R_S < 20 MΩ, and stable C_m were used for analysis. R_s was further evaluated for stability and any voltage-clamp recordings with ΔR_s >15% before and after the recording protocols were excluded from analysis; current-clamp recordings with ΔR_s >20% were excluded. There was no difference in I_{hold}, C_m, or R_s among any comparisons.

For current-clamp recordings, depolarizing and hyperpolarizing current injections (-50 pA to +50 pA for 500 ms, 5 pA steps) were applied to cells from an initial voltage of -71± 2 mV, close to their resting membrane potential -68.8±1.9 mV [137]. For voltage-clamp protocols for I_T, ACSF containing antagonists of ionotropic $GABA_A$ and glutamate receptors with TTX (2 μM) and Cs-based internal solution were used for all recordings to isolate calcium-currents. Two voltage protocols were used to isolate I_T as previously reported[167]. First, total calcium current activation was examined. Inactivation was removed by hyperpolarizing the membrane potential to −110 mV for 350 ms (not shown). Next a 250 ms prepulse of -110 mV was given. Then membrane potential was varied in 10 mV increments for 250 ms from −110 mV to -30 mV. Finally, test pulse of -40 mV for 250 ms was given. From examination of the current during the test pulse, it was evident that no sustained (high-voltage activated) calcium current was activated at potentials more hyperpolarized than -40 mV. To remove HVA contamination from the step to -30 mV, a second protocol was used in which removal of inactivation (-110 mV, 350 ms) was followed by a 250 ms prepulse at -40 mV, then a step for 250 ms at -30 mV and finally a test pulse of -40 mV for 250 ms. I_T was isolated by subtracting the trace following the -40 mV prepulse from those obtained after the -110 mV prepulse for the depolarized variable step to -30 mV; raw traces from the initial voltage protocol were used without subtraction for variable steps from -110 mV to -40 mV because of the lack of observed activation of HVA at these potentials. Activation of I_T was assessed from the resulting family of traces by peak current during the variable step phase. Inactivation of I_T was assessed from the peak current during the final -40 mV test pulse.

Post hoc identification of ERα. Pipette solution with neurobiotin was used for recordings of cells from CRISPR AAV infected mice. An outside-out patch was formed after each recording to reseal the membrane and location of the cells was marked on a brain atlas[133]. The 300 μm brain slices were fixed overnight in 10% formalin at 4°C and changed to PBS the next day. Slices were photo-bleached with a UV illuminator for ~72h and further checked to make sure no visible

fluorescent signal is observed. Sections were then placed in blocking solution (PBS containing 0.1% Triton X-100, 4% normal goat serum) for 1h, then incubated with rabbit anti-ERα (#06-935, Millipore, 1:10000 in blocking solution) for 48 h at 4°C. The sections were washed then incubated with Alexa 594-conjugated anti-rabbit and Alexa 350-conjugated neutravidin for 1h at room temperature (Molecular Probes, 1:500). Sections were mounted and coverslipped with (VWR International No. 48393 251). Images were collected on a Zeiss AXIO Imager M2 microscope. Cells with neurobiotin-labeled were imaged to determine if they showed ERα-immunoreactivity.

Data analysis and statistics. Data were analyzed offline using custom software written in IgorPro 6.31 (Wavemetrics) or MATLAB 8.4 (MathWorks, Inc.). For targeted extracellular recordings, mean firing rate in Hz was determined over 5 min of stable recording. In experiments examining I_T, the peak current amplitude at each step potential (V) was first converted to conductance using the calculated reversal potential of Ca^{2+} (E_{Ca}) and $G=I/(E_{Ca} - V)$, because driving force was linear over the range of voltages examined. The voltage dependencies of activation and steady-state inactivation were described with a single Boltzmann distribution: $G(V)= G_{max}/(1- \exp [(V_{1/2} - V_t)/k])$, where G_{max} is the maximal conductance, $V_{1/2}$ is the half-maximal voltage, and k is the voltage dependence (slope) of the distribution. Current density of I_T at each tested membrane potential was determined by dividing peak current by membrane capacitance. Data were analyzed using Prism 7 (GraphPad Software) and reported as mean ± SEM. The number of cells per group is indicated by n. Data were normally distributed and thus comparisons among groups were two-way ANOVA or two-way repeated measures (RM)with Holm-Sidak *post hoc* analysis. For categorical data analysis, Chi-square test of independence were used to test the null hypothesis that categorical variables have no correlation with each other. For each electrophysiological parameter comparison, no more than 3 cells per mouse was used in control and KERKO mice; no more than 4 cells per mouse was used for AAV infected mice. No less than 5 mice were tested per parameter. The variance

of the data was no smaller within an animal than among animals. For IHC staining, no less than 3 mice were tested per AAV vector.

Results

AVPV kisspeptin neurons exhibit decreased excitability in KERKO mice compared to control and failed to respond to estradiol.

We first used extracellular recordings to monitor the spontaneous firing rate of YFP-identified AVPV kisspeptin neurons in coronal brain slices from ovary-intact control and KERKO mice. As the persistent cornified vaginal cytology of KERKO mice is similar to estrus[168], we used mice in the estrous stage of the reproductive cycle as controls. The firing frequency in AVPV kisspeptin neurons was lower in KERKO mice compared to control (Figure 4-1a,b, two-way ANOVA/Holm-Sidak, $p=0.0001$). To test if the firing rate of AVPV kisspeptin neurons in KERKO mice responds to circulating estradiol, we repeated this study in ovariectomized (OVX) and OVX mice with an estradiol implant reproducing physiologic levels (OVX+E). Estradiol treatment increased firing rate in cells from control mice, but not KERKO mice (Figure 4-1 a,b two-way ANOVA/Holm-Sidak, control OVX vs OVX+E, $p<0.0001$, KERKO OVX vs OVX+E, $p=0.9$). We next recorded the whole-cell firing signatures of these neurons in response to current injection in all four groups described above. AVPV kisspeptin neurons in control mice exhibit more depolarization-induced bursts (DIB) and rebound bursts when estradiol is elevated, confirming previous observations[167] (Figure 4-1,c,d,e, Chi-square, DIB, $p=0.04$; rebound, $p=0.03$). These two bursting features were rare in KERKO mice under all conditions and were not regulated by estradiol (Figure 4-1, c,d,e, Chi-square, DIB, $p=0.4$, rebound, $p=0.3$). We also compared the action potential output of these cells in response to current injection (0-50 pA, 10 pA increment, 500 ms). Cells from KERKO mice generated fewer action potentials compared to ovary-intact and OVX+E controls, and were similar to cells from the OVX control group (Figure 4-1f, two-way repeated-measures ANOVA/Holm-Sidak, intact, 20pA, $p=0.03$, 30 pA, $p=0.06$; OVX+E, 20 pA,40 pA, 50 pA, $p=0.04$, 30 pA,

p=0.02). This may be attributable at least in part to decreased input resistance in cells from KERKO mice compare to controls (two-way ANOVA/Holm-Sidak, controls 1153±110 MΩ intact, 1040±142 MΩ OVX, 1341±162 MΩ OVX+E; KERKO 720±41 MΩ intact, 974±103 MΩ OVX, 989±89 MΩ OVX+E, control vs KERKO, intact p=0.02, OVX+E p=0.06).

As both depolarization-induced bursts and rebound bursts are sensitive to NiCl at levels that fairly specifically block T-type calcium channels, we measured T-type current density (I_T). I_T was decreased in AVPV Kisspeptin cells from gonad-intact KERKO mice compared to controls (Figure 4-1g,h two-way repeated-measures ANOVA/Holm-Sidak, -50 mV, p=0.003; -40 mV, p=0.002; -30 mV, p=0.003). The activation curve was not different between groups, but the inactivation curve was depolarized in cells from KERKO mice (Figure 4-1i, control vs KERKO, unpaired two-tailed Student's *t*-test, $V_{1/2}$ activation -52.7±1.6 vs -49.2±0.5 mV, p>0.1; slope 6.3 ±1.3 vs 4.7±0.4, p>0.1; $V_{1/2}$inactivation -72.5±2.7 vs -53.9±1.3 mV, p=0.02; slope -11.3±2.8 vs -7.6±1.1, p=0.01).

Design and validation of sgRNAs that target Esr1.

A caveat of studying the role of ERα in AVPV kisspeptin neurons using KERKO mice is that the deletion of ERα (encoded by *Esr1*) using cre recombinase under the control of the kisspeptin promoter is neither time-specific nor location-specific. We thus utilized the CRIPSR-Cas9 approach to achieve temporal and spatial control of *Esr1* gene knock down. We first designed two sgRNAs that target exon1 of *Esr1* based on software prediction[210] and tested the efficiency of each guide *in vitro* in C2C12 mouse myoblast cells. The sgRNAs that target *Esr1* and a sgRNA that targets *Lacz* as a control were subcloned into the lentiCRISPRv2 plasmid[214], from which Cas9 and the sgRNA are expressed after transient transfection of C2C12 cells. Puromycin was used to select successfully infected cells. After a ≥3-week selection period, we harvested the cells and sequenced the *Esr1* region. Cells infected with the sgRNAs targeting *Esr1,* but not *Lacz*, exhibited a peak-on-peak sequencing pattern, indicating disruption of

the gene (Figure 4- 2c). As these *in vitro* experiments suggested sgRNAs were able to mutate *Esr1*, we designed a Cre-dependent AAV vector that expresses the sgRNA and mCherry under control of the U6 promoter; mCherry was used to indicate infection of cre-expressing cells (Figure 4-2b). The AAV vector was bilaterally stereotaxically injected into the AVPV region of adult female mice that express Cas9 and GFP under control of the kisspeptin promoter (Figure 4-2 a,d,e). The ERα knockout efficiency of the two sgRNAs that targeted *Esr1* were comparable thus we combined them as a group in the following studies. The infection rate for AAV-*Esr1* was 79±4% (n=4, Fig2f) and only 27±1% of kisspeptin cells expressed ERα (n=3, Figure 4-2g); in mice that received AAV-*Lacz*, the infection rate was comparable at 81±2%, but 70±1% of kisspeptin neurons expressed ERα, which is comparable to control mice[121](Figure 4-2f,g).

Deletion of ERα in AVPV kisspeptin neurons in adulthood does not affect estrous cycles.

We monitored the reproductive cycles of the mice injected with AAV-sgRNAs for ≥10 days before and for up to 6wk following surgery. Neither AAV-*Esr1* nor AAV-*Lacz* disrupted reproductive cyclicity (Figure 4-2h, red dot indicates day of injection), even in mice with a high rate of bilateral infection (~80%).

Decreased excitability of AVPV kisspeptin neurons in AAV-Esr1 knockdown mice.

To test if knockdown of ERα in AVPV kisspeptin neurons alters their intrinsic excitability, we recorded firing signatures of infected and uninfected cells in OVX+E mice. Cells were loaded with neurobiotin during recording for identification and stained for ERα *post hoc* (Figure 4-3a-d). Cells not infected with AAV-*Esr1* and cells infected with either AAV-*Esr1* but in which ERα protein was detected exhibited similar firing signatures in terms of DIB and rebound bursts. In contrast, cells infected by AAV-*Esr1* that had undetectable ERα protein had reduced burst firing compared to AAV-LacZ or uninfected groups (Figure 4-3f

DIB, Chi-square, p=0.006; 4-3g, rebound, Chi-square, p=0.001). The AAV-*Esr1* group are comparable to KERKO (Figure 4-3f,g DIB and rebound, Chi-square, p>0.9 for both). These cells that lost ERα after AAV-*Esr1* infections also exhibited decreased number of action potentials with step current injection compared to cells infected with AAV-*Lacz* (Figure 4-3e, two-way repeated-measures ANOVA/Holm-Sidak, AAV-*Esr1* vs AAV-*Lacz,* 20 pA, p=0.08; 30 pA, 40 pA, p=0.02; 50 pA, p=0.01). In contrast to cells from KERKO mice, input resistance was not reduced in *Esr1* knockdown mice (one-way ANOVA/Holm-Sidak, *Esr1* vs *Lacz* vs uninfected, 1255±79 MΩ, 1324±86 MΩ, 1359±107 MΩ, p>0.8 for each comparison), suggesting the increased excitability may be due to other reasons. The relationship between current injection and number of action potentials fired (input-output curve) in cells from KERKO and in AAV-*Esr1* knockdown mice was only different at 50pA injection, with AAV-*Esr1* infected cells less excitable at this high current injection (Figure 4-3e, two-way repeated-measures ANOVA/Holm-Sidak, 50pA, p=0.01). Input resistance was greater in cells from AAV-*Esr1* knockdown mice compared to KERKO mice (unpaired two-tailed Student's *t* test, AAV-Esr1, 1255± 78 MΩ vs 989±83 MΩ, p=0.03).

Discussion

AVPV kisspeptin neurons are postulated to have a critical role mediating estradiol positive feedback signals to generate the GnRH surge. Consistent with this postulate, these neurons are more excitable during positive feedback and also receive altered fast synaptic transmission. To investigate if altered excitability depends on ERα expression by AVPV kisspeptin neurons themselves, we compared a kisspeptin promoter driven ERα deletion model (KERKO) with an adult AAV-CRIPSR/Cas9-initiated ERα knockdown model (AAV-*Esr1*) targeted to AVPV kisspeptin neurons. AVPV kisspeptin cells in both models are less excitable compared to controls, firing fewer bursts of action potentials and having a decreased numbers of action potentials in response to current injections. This indicates estradiol, via ERα in AVPV kisspeptin neurons, plays an activational

role to modulate intrinsic excitability of these cells. The increased I_T may be attributable to the generation of bursts. The inability to sense estradiol in AVPV kisspeptin neurons may thus reduce the release of kisspeptin and impair the downstream GnRH/LH surge. This may explain absence of estradiol-induced LH surges in KERKO mice[124]

One caveat of KERKO mice is that ERα is deleted when the kisspeptin gene and cre recombinase under its control are first expressed during development, about postnatal day 21 in AVPV kisspeptin neurons[121]. Decreased excitability and absence of surge may thus be due to failure of these neurons to develop in an appropriate manner. Kisspeptin expression in these cells is estradiol activated and fewer cells expressing *Kiss1* mRNA are detected in the AVPV of KERKO mice[168]. Further, if the decreased excitability and spontaneous firing observed in adults occurs during development, it may alter patterns of activity-dependent synaptogenesis and synaptic pruning[215].

The results from the AAV-*Esr1* model support and extend the data from KERKO mice and provide evidence towards accepting the hypothesis that the role of ERα in shifting excitability is activational, independent of its role in development of these cells. It further suggests that it is ERα within the AVPV population vs other kisspeptin-expressing cells as there is also spatial control of the knockdown. One caveat of AAV-*Esr1* model is that sgRNAs may have off-target actions on other regions of the genome beyond the sites predicted by the design software. To address this, we included two sgRNAs that target *Esr1* and one sgRNA that targets *Lacz* to address the possible off-target effects among groups. It is difficult, however, to assess each individual neuron to test if mutations occurred at other genes that are potentially involved in neuronal firing properties. Due to the nature of the nonhomologous end joining repair machinery activated after CRISPR-Cas9 initiated cuts, *Esr1* gene editing in each cell varies. Despite these possible variables, the firing patterns for these cells was consistent with regard to their ERα phenotype, with majority of cells without ERα firing in a tonic manner

characteristic of a low/no estradiol state. One missing physiologic link is to assess if AAV-*Esr1* infected mice are able to generate estradiol-induced LH surge. This will be studied in the future.

The reproductive phenotypes of these KERKO and AVPV-targeted ERα knockdown mice are quite different. KERKO mice tend to exhibit prolonged vaginal cornification and enlarged uteri, neither of which were observed in AAV-*Esr1* infected mice. One possible explanation is that ERα in arcuate kisspeptin neurons plays a role in maintaining normal cyclicity through the homeostatic regulation of episodic GnRH output, which drives gonadotropins and thus typical steroidogenesis, including the estradiol rise that eventually triggers positive feedback. In support of this, long-term firing output of these cells is episodic and steroid modulated[170], and activation of these cells generates a pulse of LH release[216]. Further evidence comes from Tac2-specific ERα KO mice, in which ERα is primarily deleted from the arcuate, not the AVPV, kisspeptin population. These mice also exhibit prolonged vaginal cornification[168]. It is also possible that the ~26% of AVPV kisspeptin cells with immunoreactive ERα are able to respond to an estradiol rise with a sufficient release of kisspeptin to activate downstream GnRH neurons to maintain cyclicity. In preliminary studies, however, bilateral injection of AAV-*Esr1* into the arcuate region in kisspeptin-specific Cas9 mice in adulthood is producing prolonged vaginal cornification and disrupted cycles within a month post-injection (data not shown), suggesting arcuate kisspeptin neurons are more likely to control the hormonal patterns that produce the outward expression of reproductive cycles.

In conclusion, utilizing CRISPR-Cas9 AAV, we were able to successfully knockdown ERα in kisspeptin neurons specifically in the AVPV region in adult female mice. The firing properties of these neurons after loss of ERα were less excitable when estradiol is elevated, similar to developmental knockout produced in the KERKO model. ERα in AVPV kisspeptin neurons thus plays an activational role to increase their neuronal excitability.

Figures and Legends

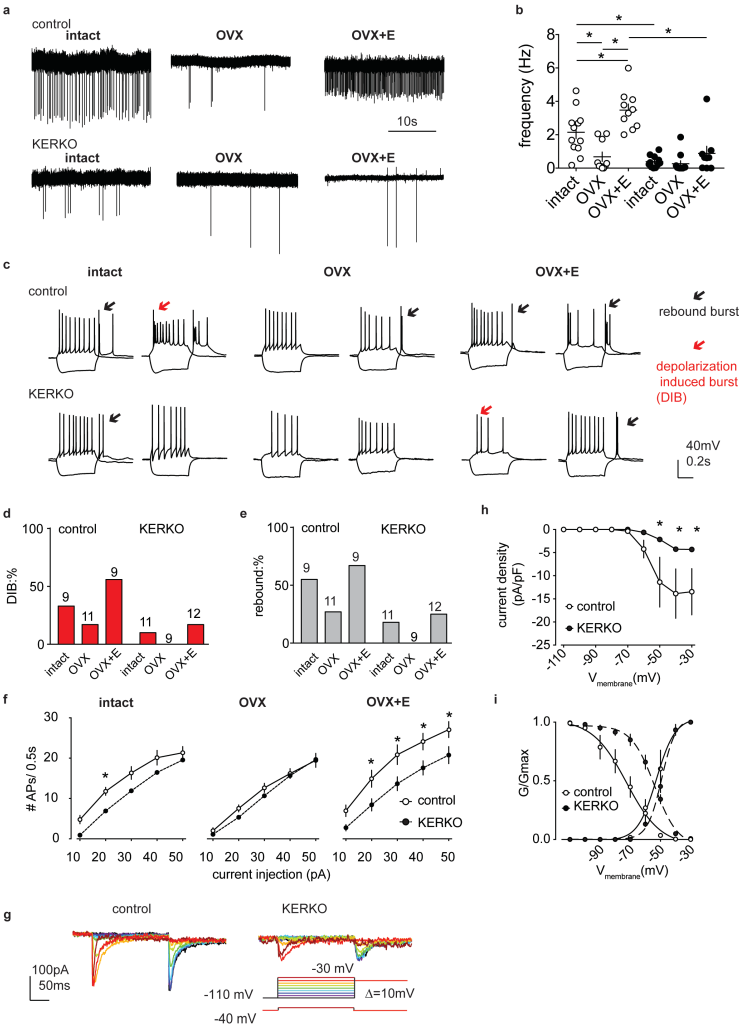

Figure 4-1 AVPV kisspeptin neurons in KERKO mice are less excitable compared to control and not regulated by estradiol.

a, representative extracellular recordings for cells from control and KERKO mice from ovary-intact, OVX and OVX+E groups. **b**, individual and mean ± SEM firing frequency of cells from control (open circles, intact n=12, OVX n=10, OVX+E, n=10) and KERKO groups (black circles, intact n=11, OVX n=11, OVX+E, n=9). **c**, representative firing signatures in response to ± 20 pA current injection for 500ms for cells in control and KERKO mice in ovary-intact, OVX and OVX+E groups, black arrows indicate rebound bursts and red arrows indicate depolarization induced bursts (DIB). **d** and **e**, percentage of cells exhibiting DIB (**d**) and rebound bursts (**e**) in all groups. Total number of cells per group is shown on top of the bar. **f**, input-output curves for cells in control and KERKO mice in ovary-intact (left), OVX (middle) and OVX+E (right) groups. g, voltage protocol (bottom) and representative subtraction-isolated I_T in control (left, n=5) and KERKO groups (right, n=6). **h**, mean ± SEM current density of I_T in in control (left, n=5) and KERKO groups (right, n=6). **i**, activation and inactivation of I_T conductance was plotted and fit with a Boltzmann function to derive $V_{1/2}$ and k value in control (n=5) and KERKO mice (n=6). All * indicate $p<0.05$.

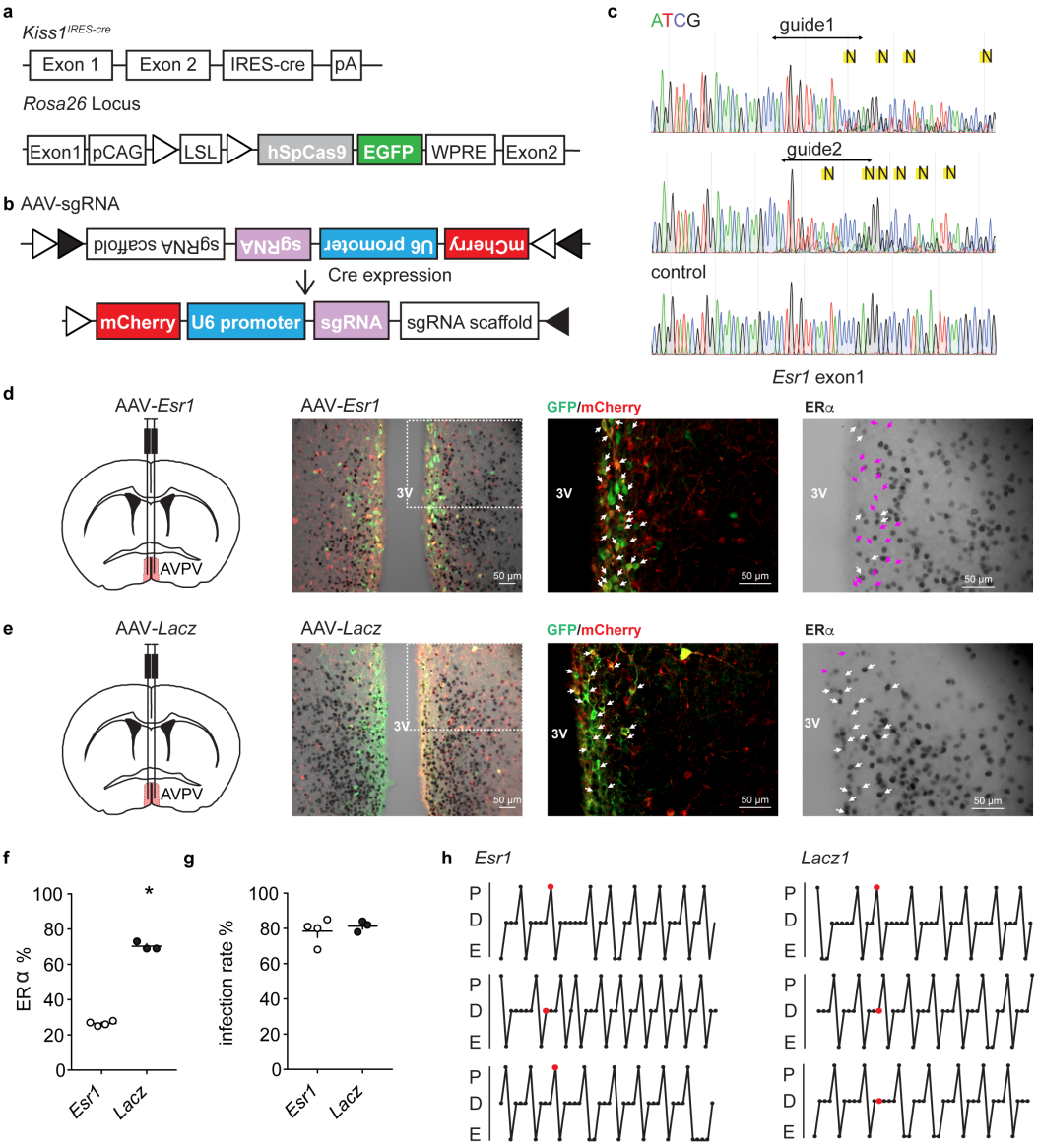

Figure 4-2 In vitro and in vivo validation of AAV-Esr1 knockdown efficiency on ERα.

a, kisspeptin-cre Cas9-GFP mice were generated by crossing Kiss1-Cre with Cas9-GFP flox mice. **b**, schematic representation of the cre-inducible AAV vector delivering sgRNAs. **c**, sequencing from C2C12 cells transiently transfected with lentiCRISPR v2 with the sgRNAs targeting Esr1 (upper, middle) or Lacz. **d** and **e**, AAV-Esr1 and AAV-Laz was bilaterally delivered to AVPV region. Brains were stained for GFP (green), mCherry (red) and ERα (black). The middle and right panels show the region in box in the left panel. **f** and **g**, infection rate of AVPV kisspeptin cells (**f**) and percentage of ERα immunoreactive AVPV kisspeptin cells (**g**) in mice bilaterally injected AAV-Esr1 or AAV-Laz. h, representative reproductive cyclicity of mice that received AAV-Esr1 (left, n=6) and AAV-Laz (right, n=4); E, estrus, D, diestrus, P proestrus. The red dot indicates the day of stereotaxic surgery.

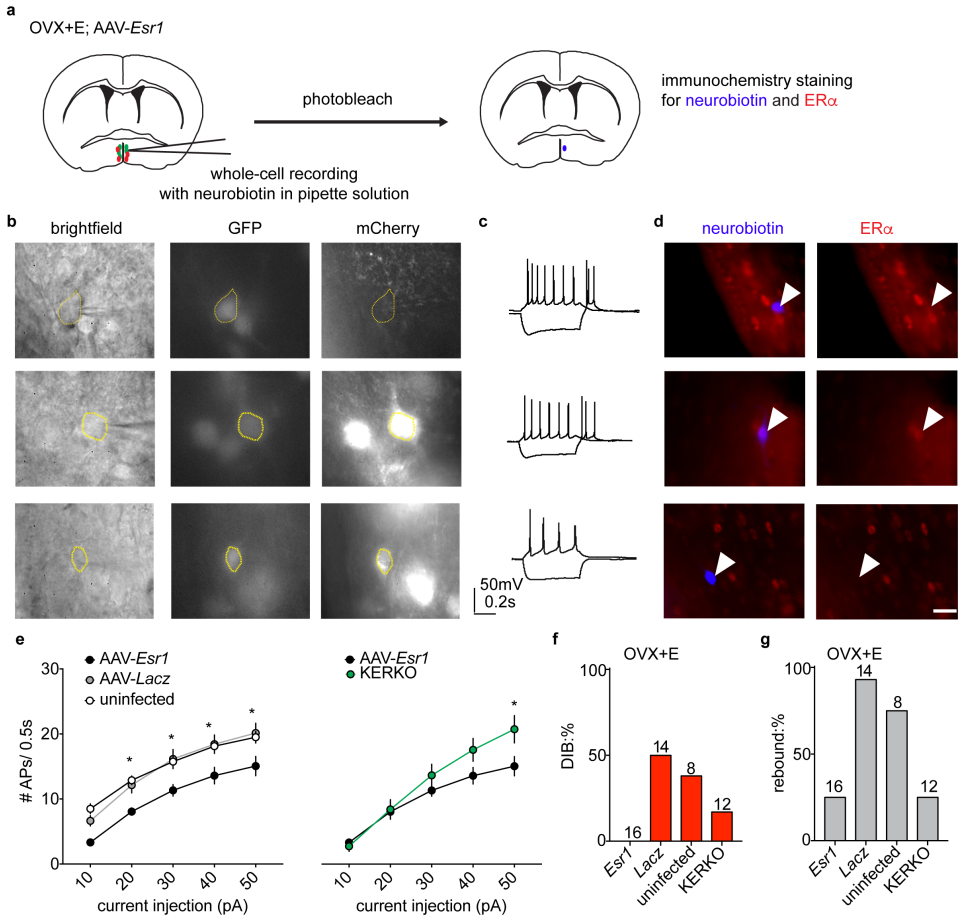

Figure 4-3 Decreased excitability of AVPV kisspeptin neurons in AAV-*Esr1* knockdown mice.

a schematic diagram for whole-cell recording and post hoc identification of ERα in recorded cells in OVX+E AAV-*Esr1* infected mice. **b-d** representative firing signatures (c) of cells (top) that were not infected by AAV-*Esr1* (b) and were immunopositive for ERα (d), infected by AAV-*Esr1* (middle, b) but still immunopositive for ERα (d) and infected by AAV-*Esr1* (bottom, b) and not immunopositive for ERα (d). **e**, input-output curves of infected cells with undetectable ERα in AAV-*Esr1* (black filled circle, n=16), cells infected by AAV-*Lacz* (grey filled circle, n=14), cells not infected by AAV (open circle, n=8), and cells from KERKO mice (green filled circle, n=12) in OVX+E groups. **f-g** percentage of cells exhibiting DIB (**f**) and rebound bursts (**g**) in all four groups. Total number of cells per group is shown on top of the bar. * indicate $p<0.05$

Chapter 5 Conclusion: Dissecting the Role of ERα on Hypothalamic Kisspeptin Neuronal Regulation of Reproduction

In this dissertation, my work has been focused on two hypothalamic kisspeptin neuronal populations, one in the anteroventral periventricular nucleus (AVPV) and the other in arcuate nucleus. I studied their role in mediating estradiol feedback from cellular, molecular and whole-body phenotype perspectives, and utilized genetic approaches to dissect the role of ERα within kisspeptin cells in each nucleus in negative and positive feedback regulation on LH release.

The intrinsic firing of AVPV kisspeptin neurons

AVPV kisspeptin neurons are thought to mediate estradiol positive feedback. The work in Chapter 2 characterized the electrophysiological properties of these neurons and their regulation by estradiol during positive feedback. We found these neurons are more excitable during estradiol positive feedback, firing more action potentials and exhibiting more bursts[167]. We and others have now identified several ionic conductances expressed by AVPV kisspeptin neurons, including hyperpolarization-activated cation channels, T-type calcium channels, and persistent sodium channels[126,127,167]. Both electrophysiological recordings measuring ionic currents and mRNA expression of these ion channel genes in pooled cells suggest these conductances are regulated by estradiol[126,127,167]. These findings are informative as they provide mechanisms on how bursts may be sculpted in AVPV kisspeptin neurons. The different firing signatures of these AVPV kisspeptin neurons demonstrate their heterogeneity, thus studies are needed to answer if subtypes of AVPV kisspeptin neurons exist with their unique molecular profiles. Combining the electrophysiological properties with molecular

signatures of these cells will help to uncover specific roles each cellular subtype may perform. The assumption is that elevated firing of AVPV kisspeptin neurons may lead to increased kisspeptin release. However, the direct measure of kisspeptin release still remains as one of the biggest challenges in the field. This estradiol modulation of intrinsic excitability is likely due to estradiol action directly on these neurons, we thus utilized genetic tools to selectively delete ERα from these cells. In Chapter 4, we compared two ERα KO models: a developmental knockout of ERα in KERKO mice and an adult deletion of ERα only in AVPV using a CRISPR/Cas9-based AAV vector. Recordings of AVPV kisspeptin cells from two models exhibit similar outcomes in the intrinsic excitability: these cells were less excitable and fired less bursts. Thus, we conclude ERα in AVPV kisspeptin neurons is required for estradiol action on their intrinsic membrane excitability.

These lost-of-function experiments suggest ERα plays a necessary role in modulating the excitability of AVPV kisspeptin neurons. However, these models have caveats, as KERKO mice have developmental deficits and CRISPR-AAV approaches may have off-target effects beyond the ERα gene *Esr1*. Several gain-of-function or restoration experiments may be considered to re-introduce ERα to AVPV kisspeptin neurons either in KERKO mice or CRISPR/Cas9-based *Esr1*-targeted AAV injected mice. The former approach helps to answer if ERα in AVPV kisspeptin neurons is sufficient to restore the failure to generate estradiol-induced LH surge in KERKO mice. The latter approach may help to demonstrate if the off-target effects of AAV-*Esr1*, if any, contribute to the decreased excitability we observed.

The intrinsic firing of arcuate kisspeptin neurons

Kisspeptin neurons in arcuate are postulated to mediate estradiol negative feedback regulation on GnRH/LH pulse release[110]. It has been debated if estradiol directly modulates arcuate kisspeptin firing. Short-term extracellular

recordings of these cells with or without circulating estradiol did to reveal any differences (Chapter 3). However, the removal of ERα from these cells in KERKO mice greatly increases their firing frequency. Long-term recordings of arcuate kisspeptin neurons in male mice suggest sex steroids, including estradiol, may modulate the long-term firing patterns but not short-term firing frequency of these cells. In females, estradiol may also exert negative feedback by decreasing the frequency of peaks in firing rate in long-term recordings. Interestingly, the firing rate of arcuate kisspeptin neurons in OVX+E KERKO mice is higher than OVX+E control mice. This suggests arcuate kisspeptin neurons require ERα to fire properly. Loss of ERα as a transcriptional factor may also alter expression of ion channel and synapse related genes and signaling pathways that lead to elevated firing.

With regard to the whole-cell firing signatures of arcuate kisspeptin neurons, others have demonstrated that they are quite different from the AVPV kisspeptin population[127], further supporting their different roles in sensing estradiol and orchestrating output to regulate reproductive circuitry. From a population activity aspect, recently Clarkson, et al. utilized calcium indicator GCaMP6 fiber photometry to measure summed arcuate kisspeptin neuron activity based on fluctuations in calcium-sensitive fluorescence. The fluorescent activity of arcuate kisspeptin neurons correlates well with LH pulse release[216]. This cell-specific readout of kisspeptin neuron activity significantly advanced the understanding of pulse-generator beyond the classical MUA study in media basal hypothalamus. However, it suffers from its own caveats that individual neuronal activity is missing. Optetrode electrophysiological recordings may be applied to distinguish individual neurons.

The afferents and efferents of kisspeptin neurons

Estradiol feedback regulation, although heavily emphasized for its direct action on kisspeptin neurons, may be exerted on a boarder network including the

afferents of kisspeptin neurons. My colleagues and I further characterized the glutamatergic (in Chapter 4) and GABAergic synaptic transmission to AVPV and arcuate kisspeptin neurons. Our results suggest glutamatergic and GABAergic synaptic inputs to AVPV and arcuate neurons are differentially regulated by estradiol[137].

In the AVPV kisspeptin population, estradiol positive feedback increases glutamate transmission and suppresses hyperpolarizing GABAergic transmission to these cells, indicating that estradiol tilts the balance toward excitatory inputs during positive feedback. Coupled with estradiol upregulation of intrinsic conductances underlying bursting firing, AVPV kisspeptin neurons are poised to increase output during positive feedback to drive the GnRH/LH surge. Interestingly, in arcuate kisspeptin neurons, estradiol suppresses the activity-dependent glutamatergic transmission, the opposite direction of its action on AVPV kisspeptin neurons. These findings extend the estradiol feedback network beyond kisspeptin neurons and suggest glutamatergic transmission to hypothalamic kisspeptin neurons may be a critical component of feedback regulation.

One critical role for neuroendocrine neurons is to release neurotransmitter and particular neuropeptides to their efferents. Only a small portion of kisspeptin neurons within the AVPV and ARC project to GnRH neurons[120,121]. Those in AVPV that connect to GnRH neurons are estrogen-sensitive and a high percent express tyrosine hydroxylase[121]. Arcuate kisspeptin neurons may not directly contact GnRH soma or proximal dendrites, but rather may primarily contact distal processes of these cells in the median eminence[120]. Further, arcuate kisspeptin neurons form close connections with one another and also project to AVPV kisspeptin neurons[169]. However, less is known about where else these kisspeptin neurons project besides themselves and GnRH neurons. This is one of the questions that the field must answer.

Arcuate kisspeptin neurons produce kisspeptin, neurokinin B(NKB) and dynorphin, thus are called KNDy neurons[96]. Ruka, et al. performed extracellular recordings on brain slices from male mice and found that NKB stimulates KNDy neuron firing frequency whereas dynorphin inhibits it[148]. Further, Qiu, et al. showed that high-frequency photostimulation on arcuate kisspeptin neurons that express light-sensitive cation channel channelrhodopsin-2 leads to postsynaptic cell membrane depolarization, likely due to neurokinin B acting on its receptors[169]. This supports the assumption that elevated firing rate potentially leads to neuropeptide release and further provides evidence on how these neuropeptides may be released endogenously to modulate membrane response. However, it is still not clear if each neuropeptide is released independently or if they are co-released. Both AVPV and arcuate kisspeptin neurons produce neurotransmitters and neuropeptides. To examine the importance of neurotransmitter release from neuropeptide release, mice with a kisspeptin neuron-specific deletion of vesicular glutamate and/or GABA transporter may need to be generated and their reproductive phenotypes be examined.

The role ERα in kisspeptin neurons plays on the HPG axis

Both Mayer C, et al. and Greenwald-Yarnell ML, et al. generated and characterized a kisspeptin-specific ERα knockout model. These KERKO mice are infertile, have precocious puberty onset and abnormal cyclicity[103,168]. Dubois, et al. demonstrated KERKO mice failed to generate estradiol-induced LH surge, suggests ERα in kisspeptin cells is required for estradiol positive feedback [124]. The role of ERα in kisspeptin cells for negative feedback regulation of LH pulses, however, was assumed to be less critical. Previous work on the estradiol negative feedback on LH in KERKO mice used a single measurement that either revealed no difference between KERKO and control mice or a blunted percent reduction[103,124,168]. The work in Chapter 3 using serial tail-tip blood LH measurements shows an increase in LH pulse frequency in KERKO mice compared to controls. As LH pulse frequency and amplitude convey critical

information for steroid production and regulating cyclicity, our results suggest ERα in kisspeptin cells may play critical roles for estradiol negative feedback regulation on LH pulse pattern. The loss of negative feedback in KERKO mice may be pointed to arcuate kisspeptin neurons, as their increased firing frequency and remarkably elevated glutamatergic transmission suggest a loss of negative feedback control on this neuronal population[208].

The KERKO model fails to response to estradiol negative and positive feedback, suggesting the role of ERα in kisspeptin cells plays is critical for these processes. However, the KERKO model is not a nucleus-specific KO model, as ERα is deleted from all kisspeptin cells. Thus, we cannot conclude the role of ERα in each nucleus. A *Tac2*-Cre ERα KO model (TERKO) may provide evidence to answer the role of ERα in arcuate kisspeptin neurons, as only arcuate but not AVPV kisspeptin neurons lose the expression of ERα[168]. Similar to KERKO mice, TERKO mice exhibit persistent cornification based on vaginal cytolog[168], linking abnormal cyclicity to loss of ERα in arcuate kisspeptin neurons. However, this model shares the same caveats with KERKO model, since deletion of ERα occurs when *Tac2* gene expression[217] (no later than P12 in the arcuate region) and it is thus not possible to distinguish between the activational vs organizational role of ERα. The CRISPR/Cas9-based AAV we developed, elaborated in Chapter 4, allows us to assess individually the role of ERα in AVPV and arcuate kisspeptin neurons in adulthood. The preliminary findings suggest ERα in arcuate kisspeptin neurons may be critical for maintaining cyclicity. Future work will focus on investigating estradiol regulation on LH pulse and surge in mice with each nucleus infected to deplete ERα. Although we only measured LH for the ongoing projects, understanding how GnRH neurons fire and release in the KERKO, TERKO and AAV CRISPR knockdown mice is critical. Fast-scan cyclic voltammetry (FSCV) using carbon-fiber microelectrodes allows GnRH to be measured on ex vivo brain slices[13]. Electrophysiological recordings of GnRH

neurons will also help reveal how loss of ERα in kisspeptin neurons affects GnRH neurons, the final common output from the brain.

Summary

The work presented in this dissertation advances the understanding of estradiol negative and positive feedback regulation of reproduction. It not only uncovers the role of estradiol and ERα in AVPV and arcuate kisspeptin neurons on regulating their intrinsic properties and received presynaptic inputs, but also reveals likely nucleus-specific roles ERα play to orchestrate LH pulsatile and surge release, and thus reproductive output. The CRISPR/Cas9 approaches further open doors to investigate genes of the interest in a spatial- and temporal-specific manner for neuroendocrine cells beyond kisspeptin neurons.

Bibliography

1. Frey, K. A. & Patel, K. S. Initial evaluation and management of infertility by the primary care physician. *Mayo Clin. Proc.* **79,** 1439–1443 (2004).

2. Bhattacharya, S. *et al.* Female infertility. *BMJ Clin. Evid.* **2010,** (2010).

3. Fink, G. Neuroendocrine Regulation of Pituitary Function. in *Neuroendocrinology in Physiology and Medicine* 107–133 (Humana Press, 2000).

4. Haisenleder, D. J. *et al.* The Frequency of Gonadotropin-Releasing Hormone Secretion Regulates Expression of α and Luteinizing Hormone β-Subunit Messenger Ribonucleic Acids in Male Rats. *Mol. Endocrinol.* **1,** 834–838 (1987).

5. Wildt, L. *et al.* Frequency and amplitude of gonadotropin-releasing hormone stimulation and gonadotropin secretion in the rhesus monkey. *Endocrinology* **109,** 376–385 (1981).

6. Marshall, J. C. & Griffin, M. L. The role of changing pulse frequency in the regulation of ovulation. *Hum. Reprod.* **8,** 57–61 (1993).

7. Plant, T. M., Zeleznik, A. & Knobil, E. *Knobil and Neill's physiology of reproduction*.

8. Goodman, R. L. & Daniel, K. Modulation of pulsatile luteinizing hormone secretion by ovarian steroids in the rat. *Biol. Reprod.* **32,** 217–25 (1985).

9. Evans, N. P., Dahl, G. E., Padmanabhan, V., Thrun, L. A. & Karsch, F. J. Estradiol Requirements for Induction and Maintenance of the Gonadotropin-Releasing Hormone Surge: Implications for Neuroendocrine Processing of the Estradiol Signal. *Endocrinology* **138,** 5408–5414 (1997).

10. Leipheimer, R. E., Bona-Gallo, A. & Gallo, R. V. Ovarian Steroid Regulation of Pulsatile Luteinizing Hormone Release during the Interval between the Mornings of Diestrus 2 and Proestrus in the Rat. *Neuroendocrinology* **41,** 252–257 (2008).

11. Adams, T. E., Norman, R. L. & Spies, H. G. Gonadotropin-Releasing Hormone Receptor Binding and Pituitary Responsiveness in Estradiol-Primed Monkeys. *Science* **213,** 1388–1390

12. Christian, C. A., Mobley, J. L. & Moenter, S. M. Diurnal and estradiol-dependent changes in gonadotropin-releasing hormone neuron firing activity. *Proc. Natl. Acad. Sci. U. S. A.* **102,** 15682–7 (2005).

13. Glanowska, K. M., Venton, B. J. & Moenter, S. M. Fast scan cyclic voltammetry as a novel method for detection of real-time gonadotropin-releasing hormone release in mouse brain slices. *J. Neurosci.* **32,** 14664–9 (2012).

14. Moenter, S. M., Brand, R. C. & Karsch, F. J. Dynamics of gonadotropin-releasing hormone (GnRH) secretion during the GnRH surge: insights into the mechanism of GnRH surge induction. *Endocrinology* **130,** 2978–84 (1992).

15. Moenter, S. M., Caraty, A. & Karsch, F. J. The estradiol-induced surge of gonadotropin-releasing hormone in the ewe. *Endocrinology* **127,** 1375–84 (1990).

16. Crowder, M. E. & Nett, T. M. Pituitary Content of Gonadotropins and Receptors for Gonadotropin-Releasing Hormone (GnRH) and Hypothalamic Content of GnRH during the Periovulatory Period of the Ewe. *Endocrinology* **114,** 234–239 (1984).

17. Kuiper, G. G., Enmark, E., Pelto-Huikko, M., Nilsson, S. & Gustafsson, J. A. Cloning of a novel receptor expressed in rat prostate and ovary. *Proc. Natl. Acad. Sci. U. S. A.* **93,** 5925–30 (1996).

18. Tremblay, G. B. *et al.* Cloning, Chromosomal Localization, and Functional Analysis of the Murine Estrogen Receptor β. *Mol. Endocrinol.* **11,** 353–365 (1997).

19. Mangelsdorf, D. J. *et al.* The nuclear receptor superfamily: the second decade. *Cell* **83,** 835–9 (1995).

20. Krege, J. H. *et al.* Generation and reproductive phenotypes of mice lacking estrogen receptor beta. *Proc. Natl. Acad. Sci. U. S. A.* **95,** 15677–82 (1998).

21. Lubahn, D. B. *et al.* Alteration of reproductive function but not prenatal sexual development after insertional disruption of the mouse estrogen receptor gene. *Proc. Natl. Acad. Sci. U. S. A.* **90,** 11162–6 (1993).

22. Wersinger, S. R., Haisenleder, D. J., Lubahn, D. B. & Rissman, E. F. Steroid Feedback on Gonadotropin Release and Pituitary Gonadotropin Subunit mRNA in Mice Lacking a Functional Estrogen Receptor α. *Endocrine* **11,** 137–144 (1999).

23. Wintermantel, T. M. *et al.* Definition of Estrogen Receptor Pathway Critical for Estrogen Positive Feedback to Gonadotropin-Releasing Hormone Neurons and Fertility. *Neuron* **52,** 271–280 (2006).

24. Clarke, I. J. & Cummins, J. T. The temporal relationship between gonadotropin releasing hormone (GnRH) and luteinizing hormone (LH) secretion in ovariectomized ewes. *Endocrinology* **111,** 1737–1739 (1982).

25. Frost, S. I., Keen, K. L., Levine, J. E. & Terasawa, E. Microdialysis methods for in vivo neuropeptide measurement in the stalk-median eminence in the Rhesus monkey. *J. Neurosci. Methods* **168,** 26–34 (2008).

26. Carmel, P. W., Araki, S. & Ferin, M. Pituitary Stalk Portal Blood Collection in Rhesus Monkeys: Evidence for Pulsatile Release of Gonadotropin-Releasing Hormone (GnRH). *Endocrinology* **99,** 243–248 (1976).

27. Gore, A. C. GnRH Pulsatility. in *GnRH: The Master Molecule of Reproduction* 29–51 (Springer US, 2002). doi:10.1007/978-1-4757-3565-9_3

28. Levine, J. E. New concepts of the neuroendocrine regulation of gonadotropin surges in rats. *Biol. Reprod.* **56,** 293–302 (1997).

29. Moenter, S. M., Caraty, A., Locatelli, A. & Karsch, F. J. Pattern of gonadotropin-releasing hormone (GnRH) secretion leading up to ovulation in the ewe: existence of a preovulatory GnRH surge. *Endocrinology* **129,** 1175–82 (1991).

30. Wester, J. R., Moenter, S., BarrellL, G. K., Lehman, M. N. & Karsch, F. J. Role of the Thyroid Gland in Seasonal Reproduction. III. Thyroidectomy Blocks Seasonal Suppression of Gonadotropin-Releasing Hormone Secretion in Sheep. *Endocrinology* **129,** 1635–1643 (1991).

31. Moenter, S. M. Leap of faith: does serum luteinizing hormone always accurately reflect central reproductive neuroendocrine activity? *Neuroendocrinology* **102,** 256–266 (2015).

32. McCartney, Christopher R. and Marshall, J. C. Neuroendocrinology of Reproduction. in *Yen & Jaffe's Reproductive Endocrinology* 3–26.e8 (Saunders, 2014).

33. Goodman, R. L. & Karsch, F. J. Pulsatile Secretion of Luteinizing Hormone: Differential Suppression by Ovarian Steroids. *Endocrinology* **107,** 1286–1290 (1980).

34. Foster DL, J. L. Puberty in the sheep. in *Physiology of reproduction* (ed. Knobil E, N. J.) 2127–2176. (Academic Press, 2006).

35. Ojeda, S. R. & Skinner, M. K. Puberty in the rat. in *Knobil and Neill's Physiology of Reproduction* (ed. Knobil E, N. J.) 2061–2126 (Academic Press, 2006). doi:10.1016/B978-012515400-0/50043-9

36. Marshall, J. C. *et al.* Gonadotropin-releasing hormone pulses: regulators of gonadotropin synthesis and ovulatory cycles. *Recent Prog. Horm. Res.* **47,** 155-87–9 (1991).

37. Belchetz, P. E., Plant, T. M., Nakai, Y., Keogh, E. J. & Knobil, E. Hypophysial responses to continuous and intermittent delivery of hypopthalamic gonadotropin-releasing hormone. *Science (80-.).* **202,** 631–3 (1978).

38. Blank, S. K., McCartney, C. R. & Marshall, J. C. The origins and sequelae

of abnormal neuroendocrine function in polycystic ovary syndrome. *Hum. Reprod. Update* **12,** 351–361 (2006).

39. Waldstreicher, J., Santoro, N. F., Hall, J. E., Filicori, M. & Crowley, W. F. Hyperfunction of the Hypothalamic-Pituitary Axis in Women with Polycystic Ovarian Disease: Indirect Evidence for Partial Gonadotroph Desensitization. *J. Clin. Endocrinol. Metab.* **66,** 165–172 (1988).

40. Adams, J. M., Taylor, A. E., Schoenfeld, D. A., Crowley, W. F. & Hall, J. E. The midcycle gonadotropin surge in normal women occurs in the face of an unchanging gonadotropin-releasing hormone pulse frequency. *J. Clin. Endocrinol. Metab.* **79,** 858–864 (1994).

41. Knobil, E., Plant, T. M., Wildt, L., Belchetz, P. E. & Marshall, G. Control of the rhesus monkey menstrual cycle: permissive role of hypothalamic gonadotropin-releasing hormone. *Science (80-.).* **207,** 1371–3 (1980).

42. Pau, K. Y., Berria, M., Hess, D. L. & Spies, H. G. Preovulatory gonadotropin-releasing hormone surge in ovarian-intact rhesus macaques. *Endocrinology* **133,** 1650–1656 (1993).

43. Xia, L., Van Vugt, D., Alston, E. J., Luckhaus, J. & Ferin, M. A surge of gonadotropin-releasing hormone accompanies the estradiol-induced gonadotropin surge in the rhesus monkey. *Endocrinology* **131,** 2812–2820 (1992).

44. Sarkar, D. K., Chiappa, S. A., Fink, G. & Sherwood, N. M. Gonadotropin-releasing hormone surge in pro-oestrous rats. *Nature* **264,** 461–3 (1976).

45. Karsch, F. J., Bowen, J. M., Caraty, A., Evans, N. P. & Moenter, S. M. Gonadotropin-releasing hormone requirements for ovulation. *Biol. Reprod.* **56,** 303–9 (1997).

46. Wilson, R. C. *et al.* Central Electrophysiologic Correlates of Pulsatile Luteinizing Hormone Secretion in the Rhesus Monkey. *Neuroendocrinology* **39,** 256–260 (1984).

47. Suter, K. J. *et al.* Genetic Targeting of Green Fluorescent Protein to Gonadotropin-Releasing Hormone Neurons: Characterization of Whole-

Cell Electrophysiological Properties and Morphology [1]. *Endocrinology* **141,** 412–419 (2000).

48. Spergel, D. J., Krüth, U., Shimshek, D. R., Sprengel, R. & Seeburg, P. H. Using reporter genes to label selected neuronal populations in transgenic mice for gene promoter, anatomical, and physiological studies. *Prog. Neurobiol.* **63,** 673–86 (2001).

49. Herbison, A. E., Pape, J.-R., Simonian, S. X., Skynner, M. J. & Sim, J. A. Molecular and cellular properties of GnRH neurons revealed through transgenics in the mouse. *Mol. Cell. Endocrinol.* **185,** 185–194 (2001).

50. Abe, H. & Terasawa, E. Firing pattern and rapid modulation of activity by estrogen in primate luteinizing hormone releasing hormone-1 neurons. *Endocrinology* **146,** 4312–20 (2005).

51. Nunemaker, C. S., DeFazio, R. A. & Moenter, S. M. Estradiol-Sensitive Afferents Modulate Long-Term Episodic Firing Patterns of GnRH Neurons. *Endocrinology* **143,** 2284–2292 (2002).

52. Sim, J. A., Skynner, M. J. & Herbison, A. E. Heterogeneity in the basic membrane properties of postnatal gonadotropin-releasing hormone neurons in the mouse. *J. Neurosci.* **21,** 1067–75 (2001).

53. van den Pol, A. N. Neuropeptide Transmission in Brain Circuits. *Neuron* **76,** 98–115 (2012).

54. Nunemaker, C. S., Straume, M., DeFazio, R. A. & Moenter, S. M. Gonadotropin-Releasing Hormone Neurons Generate Interacting Rhythms in Multiple Time Domains. *Endocrinology* **144,** 823–831 (2003).

55. Dror, T., Franks, J. & Kauffman, A. S. Analysis of Multiple Positive Feedback Paradigms Demonstrates a Complete Absence of LH Surges and GnRH Activation in Mice Lacking Kisspeptin Signaling. *Biol. Reprod.* **88,** 146–146 (2013).

56. Christian, C. A. & Moenter, S. M. Estradiol induces diurnal shifts in GABA transmission to gonadotropin-releasing hormone neurons to provide a neural signal for ovulation. *J. Neurosci.* **27,** 1913–21 (2007).

57. Sun, J., Chu, Z. & Moenter, S. M. Diurnal in vivo and rapid in vitro effects of estradiol on voltage-gated calcium channels in gonadotropin-releasing hormone neurons. *J. Neurosci.* **30,** 3912–23 (2010).

58. Chu, Z., Takagi, H. & Moenter, S. M. Hyperpolarization-activated currents in gonadotropin-releasing hormone (GnRH) neurons contribute to intrinsic excitability and are regulated by gonadal steroid feedback. *J. Neurosci.* **30,** 13373–83 (2010).

59. Christian, C. A., Pielecka-Fortuna, J. & Moenter, S. M. Estradiol suppresses glutamatergic transmission to gonadotropin-releasing hormone neurons in a model of negative feedback in mice. *Biol. Reprod.* **80,** 1128–35 (2009).

60. Noel, S. D., Keen, K. L., Baumann, D. I., Filardo, E. J. & Terasawa, E. Involvement of G Protein-Coupled Receptor 30 (GPR30) in Rapid Action of Estrogen in Primate LHRH Neurons. *Mol. Endocrinol.* **23,** 349–359 (2009).

61. Hrabovszky, E. *et al.* Estrogen receptor-beta immunoreactivity in luteinizing hormone-releasing hormone neurons of the rat brain. *Endocrinology* **142,** 3261–4 (2001).

62. Chu, Z. & Moenter, S. M. Physiologic Regulation of a Tetrodotoxin-Sensitive Sodium Influx That Mediates a Slow Afterdepolarization Potential in Gonadotropin-Releasing Hormone Neurons: Possible Implications for the Central Regulation of Fertility. *J. Neurosci.* **26,** 11961–11973 (2006).

63. Decavel, C. & Van Den Pol, A. N. GABA: A dominant neurotransmitter in the hypothalamus. *J. Comp. Neurol.* **302,** 1019–1037 (1990).

64. van den Pol, A. N., Wuarin, J. P. & Dudek, F. E. Glutamate, the dominant excitatory transmitter in neuroendocrine regulation. *Science* **250,** 1276–8 (1990).

65. DeFazio, R. A., Heger, S., Ojeda, S. R. & Moenter, S. M. Activation of A-type gamma-aminobutyric acid receptors excites gonadotropin-releasing hormone neurons. *Mol. Endocrinol.* **16,** 2872–91 (2002).

66. Kuehl-Kovarik, M. C. *et al.* Episodic Bursting Activity and Response to

Excitatory Amino Acids in Acutely Dissociated Gonadotropin-Releasing Hormone Neurons Genetically Targeted with Green Fluorescent Protein. *J. Neurosci.* **22,** 2313–2322 (2002).

67. Chu, Z., Andrade, J., Shupnik, M. A. & Moenter, S. M. Differential regulation of gonadotropin-releasing hormone neuron activity and membrane properties by acutely applied estradiol: dependence on dose and estrogen receptor subtype. *J. Neurosci.* **29,** 5616–27 (2009).

68. Gaskins, G. T. & Moenter, S. M. Orexin A suppresses gonadotropin-releasing hormone (GnRH) neuron activity in the mouse. *Endocrinology* **153,** 3850–3860 (2012).

69. Messager, S. *et al.* Kisspeptin directly stimulates gonadotropin-releasing hormone release via G protein-coupled receptor 54. *Proc. Natl. Acad. Sci. U. S. A.* **102,** 1761–1766 (2005).

70. Christian, C. A. & Moenter, S. M. Vasoactive intestinal polypeptide can excite gonadotropin-releasing hormone neurons in a manner dependent on estradiol and gated by time of day. *Endocrinology* **149,** 3130–6 (2008).

71. Pielecka-Fortuna, J., DeFazio, R. A. & Moenter, S. M. Voltage-gated potassium currents are targets of diurnal changes in estradiol feedback regulation and kisspeptin action on gonadotropin-releasing hormone neurons in mice. *Biol. Reprod.* **85,** 987–95 (2011).

72. Pielecka-Fortuna, J., Chu, Z. & Moenter, S. M. Kisspeptin acts directly and indirectly to increase gonadotropin-releasing hormone neuron activity and its effects are modulated by estradiol. *Endocrinology* **149,** 1979–86 (2008).

73. van der Beek, E. M. *et al.* Preferential induction of c-fos immunoreactivity in vasoactive intestinal polypeptide-innervated gonadotropin-releasing hormone neurons during a steroid-induced luteinizing hormone surge in the female rat. *Endocrinology* **134,** 2636–2644 (1994).

74. Campbell, R. E., Grove, K. L. & Smith, M. S. Gonadotropin-Releasing Hormone Neurons Coexpress Orexin 1 Receptor Immunoreactivity and Receive Direct Contacts by Orexin Fibers. *Endocrinology* **144,** 1542–1548 (2003).

75. de Roux, N. *et al.* Hypogonadotropic hypogonadism due to loss of function of the KiSS1-derived peptide receptor GPR54. *Proc. Natl. Acad. Sci.* **100,** 10972–10976 (2003).

76. Seminara, S. B. *et al.* The GPR54 Gene as a Regulator of Puberty. *N. Engl. J. Med.* **349,** 1614–1627 (2003).

77. d'Anglemont de Tassigny, X. *et al.* Hypogonadotropic hypogonadism in mice lacking a functional Kiss1 gene. *Proc. Natl. Acad. Sci.* **104,** 10714–10719 (2007).

78. Lapatto, R. *et al. Kiss1* $^{-/-}$ Mice Exhibit More Variable Hypogonadism than *Gpr54* $^{-/-}$ Mice. *Endocrinology* **148,** 4927–4936 (2007).

79. Chan, Y. M., Broder-Fingert, S., Wong, K. M. & Seminara, S. B. Kisspeptin/Gpr54-Independent Gonadotrophin-Releasing Hormone Activity in *Kiss1* and *Gpr54* Mutant Mice. *J. Neuroendocrinol.* **21,** 1015–1023 (2009).

80. Herbison, A. E., d'Anglemont de Tassigny, X., Doran, J. & Colledge, W. H. Distribution and Postnatal Development of Gpr54 Gene Expression in Mouse Brain and Gonadotropin-Releasing Hormone Neurons. *Endocrinology* **151,** 312–321 (2010).

81. Lee, D. K. *et al.* Discovery of a receptor related to the galanin receptors. *FEBS Lett.* **446,** 103–7 (1999).

82. Irwig, M. S. *et al.* Kisspeptin Activation of Gonadotropin Releasing Hormone Neurons and Regulation of KiSS-1 mRNA in the Male Rat. *Neuroendocrinology* **80,** 264–272 (2005).

83. Han, S. *et al.* Activation of gonadotropin-releasing hormone neurons by kisspeptin as a neuroendocrine switch for the onset of puberty. *J. Neurosci.* **25,** 11349–56 (2005).

84. Roseweir, A. K. *et al.* Discovery of Potent Kisspeptin Antagonists Delineate Physiological Mechanisms of Gonadotropin Regulation. *J. Neurosci.* **29,** 3920–3929 (2009).

85. Clarkson, J. & Herbison, A. E. Postnatal Development of Kisspeptin Neurons in Mouse Hypothalamus; Sexual Dimorphism and Projections to Gonadotropin-Releasing Hormone Neurons. *Endocrinology* **147,** 5817–5825 (2006).

86. Yeo, S. H. & Herbison, A. E. Projections of arcuate nucleus and rostral periventricular kisspeptin neurons in the adult female mouse brain. *Endocrinology* **152,** 2387–2399 (2011).

87. Cravo, R. M. *et al.* Characterization of Kiss1 neurons using transgenic mouse models. *Neuroscience* **173,** 37–56 (2011).

88. Smith, J. T., Cunningham, M. J., Rissman, E. F., Clifton, D. K. & Steiner, R. A. Regulation of Kiss1 gene expression in the brain of the female mouse. *Endocrinology* **146,** 3686–3692 (2005).

89. Smith, J. T. *et al.* Differential Regulation of KiSS-1 mRNA Expression by Sex Steroids in the Brain of the Male Mouse. *Endocrinology* **146,** 2976–2984 (2005).

90. PLANT, T. M. *et al.* The Arcuate Nucleus and the Control of Gonadotropin and Prolactin Secretion in the Female Rhesus Monkey (*Macaca mulatta*). *Endocrinology* **102,** 52–62 (1978).

91. SOPER, B. D. & WEICK, R. F. Hypothalamic and Extrahypothalamic Mediation of Pulsatile Discharges of Luteinizing Hormone in the Ovariectomized Rat. *Endocrinology* **106,** 348–355 (1980).

92. Mori, Y. *et al.* Chronic Recording of Electrophysiological Manifestation of the Hypothalamic Gonadotropin-Releasing Hormone Pulse Generator Activity in the Goat. *Neuroendocrinology* **53,** 392–395 (1991).

93. Kawakami, M., Uemura, T. & Hayashi, R. Electrophysiological Correlates of Pulsatile Gonadotropin Release in Rats. *Neuroendocrinology* **35,** 63–67 (1982).

94. Goldsmith, P. C., Thind, K. K., Song, T., Kim, E. J. & Boggant, J. E. Location of the Neuroendocrine Gonadotropin-Releasing Hormone Neurons in the Monkey Hypothalamus by Retrograde Tracing and

Immunostaining. *J. Neuroendocrinol.* **2,** 157–168 (1990).

95. Witkin, J. W., Paden, C. M. & Silverman, A.-J. The Luteinizing Hormone-Releasing Hormone (LHRH) Systems in the Rat Brain. *Neuroendocrinology* **35,** 429–438 (1982).

96. Lehman, M. N., Coolen, L. M. & Goodman, R. L. Minireview: Kisspeptin/neurokinin B/dynorphin (KNDy) cells of the arcuate nucleus: a central node in the control of gonadotropin-releasing hormone secretion. *Endocrinology* **151,** 3479–3489 (2010).

97. Navarro, V. M. *et al.* Interactions between kisspeptin and neurokinin B in the control of GnRH secretion in the female rat. *Am. J. Physiol. Metab.* **300,** E202–E210 (2011).

98. Navarro, V. M. *et al.* Regulation of Gonadotropin-releasing hormone secretion by kisspeptin/Dynorphin/Neurokinin B neurons in the arcuate uucleus of the mouse. *J. Neurosci.* **29,** 11859–11866 (2009).

99. Foradori, C. D., Amstalden, M., Goodman, R. L. & Lehman, M. N. Colocalisation of Dynorphin A and Neurokinin B Immunoreactivity in the Arcuate Nucleus and Median Eminence of the Sheep. *J. Neuroendocrinol.* **18,** 534–541 (2006).

100. Krajewski, S. J. *et al.* Morphologic evidence that neurokinin B modulates gonadotropin-releasing hormone secretion via neurokinin 3 receptors in the rat median eminence. *J. Comp. Neurol.* **489,** 372–386 (2005).

101. Wakabayashi, Y. *et al.* Neurokinin B and Dynorphin A in Kisspeptin Neurons of the Arcuate Nucleus Participate in Generation of Periodic Oscillation of Neural Activity Driving Pulsatile Gonadotropin-Releasing Hormone Secretion in the Goat. *J. Neurosci.* **30,** 3124–3132 (2010).

102. Goodman, R. L. *et al.* Kisspeptin, Neurokinin B, and Dynorphin Act in the Arcuate Nucleus to Control Activity of the GnRH Pulse Generator in Ewes. *Endocrinology* **154,** 4259–4269 (2013).

103. Mayer, C. *et al.* Timing and completion of puberty in female mice depend on estrogen receptor alpha-signaling in kisspeptin neurons. *Proc. Natl.*

Acad. Sci. U. S. A. **107,** 22693–22698 (2010).

104. Gu, G. B. & Simerly, R. B. Projections of the sexually dimorphic anteroventral periventricular nucleus in the female rat. *J. Comp. Neurol.* **384,** 142–64 (1997).

105. Le, W. W., Berghorn, K. A., Rassnick, S. & Hoffman, G. E. Periventricular Preoptic Area Neurons Coactivated with Luteinizing Hormone (LH)-Releasing Hormone (LHRH) Neurons at the Time of the LH Surge Are LHRH Afferents. *Endocrinology* **140,** 510–519 (1999).

106. Wiegand, S. J. & Terasawa, E. Discrete lesions reveal functional heterogeneity of suprachiasmatic structures in regulation of gonadotropin secretion in the female rat. *Neuroendocrinology* **34,** 395–404 (1982).

107. Wiegand, S. J., Terasawa, E., Bridson, W. E. & Goy, R. W. Effects of Discrete Lesions of Preoptic and Suprachiasmatic Structures in the Female Rat. *Neuroendocrinology* **31,** 147–157 (1980).

108. Wiegand, S. J., Terasawa, E. & Bridson, W. E. Persistent estrus and blockade of progesterone-induced lh release follows lesions which do not damage the suprachiasmatic nucleus. *Endocrinology* **102,** 1645–1648 (1978).

109. Kauffman, A. S. *et al.* Sexual Differentiation of *Kiss1* Gene Expression in the Brain of the Rat. *Endocrinology* **148,** 1774–1783 (2007).

110. Oakley, A. E., Clifton, D. K. & Steiner, R. A. Kisspeptin signaling in the brain. *Endocr. Rev.* **30,** 713–743 (2009).

111. Clarkson, J. & Herbison, A. E. Dual Phenotype Kisspeptin-Dopamine Neurones of the Rostral Periventricular Area of the Third Ventricle Project to Gonadotrophin-Releasing Hormone Neurones. *J. Neuroendocrinol.* **23,** 293–301 (2011).

112. Clarkson, J., d'Anglemont de Tassigny, X., Moreno, A. S., Colledge, W. H. & Herbison, A. E. Kisspeptin-GPR54 signaling is essential for preovulatory gonadotropin-releasing hormone neuron activation and the luteinizing hormone surge. *J. Neurosci.* **28,** 8691–7 (2008).

113. Robertson, J. L., Clifton, D. K., De La Iglesia, H. O., Steiner, R. a. & Kauffman, A. S. Circadian regulation of Kiss1 neurons: Implications for timing the preovulatory gonadotropin-releasing hormone/luteinizing hormone surge. *Endocrinology* **150,** 3664–3671 (2009).

114. Karsch, F. J., Cummins, J. T., Thomas, G. B. & Clarke, I. J. Steroid feedback inhibition of pulsatile secretion of gonadotropin-releasing hormone in the ewe. *Biol. Reprod.* **36,** 1207–18 (1987).

115. Lubbers, L. S., Hileman, S. M., Kuehl, D. E., Ferreira, S. A. & Jackson, G. L. Temporal effects of estradiol (E) on luteinizing hormone-releasing hormone (LHRH) and LH release in castrated male sheep. *Domest. Anim. Endocrinol.* **15,** 511–524 (1998).

116. Christian, C. A. & Moenter, S. M. The neurobiology of preovulatory and estradiol-induced gonadotropin-releasing hormone surges. *Endocr. Rev.* **31,** 544–77 (2010).

117. Skynner, M. J., Sim, J. a & Herbison, a E. Detection of estrogen receptor alpha and beta messenger ribonucleic acids in adult gonadotropin-releasing hormone neurons. *Endocrinology* **140,** 5195–5201 (1999).

118. Couse, J. F. *et al.* Postnatal sex reversal of the ovaries in mice lacking estrogen receptors alpha and beta. *Science (80-.).* **286,** 2328–31 (1999).

119. Christian, C. A., Glidewell-Kenney, C., Jameson, J. L. & Moenter, S. M. Classical estrogen receptor α signaling mediates negative and positive feedback on gonadotropin-releasing hormone neuron firing. *Endocrinology* **149,** 5328–5334 (2008).

120. Yip, S. H., Boehm, U., Herbison, A. E. & Campbell, R. E. Conditional viral tract tracing delineates the projections of the distinct kisspeptin neuron populations to gonadotropin-releasing hormone (GnRH) neurons in the mouse. *Endocrinology* **156,** 2582–94 (2015).

121. Kumar, D. *et al.* Specialized subpopulations of kisspeptin neurons communicate with GnRH neurons in female mice. *Endocrinology* **156,** 32–38 (2015).

122. Smith, J. T., Popa, S. M., Clifton, D. K., Hoffman, G. E. & Steiner, R. A. Kiss1 neurons in the forebrain as central processors for generating the preovulatory luteinizing hormone surge. *J. Neurosci.* **26,** 6687–94 (2006).

123. Kinoshita, M. *et al.* Involvement of central metastin in the regulation of preovulatory luteinizing hormone surge and estrous cyclicity in female rats. *Endocrinology* **146,** 4431–6 (2005).

124. Dubois, S. L. *et al.* Positive, but not negative feedback actions of estradiol in adult female mice require estrogen receptor α in kisspeptin neurons. *Endocrinology* 156(3):1111-20 (2015).

125. Piet, R., Boehm, U. & Herbison, A. E. Estrous Cycle Plasticity in the Hyperpolarization-Activated Current Ih Is Mediated by Circulating 17 - Estradiol in Preoptic Area Kisspeptin Neurons. *J. Neurosci.* **33,** 10828–10839 (2013).

126. Zhang, C. *et al.* Molecular mechanisms that drive estradiol-dependent burst firing of Kiss1 neurons in the rostral periventricular preoptic area. *Am. J. Physiol. Endocrinol. Metab.* **305,** E1384-97 (2013).

127. Zhang, C., Bosch, M. A., Qiu, J., Rønnekleiv, O. K. & Kelly, M. J. 17β-Estradiol Increases Persistent Na + Current and Excitability of AVPV/PeN Kiss1 Neurons in Female Mice. *Mol. Endocrinol.* **29,** 518–527 (2015).

128. Gallo, R. V & Bona-Gallo, A. Lack of ovarian steroid negative feedback on pulsatile luteinizing hormone release between estrus and diestrous day 1 in the rat estrous cycle. *Endocrinology* **116,** 1525–8 (1985).

129. Andrews, W. W., Mizejewski, G. J. & Ojeda, S. R. Development of estradiol-positive feedback on luteinizing hormone release in the female rat: a quantitative study. *Endocrinology* **109,** 1404–13 (1981).

130. Cravo, R. M. *et al.* Leptin signaling in Kiss1 neurons arises after pubertal development. *PLoS One* **8,** e58698 (2013).

131. Shim, W. S. *et al.* Estradiol hypersensitivity and mitogen-activated protein kinase expression in long-term estrogen deprived human breast cancer cells in vivo. *Endocrinology* **141,** 396–405 (2000).

132. Dror, T., Franks, J. & Kauffman, A. S. Analysis of multiple positive feedback paradigms demonstrates a complete absence of LH surges and GnRH activation in mice lacking kisspeptin signaling. *Biol. Reprod.* **88,** 146 (2013).

133. Paxinos, G. & Franklin, K. *The Mouse Brain in Stereotaxic Coordinates: Second Edition.* (Elsevier Academic Press, 2001).

134. Nunemaker, C. S., DeFazio, R. A. & Moenter, S. M. A targeted extracellular approach for recording long-term firing patterns of excitable cells: a practical guide. *Biol. Proced. Online* **5,** 53–62 (2003).

135. Alcami, P., Franconville, R., Llano, I. & Marty, A. Measuring the firing rate of high-resistance neurons with cell-attached recording. *J. Neurosci.* **32,** 3118–30 (2012).

136. Barry, P. H. JPCalc, a software package for calculating liquid junction potential corrections in patch-clamp, intracellular, epithelial and bilayer measurements and for correcting junction potential measurements. *J. Neurosci. Methods* **51,** 107–16 (1994).

137. DeFazio, R. A., Elias, C. F. & Moenter, S. M. GABAergic transmission to kisspeptin neurons is differentially regulated by time of day and estradiol in female mice. *J. Neurosci.* **34,** 16296–308 (2014).

138. DeFazio, R. A. & Moenter, S. M. Estradiol feedback alters potassium currents and firing properties of gonadotropin-releasing hormone neurons. *Mol. Endocrinol.* **16,** 2255–65 (2002).

139. Khaliq, Z. M. & Bean, B. P. Pacemaking in dopaminergic ventral tegmental area neurons: depolarizing drive from background and voltage-dependent sodium conductances. *J. Neurosci.* **30,** 7401–7413 (2010).

140. Perez-Reyes, E. Molecular physiology of low-voltage-activated t-type calcium channels. *Physiol. Rev.* **83,** 117–161 (2003).

141. Tadayonnejad, R. *et al.* Rebound discharge in deep cerebellar nuclear neurons in vitro. *Cerebellum* **9,** 352–74 (2010).

142. Jacobs, J. M. & Meyer, T. Control of Action Potential-Induced Ca2+ Signaling in the Soma of Hippocampal Neurons by Ca2+ Release from Intracellular Stores. *J. Neurosci.* **17,** 4129–4135 (1997).

143. Suzuki, S. & Rogawski, M. a. T-type calcium channels mediate the transition between tonic and phasic firing in thalamic neurons. *Proc. Natl. Acad. Sci. U. S. A.* **86,** 7228–7232 (1989).

144. Molineux, M. L. *et al.* Specific T-type calcium channel isoforms are associated with distinct burst phenotypes in deep cerebellar nuclear neurons. *Proc. Natl. Acad. Sci. U. S. A.* **103,** 5555–5560 (2006).

145. Lee, J. H., Gomora, J. C., Cribbs, L. L. & Perez-Reyes, E. Nickel block of three cloned T-type calcium channels: low concentrations selectively block alpha1H. *Biophys. J.* **77,** 3034–42 (1999).

146. Perreault, P. & Avoli, M. Physiology and pharmacology of epileptiform activity induced by 4-aminopyridine in rat hippocampal slices. *J. Neurophysiol.* **65,** 771–85 (1991).

147. Amendola, J., Woodhouse, A., Martin-Eauclaire, M.-F. & Goaillard, J.-M. Ca^{2+}/cAMP-sensitive covariation of I(A) and I(H) voltage dependences tunes rebound firing in dopaminergic neurons. *J. Neurosci.* **32,** 2166–81 (2012).

148. Ruka, K. A., Burger, L. L. & Moenter, S. M. Regulation of arcuate neurons coexpressing kisspeptin, neurokinin B, and dynorphin by modulators of neurokinin 3 and κ-opioid receptors in adult male mice. *Endocrinology* **154,** 2761–71 (2013).

149. Pinilla, L., Aguilar, E., Dieguez, C., Millar, R. P. & Tena-Sempere, M. Kisspeptins and reproduction: physiological roles and regulatory mechanisms. *Physiol. Rev.* **92,** 1235–316 (2012).

150. Krahe, R. & Gabbiani, F. Burst firing in sensory systems. *Nat. Rev. Neurosci.* **5,** 13–23 (2004).

151. Jackson, M. B., Konnerth, A. & Augustine, G. J. Action potential broadening and frequency-dependent facilitation of calcium signals in

pituitary nerve terminals. *Proc. Natl. Acad. Sci. U. S. A.* **88,** 380–4 (1991).

152. Muschol, M. & Salzberg, B. M. Dependence of transient and residual calcium dynamics on action-potential patterning during neuropeptide secretion. *J. Neurosci.* **20,** 6773–6780 (2000).

153. Ducret, E., Gaidamaka, G. & Herbison, A. E. Electrical and morphological characteristics of anteroventral periventricular nucleus kisspeptin and other neurons in the female mouse. *Endocrinology* **151,** 2223–2232 (2010).

154. De Croft, S. *et al.* Spontaneous kisspeptin neuron firing in the adult mouse reveals marked sex and brain region differences but no support for a direct role in negative feedback. *Endocrinology* **153,** 5384–5393 (2012).

155. Piet, R., Fraissenon, A., Boehm, U. & Herbison, a. E. Estrogen Permits Vasopressin Signaling in Preoptic Kisspeptin Neurons in the Female Mouse. *J. Neurosci.* **35,** 6881–6892 (2015).

156. Kriegsfeld, L. J. Circadian regulation of kisspeptin in female reproductive functioning. *Adv. Exp. Med. Biol.* **784,** 385–410 (2013).

157. Frazao, R. *et al.* Shift in Kiss1 Cell Activity Requires Estrogen Receptor. *J. Neurosci.* **33,** 2807–2820 (2013).

158. Bean, B. P. The action potential in mammalian central neurons. *Nat. Rev. Neurosci.* **8,** 451–465 (2007).

159. Puopolo, M., Raviola, E. & Bean, B. P. Roles of subthreshold calcium current and sodium current in spontaneous firing of mouse midbrain dopamine neurons. *J. Neurosci.* **27,** 645–656 (2007).

160. Itri, J. N. *et al.* Circadian regulation of a-type potassium currents in the suprachiasmatic nucleus. *J. Neurophysiol.* **103,** 632–40 (2010).

161. Goldman, M. S., Golowasch, J., Marder, E. & Abbott, L. F. Global Structure, Robustness, and Modulation of Neuronal Models. *J. Neurosci.* **21,** 5229–5238 (2001).

162. Swensen, A. M. & Bean, B. P. Robustness of burst firing in dissociated

purkinje neurons with acute or long-term reductions in sodium conductance. *J. Neurosci.* **25,** 3509–20 (2005).

163. Prinz, A. A., Bucher, D. & Marder, E. Similar network activity from disparate circuit parameters. *Nat. Neurosci.* **7,** 1345–52 (2004).

164. Vasudevan, N. & Pfaff, D. W. Non-genomic actions of estrogens and their interaction with genomic actions in the brain. *Front. Neuroendocrinol.* **29,** 238–257 (2008).

165. Morissette, M. *et al.* Contribution of estrogen receptors alpha and beta to the effects of estradiol in the brain. *J. Steroid Biochem. Mol. Biol.* **108,** 327–338 (2008).

166. Zhang, C., Bosch, M. A., Rønnekleiv, O. K. & Kelly, M. J. Kisspeptin activation of TRPC4 channels in female GnRH neurons requires PIP2 depletion and cSrc kinase activation. *Endocrinology* **154,** 2772–83 (2013).

167. Wang, L., DeFazio, R. A. & Moenter, S. M. Excitability and burst generation of AVPV kisspeptin neurons are regulated by the estrous cycle via multiple conductances modulated by estradiol action. *eNeuro* **3,** e0094-16 (2016).

168. Greenwald-Yarnell, M. L. *et al.* ERα in Tac2 neurons regulates puberty onset in female mice. *Endocrinology* **157,** 1555–1565 (2016).

169. Qiu, J. *et al.* High-frequency stimulation-induced peptide release synchronizes arcuate kisspeptin neurons and excites GnRH neurons. *eLife* **5,** e16246 (2016).

170. Vanacker, C., Moya, M. R., DeFazio, R. A., Johnson, M. L. & Moenter, S. M. Long-term recordings of arcuate nucleus kisspeptin neurons reveal patterned activity that is modulated by gonadal steroids in male mice. *Endocrinology* (2017). doi:10.1210/en.2017-00382

171. López, F. J., Donoso, A. O. & Negro-Vilar, A. Endogenous excitatory amino acids and glutamate receptor subtypes involved in the control of hypothalamic luteinizing hormone-releasing hormone secretion. *Endocrinology* **130,** 1986–92 (1992).

172. Ping, L., Mahesh, V. B., Bhat, G. K. & Brann, D. W. Regulation of gonadotropin-releasing hormone and luteinizing hormone secretion by AMPA receptors. *Neuroendocrinology* **66,** 246–53 (1997).

173. Brann, D. W. Glutamate: a major excitatory transmitter in neuroendocrine regulation. *Neuroendocrinology* **61,** 213–25 (1995).

174. Iremonger, K. J., Constantin, S., Liu, X. & Herbison, A. E. Glutamate regulation of GnRH neuron excitability. *Brain Res.* **1364,** 35–43 (2010).

175. Gu, G., Varoqueaux, F. & Simerly, R. B. Hormonal regulation of glutamate receptor gene expression in the anteroventral periventricular nucleus of the hypothalamus. *J. Neurosci.* **19,** 3213–22 (1999).

176. Ottem, E. N., Godwin, J. G., Krishnan, S. & Petersen, S. L. Dual-phenotype GABA/glutamate neurons in adult preoptic area: sexual dimorphism and function. *J. Neurosci.* **24,** (2004).

177. Belousov, A. B. & van den Pol, A. N. Local synaptic release of glutamate from neurons in the rat hypothalamic arcuate nucleus. *J. Physiol.* **499,** 747–761 (1997).

178. Czieselsky, K. *et al.* Pulse and surge profiles of luteinizing hormone secretion in the mouse. *Endocrinology* **157,** 4794–4802 (2016).

179. Steyn, F. J. *et al.* Development of a methodology for and assessment of pulsatile luteinizing hormone secretion in juvenile and adult male mice. *Endocrinology* **154,** 4939–4945 (2013).

180. Hanchate, N. K. *et al.* Kisspeptin-GPR54 signaling in mouse NO-synthesizing neurons participates in the hypothalamic control of ovulation. *J. Neurosci.* **32,** (2012).

181. Sullivan, S. D., DeFazio, R. A. & Moenter, S. M. Metabolic regulation of fertility through presynaptic and postsynaptic signaling to gonadotropin-releasing hormone neurons. *J. Neurosci.* **23,** (2003).

182. Veldhuis, J. D. & Johnson, M. L. Cluster analysis: a simple, versatile, and robust algorithm for endocrine pulse detection. *Am. J. Physiol.* **250,** E486-

93 (1986).

183. Livak, K. J. & Schmittgen, T. D. Analysis of relative gene expression data using real-time quantitative PCR and the 2−ΔΔCT method. *Methods* **25,** 402–408 (2001).

184. Auger, C. & Marty, A. Quantal currents at single-site central synapses. *J. Physiol.* **526 Pt 1,** 3–11 (2000).

185. Zhang, X. & van den Pol, A. N. Direct inhibition of arcuate proopiomelanocortin neurons: a potential mechanism for the orexigenic actions of dynorphin. *J. Physiol.* **591,** 1731–1747 (2013).

186. Hentges, S. T., Otero-Corchon, V., Pennock, R. L., King, C. M. & Low, M. J. Proopiomelanocortin expression in both GABA and glutamate neurons. *J. Neurosci.* **29,** (2009).

187. Jarvie, B. C. & Hentges, S. T. Expression of GABAergic and glutamatergic phenotypic markers in hypothalamic proopiomelanocortin neurons. *J. Comp. Neurol.* **520,** 3863–3876 (2012).

188. Ruka, K. A., Burger, L. L. & Moenter, S. M. Both estrogen and androgen modify the response to activation of neurokinin-3 and κ-opioid receptors in arcuate kisspeptin neurons from male mice. *Endocrinology* **157,** 752–763 (2016).

189. Glanowska, K. M., Burger, L. L. & Moenter, S. M. Development of Gonadotropin-releasing hormone secretion and pituitary response. *J. Neurosci.* **34,** (2014).

190. Zou, K. & Ing, N. H. Oestradiol up-regulates oestrogen receptor, cyclophilin, and glyceraldehyde phosphate dehydrogenase mRNA concentrations in endometrium, but down-regulates them in liver. *J. Steroid Biochem. Mol. Biol.* **64,** 231–237 (1998).

191. Witham, E. A. *et al.* Kisspeptin regulates gonadotropin genes via immediate early gene induction in pituitary gonadotropes. *Mol. Endocrinol.* **27,** 1283–94 (2013).

192. Burger, L. L., Dalkin, A. C., Aylor, K. W., Haisenleder, D. J. & Marshall, J. C. GnRH pulse frequency modulation of gonadotropin subunit gene transcription in normal gonadotropes—assessment by primary transcript assay provides evidence for roles of GnRH and follistatin. *Endocrinology* **143,** 3243–3249 (2002).

193. Eyigor, O., Lin, W. & Jennes, L. Identification of neurones in the female rat hypothalamus that express oestrogen receptor-alpha and vesicular glutamate transporter-2. *J. Neuroendocrinol.* **16,** 26–31 (2004).

194. Woolley, C. S. Estrogen-mediated structural and functional synaptic plasticity in the female rat hippocampus. *Horm. Behav.* **34,** 140–148 (1998).

195. Schwarz, J. M., Liang, S.-L., Thompson, S. M. & McCarthy, M. M. Estradiol induces hypothalamic dendritic spines by enhancing glutamate release: a mechanism for organizational sex differences. *Neuron* **58,** 584–98 (2008).

196. Cholanian, M., Krajewski-Hall, S. J., Levine, R. B., McMullen, N. T. & Rance, N. E. Electrophysiology of arcuate neurokinin B neurons in female Tac2-EGFP transgenic mice. *Endocrinology* **155,** 2555–2565 (2014).

197. Mercer, A. J., Hentges, S. T., Meshul, C. K. & Low, M. J. Unraveling the central proopiomelanocortin neural circuits. *Front. Neurosci.* **7,** 19 (2013).

198. Manfredi-Lozano, M. *et al.* Defining a novel leptin-melanocortin-kisspeptin pathway involved in the metabolic control of puberty. *Mol. Metab.* **5,** 844–57 (2016).

199. Nestor, C. C. *et al.* Optogenetic stimulation of arcuate nucleus Kiss1 neurons reveals a steroid-dependent glutamatergic input to POMC and AgRP neurons in male mice. *Mol. Endocrinol.* **30,** 630–644 (2016).

200. Drake, C. T. *et al.* Dynorphin opioids present in dentate granule cells may function as retrograde inhibitory neurotransmitters. *J. Neurosci.* **14,** 3736–50 (1994).

201. Iremonger, K. J. & Bains, J. S. Retrograde opioid signaling regulates glutamatergic transmission in the hypothalamus. *J. Neurosci.* **29,** (2009).

202. Semaan, S. J. *et al.* BAX-dependent and BAX-independent regulation of Kiss1 neuron development in mice. *Endocrinology* **151,** 5807–5817 (2010).

203. Kumar, D. *et al.* Murine arcuate nucleus kisspeptin neurons communicate with GnRH neurons in utero. *J. Neurosci.* **34,** (2014).

204. Caraty, A., Locatelli, A. & Schanbacher, B. Augmentation, by naloxone, of the frequency and amplitude of LHRH pulses in hypothalamo-hypophyseal portal blood in the castrated ram. *C. R. Acad. Sci. III.* **305,** 369–74 (1987).

205. Dalkin, A. C., Haisenleder, D. J., Ortolano, G. A., Ellis, T. R. & Marshall, J. C. The frequency of gonadotropin-releasing hormone stimulation differentially regulates gonadotropin subunit messenger ribonucleic acid expression. *Endocrinology* **125,** 917–923 (1989).

206. Macaluso, M. *et al.* A public health focus on infertility prevention, detection, and management. *Fertil. Steril.* **93,** 16.e1-10 (2010).

207. Helm, K. D., Nass, R. M., Evans, W. S., Nass, R. M. & Evans, W. S. Physiologic and Pathophysiologic Alterations of the Neuroendocrine Components of the Reproductive Axis. in *Yen & Jaffe's Reproductive Endocrinology* 441–488 (Elsevier, 2009). doi:10.1016/B978-1-4160-4907-4.00019-X

208. Wang, L., Burger, L. L., Greenwald-Yarnell, M. L., Myers, M. G. & Moenter, S. M. Glutamatergic Transmission to Hypothalamic Kisspeptin Neurons Is Differentially Regulated by Estradiol through Estrogen Receptor α in Adult Female Mice. *J. Neurosci.* **38,** 1061 LP-1072 (2018).

209. Swiech, L. *et al.* In vivo interrogation of gene function in the mammalian brain using CRISPR-Cas9. *Nat. Biotechnol.* **33,** 102–106 (2014).

210. Ran, F. A. *et al.* Genome engineering using the CRISPR-Cas9 system. *Nat. Protoc.* **8,** 2281–308 (2013).

211. Doench, J. G. *et al.* Rational design of highly active sgRNAs for CRISPR-Cas9–mediated gene inactivation. *Nat. Biotechnol.* **32,** 1262–1267 (2014).

212. Ramakrishnan, S. K. *et al.* HIF2α Is an Essential Molecular Brake for

Postprandial Hepatic Glucagon Response Independent of Insulin Signaling. *Cell Metab.* **23,** 505–516 (2016).

213. Flak, J. N. *et al.* A leptin-regulated circuit controls glucose mobilization during noxious stimuli. *J. Clin. Invest.* **127,** 3103–3113 (2017).

214. Sanjana, N. E., Shalem, O. & Zhang, F. Improved vectors and genome-wide libraries for CRISPR screening. *Nat. Methods* **11,** 783–784 (2014).

215. Tau, G. Z. & Peterson, B. S. Normal development of brain circuits. *Neuropsychopharmacology* **35,** 147–68 (2010).

216. Clarkson, J. *et al.* Definition of the hypothalamic GnRH pulse generator in mice. *Proc. Natl. Acad. Sci.* **114,** E10216–E10223 (2017).

217. Gill, J. C. *et al.* Increased Neurokinin B (*Tac2*) Expression in the Mouse Arcuate Nucleus Is an Early Marker of Pubertal Onset with Differential Sensitivity to Sex Steroid-Negative Feedback than *Kiss1*. *Endocrinology* **153,** 4883–4893 (2012).